

**Synthesis and Evaluation of Ionic Liquids for their Applications in
Antibacterial Paints**



Rabia Hassan

Reg. No. 00000203189

**This thesis is submitted as a partial fulfillment of the requirements for the
degree of MS in Chemistry**

Supervisor: Dr. Mudassir Iqbal

Department of Chemistry

School of Natural Sciences

National University of Sciences and Technology,

Islamabad, Pakistan.

National University of Sciences & Technology**MS THESIS WORK**

We hereby recommend that the dissertation prepared under our supervision by: Rabia Hassan, Regn No. 00000203189 Titled: Synthesis and Evaluation of Ionic Liquids for their Application in Antibacterial Paint be accepted in partial fulfillment of the requirements for the award of **MS** degree.

Examination Committee Members1. Name: DR. SYED RIZWAN HUSSAINSignature: 2. Name: DR. FAHEEM AMINSignature: External Examiner: DR. SAIMA KALSOOMSignature: Supervisor's Name DR. MUDASSIR IQBALSignature: 


Head of Department

11/11/19
Date

COUNTERSIGNEDDate: 11/11/2019


Dean/Principal

THESIS ACCEPTANCE CERTIFICATE

Certified that final copy of MS thesis written by Ms. Rabia Hassan, (Registration No. 00000203189), of School of Natural Sciences has been vetted by undersigned, found complete in all respects as per NUST statutes/regulations, is free of plagiarism, errors, and mistakes and is accepted as partial fulfillment for award of MS/M.Phil degree. It is further certified that necessary amendments as pointed out by GEC members and external examiner of the scholar have also been incorporated in the said thesis.

Signature: _____ 

Name of Supervisor: Dr. Mudassir Iqbal

Date: _____

Signature (HoD): _____ 

Date: 11/11/11

Signature (Dean/Principal): 

Date: 11/11/2011

To my mother for her unconditional love, inspiration , and support.

ACKNOWLEDGEMENT

Words are bound and knowledge is limited to praise Almighty ALLAH. The beneficent, and the merciful who created the universe and ability to think into His secrets. Peace and blessings of ALLAH upon Holy prophet Muhammad (peace be upon him) the everlasting source of guidance and knowledge for humanity.

I would like to thank my mother, for her limitless support, love, and encouragement. Without her being there for me when things got tough, this never could have been possible. She has been there for me since the beginning, and I know she always will be.

I consider myself very fortune to work under the kind supervision and guidance of Dr. Mudassir Iqbal whose personal interest and dedication, thought provoking guidance, valuable suggestions and discussions enabled me to complete this task. He really encourages my all attempts in designing this research work and helped at each and every stage of the project. I am thankful to GEC members Dr. Rizwan Hussain and Dr. Faheem Amin. I offer my regards to principal SNS and HOD Dr. Mohammad Arfan who provided me an opportunity to complete this project.

I would also like to thank to Mr. Ishrat, and other staff members for their cooperation during my research work. To those who indirectly contributed in

Rabia Hassan

ABSTRACT

Thirty six Ionic Liquids were prepared cationic parts were Imidazolium, Pyridinium, Quaternary ammonium and phosphonium with varying chain lengths and anionic parts were Bromide, Sodium Methane sulphonate, Lithium Bis(trifluoromethane-sulfonyl)imide ,Sodium Dichloroacetate and Sodium Tetrafluoroborate ,Potassium Hydrogen sulphate. The prepared ionic liquids were characterized with different characterization techniques TLC, FTIR and NMR. Then these thirty six samples were tested for their antibacterial activity against most commonly occurring bacteria in environment. Most of the ionic liquids show good antibacterial property, among them ionic liquid showing highest antibacterial activity were selected and there different composition were made in paint in order to check antibacterial activity. All compositions were highly antibacterial as all compositions show minimum bacterial growth.

Table of Contents

ACKNOWLEDGEMENT.....	i
ABSTRACT.....	ii
Abbreviations	ix
Chapter 1	1
1. INTRODUCTION.....	1
1.1 Problem.....	1
1.2 What is bacteria	1
1.3 Structure of bacteria.....	2
1.4 Types of bacteria.....	2
1.5 Most common bacteria and their infections	3
1.5.1.Escherichia coli.....	3
1.5.2. <i>Enterobacter aerogenes</i>	3
1.5.3. <i>Klebsiella pneumoniae</i>	3
1.5.4. <i>Proteus vulgaris</i>	4
1.5.5. <i>Streptococcus pneumoniae</i>	4
1.5.6. <i>Streptococcus pyogenes</i>	4
1.5.7. <i>Pseudomonas aeruginosa</i>	4
1.6 Role of Surface contamination in bacterial infections transmission	5
1.7 Hospitals Acquired Bacterial Infections	6
1.8 Measures to control bacterial infections:.....	7
1.9 Ionic liquids and properties of ionic liquids:	8
2. LITERATURE REVIEW	10
2.1. Nanoparticles based antibacterial paint.....	10
2.2. Ionic liquids antibacterial activity	13
2.3. Drug derived ionic liquids and their antibacterial activity	14
2.4. Research work aims.....	17
Chapter 3	18
3.1 Solvents and chemicals	18
3.2 Apparatus and Glassware	18
3.3 Experimental procedure.....	18
Synthesis of ionic liquids.....	19
3.3.1. Synthesis of Sodium Methanesulphonate.....	21
3.3.2. Synthesis of Sodium Dichloroacetate	21
3.3.3. 1-Methyl-3-octylimidazolium bromide synthesis	22

3.3.4.	1-Methyl-3-octylimidazolium methanesulphonate synthesis	22
3.3.5.	1-Methyl-3-octyl-imidazolium Bis(trifluoromethane-sulfonyl)imide	23
	[C ₈ mim][Tf ₂ N] synthesis	23
3.3.6.	1-Methyl-3-octylimidazolium dichloroacetate [C ₈ mim][CHCl ₂ CO ₂] synthesis	23
3.3.7.	1-Methyl-3-octylimidazolium tetrafluoroborate[C ₈ mim][BF ₄] synthesis	24
3.3.8.	1-Methyl-3-octylimidazolium hydrogen sulphate[C ₈ mim][HSO ₄] synthesis	24
3.3.9.1	1-Methyl- 3-butylimidazolium bromide synthesis.....	25
3.3.10.	1-Butyl-3-methylimidazolium methanesulphonate synthesis.....	25
3.3.11.	3-Butyl-1-methylimidazolium Bis(trifluoromethane-sulfonyl)imide.....	26
	[C ₄ mim][Tf ₂ N] synthesis.....	26
3.3.12.	3-Butyl-1-methylimidazolium dichloroacetate [C ₄ mim][CHCl ₂ CO ₂] synthesis	26
3.3.13.	1-Methyl-3-butylimidazolium tetrafluoroborate [C ₄ mim][BF ₄] synthesis.....	27
3.3.14.	1-Methyl-3-butylimidazolium hydrogen sulphate[C ₄ mim][HSO ₄] synthesis.....	27
3.3.15	Octyl pyridinium bromide synthesis	28
3.3.16.	Octyl pyridinium methanesulphonate synthesis	28
3.3.17.	Octyl pyridinium Bis(trifluoromethane-sulfonyl)imide [C ₈ py][Tf ₂ N] synthesis ...	29
3.3.18.	Octyl pyridinium dichloroacetate[C ₈ py] [CHCl ₂ CO ₂] synthesis	29
3.3.19.	Octyl pyridinium tetrafluoroborate [C ₈ py][BF ₄] synthesis	30
3.3.20.	Octyl pyridinium hydrogen sulphate[C ₈ py][HSO ₄] synthesis.....	30
3.3.21.	Butyl pyridinium bromide synthesis	31
3.3.22.	Butyl pyridinium methanesulphonate synthesis	31
3.3.23.	Butyl pyridinium Bis(trifluoromethane-sulfonyl)imide [C ₄ py] [Tf ₂ N] synthesis .	32
3.3.24.	Butyl pyridinium dichloroacetate [C ₄ py][CHCl ₂ CO ₂] synthesis	32
3.3.25.	Butyl pyridinium tetrafluoroborate[C ₄ py][BF ₄] synthesis	33
3.3.26.	Butyl pyridinium hydrogen sulphate [C ₄ py][HSO ₄] synthesis.....	33
3.3.27.	Mono-butyl tri-octyl phosphonium bromide synthesis.....	34
3.3.28.	Mono-butyl tri-octyl phosphonium methanesulphonate synthesis.....	34
3.3.29.	Butyl-tri-octyl phosphonium Bis(trifluoromethane-sulfonyl)imide [P ₄₈₈₈][Tf ₂ N]synthesis.....	35
3.3.30.	Butyl-Tri-octyl phosphonium dichloroacetate [P ₄₈₈₈][CHCl ₂ CO ₂] synthesis	35
3.3.31.	Tri-octyl mono-butyl phosphonium tetrafluoroborate[P ₄₈₈₈][BF ₄] synthesis.....	36
3.3.32.	Tri-octyl mono-butyl phosphonium hydrogen sulphate[P ₄₈₈₈][HSO ₄] synthesis 36	
3.3.33.	Diethyl dibutyl ammonium bromide	37
3.3.34.	Diethyl dibutyl ammonium methanesulphonate synthesis	37
3.3.35.	Diethyl dibutyl ammonium Bis(trifluoromethane-sulfonyl)imide [N ₂₂₄₄][Tf ₂ N] synthesis 38	

3.3.36.	Diethyl dibutyl ammonium dichloroacetate [N ₂ 2 4 4][CHCl ₂ CO ₂] synthesis.....	38
3.3.37.	Diethyl dibutyl ammonium tetrafluoroborate[N ₂ 2 4 4][BF ₄] synthesis	39
3.3.38.	Diethyl dibutyl ammonium hydrogen sulphate[N ₂ 2 4 4][HSO ₄] synthesis.....	39
Chapter 4	40
4.	RESULT AND DISCUSSION.....	41
4.1	Thin layer chromatography (TLC)	41
4.2.	Attenuated Total Reflection-Fourier Transformation Infrared spectroscopy	42
4.2.1.	FT-IR analysis of 1-Methyl-3-octylimidazolium bromide [C ₈ mim]Br	42
4.2.2.	FT-IR analysis of 1-Methyl-3-octylimidazolium methane sulphonate	43
4.2.3.	FT-IR analysis of 1-Methyl-3-octylimidazolium Bis(trifluoromethanesulfonyl) imide	44
4.2.4.	FT-IR analysis of 1-Methyl-3-octylimidazolium dichloroacetate	44
4.2.5.	FT-IR analysis of 1-Methyl-3-octylimidazolium tetrafluoroborate.....	45
4.2.6.	FT-IR analysis for 1-Methyl-3-Octylimidazolium hydrogen sulphate.....	46
4.2.7.	FT-IR analysis for 1-Methyl-3-butylimidazolium bromide [C ₄ mim]Br	47
4.2.8.	FT-IR analysis of 1-Methyl-3-butylimidazolium methanesulphonate	48
4.2.9.	FT-IR analysis of 1-Methyl-3-butylimidazolium Bis(trifluoromethane-sulfonyl) Imide	48
4.2.10.	FT-IR analysis for 3-Butyl-1-methylimidazolium dichloroacetate.....	49
4.2.11.	FT-IR analysis of 1-Methyl-3-butylimidazolium tetrafluoroborate.....	49
4.2.12.	FT-IR analysis for 1-Methyl-3-butylimidazolium hydrogen sulphate	50
4.2.13.	FT-IR analysis for Octyl pyridinium bromide [C ₈ py]Br.....	51
4.2.14.	FT-IR analysis for Octyl pyridinium bromide [C ₈ py][MeSO ₃]	52
4.2.15.	FT-IR analysis for Octyl pyridinium Bis(trifluoromethane-sulfonyl)imide.....	53
4.2.16.	FT-IR analysis for Octyl pyridinium dichloroacetate	53
4.2.17.	FT-IR analysis for Octyl pyridinium tetrafluoroborate [C ₈ py][BF ₄].....	54
4.2.18.	FT-IR analysis for Octyl pyridinium bromide [C ₈ py][HSO ₄].....	55
4.2.19.	FT-IR analysis for Butyl pyridinium bromide [C ₄ py]Br.....	56
4.2.20.	FT-IR analysis for Butyl pyridinium bromide	56
4.2.21.	FT-IR analysis for Butyl pyridinium Bis(trifluoromethane-sulfonyl)imide.....	57
4.2.22.	FT-IR analysis for Butyl pyridinium dichloroacetate	58
4.2.23.	FT-IR analysis for Butyl pyridinium tetrafluoroborate.....	58
4.2.24.	FT-IR analysis for Butyl pyridinium hydrogen sulphate.....	59
4.2.25.	FT-IR analysis of Mono-butyl tri-octyl phosphonium Bromide	60
4.2.26.	FT-IR analysis of Mono-butyl tri-octyl phosphonium methane sulphonate.....	60
4.2.27.	FT-IR analysis of Mono-butyl tri-octyl phosphonium Bis(trifluoromethane- sulfonyl) imide	61

4.2.28.	FT-IR analysis of Butyl-Tri-octyl phosphonium dichloroacetate.....	62
4.2.29.	FT-IR analysis of Tri-octyl mono-butyl phosphonium tetrafluoroborate [P ₄₈₈₈][BF ₄].....	63
4.2.30.	Tri-octyl mono-butyl phosphonium hydrogen sulphate.....	63
4.2.31.	FT-IR analysis of Di-butyl di-ethyl ammonium bromide.....	64
4.2.32.	FT-IR analysis of Di-butyl di-ethyl ammonium methanesulphonate.....	65
4.2.33.	FT-IR analysis Di-butyl di-ethyl ammonium Bis(trifluoromethane-sulfonyl) imide 65	65
4.2.34.	FT-IR analysis of Di-butyl di-ethyl ammonium dichloroacetate.....	66
4.2.35.	FT-IR analysis for Di-butyl di-ethyl ammonium hydrogen tetrafluoroborate.....	67
4.2.36.	FT-IR analysis for Di-butyl di-ethyl ammonium hydrogen sulphate.....	68
4.4.	Anti-bacterial Susceptibility of 36 different ionic liquids.....	69
4.4.1.	Sample preparation:.....	69
4.4.2.	Anti-bacterial susceptibility Test 1 using Agar Well Diffusion Assay.....	69
	Table 4.1 Antibacterial activity of ionic liquids against most common bacteria.....	73
4.5.	Antibacterial Activity Graphs.....	74
4.6	Antibacterial Paint.....	77
Chapter 5	78
5.	CONCLUSION.....	78
REFERENCES	1

List of Figures

Figure 1.1 Structure of bacteria.....	2
Figure 1.2 Types of bacteria	2
Figure 1.3 Bacterial infections through surfaces	5
Figure 1.4 Role of hands in bacterial in bacterial infection transmission	6
Figure 1.5 Measures to control bacterial infections.....	7
Figure 1.6 Control of infections by antibacterial surfaces	8
Figure 4.1 FTIR spectrum of [C ₈ mim]Br.....	43
Figure 4.2 FTIR spectrum of [C ₈ mim][MeSO ₃]	43
Figure 4.3 FTIR spectrum of [C ₈ mim][Tf ₂ N]	44
Figure 4.4 FTIR spectrum of [C ₈ mim][CHCl ₂ CO ₂]	45
Figure 4.5 FTIR spectrum of [C ₈ mim][BF ₄].....	45
Figure 4.6 FTIR spectrum of [C ₈ mim][HSO ₄].....	46
Figure 4.7 FTIR for comparison of different exchanged anions with [C ₈ mim].....	47
Figure 4.8 FT-IR spectrum [C ₄ mim]Br.....	47
Figure 4.9 FT-IR spectrum of [C ₄ mim][MeSO ₃]	48
Figure 4.10 FTIR spectrum [C ₈ mim][Tf ₂ N]	49
Figure 4.11 FTIR spectrum of [C ₄ mim][CHCl ₂ CO ₂].....	49
Figure 4.12 FTIR spectrum of [C ₄ mim][BF ₄].....	50
Figure 4.14 FTIR for comparison of different exchanged anions with [C ₄ mim].....	51
Figure 4.15 FTIR spectrum of [C ₈ py][Br]	52
Figure 4.16 FTIR spectrum of [C ₈ py][MeSO ₃].....	52
Figure 4.17 FTIR spectrum of [C ₈ mim][Tf ₂ N]	53
Figure 4.18 FTIR spectrum of [C ₈ py][CHCl ₂ CO ₂].....	54
Figure 4.19 FTIR spectrum of [C ₈ py][BF ₄]	54
Figure 4.20 FTIR spectrum of [C ₈ py][HSO ₄]	55
Figure 4.21 FTIR for comparison of different exchanged anions with [C ₈ py].....	55
Figure 4.22 FTIR spectrum of [C ₄ py][Br]	56
Figure 4.23 FTIR spectrum of [C ₄ py][MeSO ₃].....	57
Figure 4.24 FTIR spectrum of [C ₄ mim][Tf ₂ N]	57
Figure 4.25 FTIR spectrum of [C ₄ py][CHCl ₂ CO ₂].....	58
Figure 4.26 FTIR spectrum of [C ₄ py][BF ₄]	59
Figure 4.27 FTIR spectrum of [C ₄ py][HSO ₄]	59
Figure 4.28 FTIR for comparison of different exchanged anions with [C ₄ py].....	60
Figure 4.29 FT-IR spectrum of [P ₄₈₈₈][Br]	60

Figure 4.30 FTIR spectrum of $[P_{4888}][MeSO_3]$	61
Figure 4.31 FTIR spectrum of $[P_{4888}][Tf_2N]$	62
Figure 4.32 FTIR spectrum of $[P_{4888}][CHCl_2CO_2]$	62
Figure 4.33 FTIR spectrum of $[P_{4888}][BF_4]$	63
Figure 4.34 FTIR spectrum of $[P_{4888}][HSO_4]$	64
Figure 4.35 FTIR for comparison of different exchanged anions with $[P_{4888}]$	64
Figure 4.36 FTIR spectrum of $[N_{2244}][Br]$	65
Figure 4.37 FTIR spectrum of $[N_{2244}][MeSO_3]$	65
Figure 4.38 FTIR spectrum of $[N_{2244}][Tf_2N]$	66
Figure 4.39 FTIR spectrum of $[N_{2244}][CHF_2CO_2]$	67
Figure 4.40 FTIR spectrum of $[N_{2244}][BF_4]$	67
Figure 4.41 FTIR spectrum of $[N_{2244}][HSO_4]$	68
Figure 4.42 FTIR for comparison of different exchanged anions with $[N_{2244}]$	68

Abbreviations

Na[CH ₃ SO ₃]	Sodium Methane sulphonate (X)
Li[Tf ₂ N]	Lithium Bis(trifluoromethane-sulfonyl)imide (XI)
Na[CHCl ₂ CO ₂]	Sodium Dichloroacetate (XII)
Na[BF ₄]	Sodium Tetrafluoroborate (XIII)
K[HSO ₄]	Potassium Hydrogen sulphate (XIV)
[C ₈ mim]Br	1-Methyl-3-octylimidazolium bromide (XV)
[C ₈ mim][CH ₃ SO ₃]	1-Methyl-3-octylimidazolium Methane sulphonate (XVI)
[C ₈ mim][Tf ₂ N]	1-Methyl-3-octylimidazolium Bis(trifluoromethane-sulfonyl)imide (XVII)
[C ₈ mim][CHCl ₂ CO ₂]	1-Methyl-3-octylimidazolium Dichloroacetate (XVIII)
[C ₈ mim][BF ₄]	1-Methyl-3-octylimidazolium Tetrafluoroborate (XIX)
[C ₈ mim][HSO ₄]	1-Methyl-3-octylimidazolium Hydrogen sulphate (XX)
[C ₄ mim]Br	1-Methyl- 3-butylimidazolium bromide (XXI)
[C ₄ mim][CH ₃ SO ₃]	1-Methyl- 3-butylimidazolium Methane sulphonate (XXII)
[C ₄ mim][Tf ₂ N]	1-Methyl- 3-butylimidazolium Bis(trifluoromethane-sulfonyl)imide(XXIII)
[C ₄ mim][CHCl ₂ CO ₂]	1-Methyl- 3-butylimidazolium Dichloroacetate (XXIV)
[C ₄ mim][BF ₄]	1-Methyl- 3-butylimidazolium Tetrafluoroborate (XXV)
[C ₄ mim][HSO ₄]	1-Methyl- 3-butylimidazolium Hydrogen sulphate (XXVI)
[C ₈ py]Br	Octyl pyridinium bromide (XXVII)
[C ₈ py][CH ₃ SO ₃]	Octyl pyridinium Methane sulphonate (XXVIII)
[C ₈ py][Tf ₂ N]	Octyl pyridinium Bis(trifluoromethane-sulfonyl) imide (XXIX)
[C ₈ py][CHCl ₂ CO ₂]	Octyl pyridinium Dichloroacetate (XXX)
[C ₈ py][BF ₄]	Octyl pyridinium Tetrafluoroborate (XXXI)
[C ₈ py][HSO ₄]	Octyl pyridinium Hydrogen sulphate (XXXII)

[C ₄ py]Br.....	Butyl pyridinium bromide (XXXIII)
[C ₄ py][CH ₃ SO ₃]	Butyl pyridinium Methane sulphonate (XXXIV)
[C ₄ py][Tf ₂ N].....	Butyl pyridinium Bis(trifluoromethane-sulfonyl)imide (XXXV)
[C ₄ py][CHCl ₂ CO ₂]	Butyl pyridinium Dichloroacetate (XXXVI)
[C ₄ py][BF ₄]	Butyl pyridinium Tetrafluoroborate (XXXVII)
[C ₄ py][HSO ₄]	Butyl pyridinium Hydrogen sulphate (XXXVIII)
[P ₄₈₈₈]Br	Tri-octyl mono-butyl phosphonium bromide (XXXIX)
[P ₄₈₈₈][CH ₃ SO ₃].....	Tri-octyl mono-butyl phosphonium Methane sulphonate (XL)
[P ₄₈₈₈][Tf ₂ N].	Tri-octyl mono-butyl phosphonium Bis(trifluoromethane-sulfonyl)imide (XLI)
[P ₄₈₈₈][CHCl ₂ CO ₂].....	Tri-octyl mono-butyl phosphonium Dichloroacetate(XLII)
[P ₄₈₈₈][BF ₄]	Tri-octyl mono-butyl phosphonium Tetrafluoroborate(XLIII)
[P ₄₈₈₈][HSO ₄]	Tri-octyl mono-butyl phosphonium Hydrogen sulphate(XLIV)
[N ₂₂₄₄]Br	Diethyl dibutyl ammonium bromide (XLV)
[N ₂₂₄₄][CH ₃ SO ₃]	Diethyl dibutyl ammonium Methane sulphonate (XLVI)
[N ₂₂₄₄][Tf ₂ N].....	Diethyl dibutyl ammonium Bis(trifluoromethane-sulfonyl)imide (XLVII)
[N ₂₂₄₄][CHCl ₂ CO ₂].....	Diethyl dibutyl ammonium Dichloroacetate(XLVIII)
[N ₂₂₄₄][BF ₄].....	Diethyl dibutyl ammonium Tetrafluoroborate(IL)
[N ₂₂₄₄][HSO ₄].....	Diethyl dibutyl ammonium Hydrogen sulphate(L)

Chapter 1

1. INTRODUCTION

1.1 Problem

Bacteria are the major cause of many diseases and thus are very harmful for human health. Bacteria are the most important pathogen of humans as they cause life threatening infections and that's why a number of biocides have been used to kill and control bacteria but to all of these biocides bacteria gain resistance and their number is increasing day by day with increased resistance so there is always a need of new antibacterial agent. They have tendency to attach to any kind of surface for a longer period upon favorable condition divide into number of cells. Hospitals, schools, ATM and other public places surfaces are contaminated with bacteria and most commonly hospitals are the main cause of bacterial transmission from one person to another person. Sanitization, sterilization, disinfection help in control of germs but it is difficult to do all such practices on regular basis so surface must be made antibacterial in order to control bacterial infections nanoparticle based coatings are in practice, but they are expensive and release of toxic nanoparticles in to atmosphere is very harmful for human health.

1.2 What is bacteria

Bacteria are single celled microorganism and are present everywhere as they can survive in any kind of environment because of their dormant nature for longer periods and upon favorable condition they divide into several cells in such a way that within eight hours a single bacterium produces a population of 500,000 bacteria. Bacteria are present in air, water, soil, at the bottom of deepest ocean and even at mountain top and are able to live in plant, animal and people.

Bacteria cause disease by gaining an access route to the body and access routes for the bacteria are contact to contaminated surfaces, infected person ,contaminated food and contaminated water. Hospitals, schools and other public building are sources for germ spreading to stop the transmission of germs these public places must be germs free.

1.3 Structure of bacteria

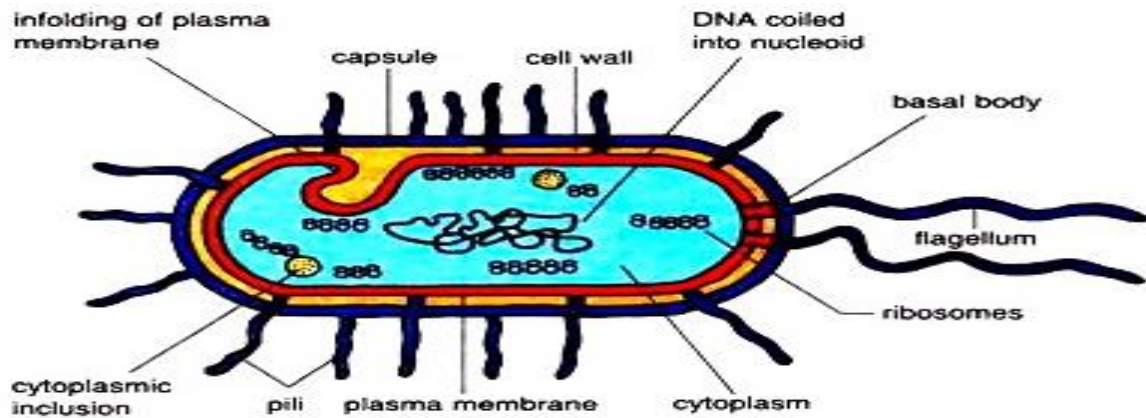


Figure 1.1 Structure of bacteria

1.4 Types of bacteria



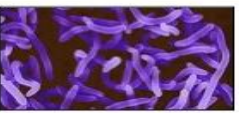
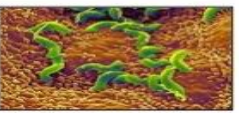








Circular	Rod-shaped	Curved Forms	Other Shapes
 Diplo- (in pairs)	 Coccobacilli (oval)	 Vibrio (curved rod)	 Helicobacter (helical)
 Strepto- (in chains)	 Streptobacilli	 Spirilla (coil)	 Corynebacter (club)
 Staphylo- (clusters)	 Mycobacteria	 Spirochete (spiral)	 Streptomycetes

Figure 1.2 Types of bacteria

Bacteria are classified in a number of ways on the basis of

1.4.1 Composition of cell wall

Gram +ve bacterial cell wall consist of thick peptidoglycan and retain violet color of gram during gram test while gram negative has thin peptidoglycan and does not retain color of gram during gram stain test, Hans Christian Gram developed this test in 1884.

1.4.2 Gaseous requirement

Aerobic bacteria need oxygen to respire, anaerobic bacteria can survive without presence of oxygen, and facultative bacteria either utilize oxygen or even they can live without oxygen

1.4.3 Shape

They can be rod shaped, circular, comma or spiral shaped bacteria.

1.5 Most common bacteria and their infections

1.5.1. Escherichia coli

E. coli is rod shaped, facultative aerobic, Gram-negative bacteria they are the most diverse and large group of bacteria that are present everywhere in environment.

1.5.1.1. E. coli infections

E. coli strains are very common and present in everywhere they can be very harmful and can cause many disease problems such as diarrhea, abdominal pain, pneumonia, food poisoning and urinary tract infections when they are taken from raw food. [1]

One strain of *E. coli* O157:H7 is very harmful and can cause serious problems such as bloody diarrhea, abdominal pain and vomiting in children it can cause kidney failure and life threatening symptoms are also caused by it fever, confusion and bleeding. [2, 3]

Some *Escherichia coli* produce toxin termed as Shiga it infects lining of intestine and damages it. [4, 5]

1.5.2. Enterobacter aerogenes

Enterobacter aerogenes are rod shaped, Gram -ve , nonmotile, facultatively anaerobic bacteria that causes nosocomial and opportunistic infections . Gastrointestinal tract is favorite place for *Enterobacter aerogenes* to live it can survive also in environment and is present at different surfaces and in soil also. [6]

E. aerogenes are mostly resistant to drugs for example ciprofloxacin resistant *E. aerogenes*, multi drug resistant *E. aerogene* [7] . Beta lactamase secreted by these bacteria will open ring of beta lactam antibiotics and thus causing resistance to wide range of beta lactam antibiotics such as cephalosporin and imipenem, genetic element integron of these bacteria also have antibacterial resistance against aminoglycosides

1.5.2.1. Enterobacter aerogenes infections

E. aerogenes mostly cause gastrointestinal infection, heart infections, urinary tract infections, septic arthritis, osteomyelitis, eye, skin and tissue infections in unhealthy persons.

1.5.3. Klebsiella pneumoniae

K. pneumoniae present in nasopharynx is a rod shaped, nonmotile, encapsulated, Gram-negative bacteria that causes pneumoniae. Capsule presence is the major virulence factor of this bacteria which causes it to be drug resistant.

1.5.3.1. *Klebsiella pneumoniae* infections

Klebsiella pneumoniae causes two types of pneumoniae, Hospital acquired, and community acquired pneumoniae. *K. pneumoniae* along with pneumonia causes necrosis and inflammation of tissues thus sputum produced upon cough is currant jelly while by *S. pneumonia* rust colored sputum is produced by the patient. Ventilated patients have more chances of getting pneumonia as compare to nonventilated patient.[8]

Lung abscesses, bacteremia, empyema (collection of pus in body) are some more infections caused by *K. pneumoniae*.[9]

1.5.4. *Proteus vulgaris*

Proteus vulgaris are motile, aerobic ,gram negative rods type bacteria. They are found in gastrointestinal tract of humans so cause urinary tract infections[10], other infections caused by this bacteria are wound, bloodstream, burn and respiratory tract infections, and is multidrug resistant. [11]

1.5.5. *Streptococcus pneumoniae*

Strepto means chain ,it is cocci type bacteria it is major cause of community acquired infections and causes diseases in both children and adults[12], respiratory tract infections are caused by it syndromes[13, 14] are also major cause of this bacteria it is drug resistant so infections are difficult to control.

1.5.6. *Streptococcus pyogenes*

Streptococcus pyogenes is a nonmotile cocci type bacteria. In addition to causing skin infections and upper respiratory tract infections these bacteria are also responsible for systemic infections [14]. They can survive on a dry surface from 3 days to 7 months.

1.5.7. *Pseudomonas aeruginosa*

Motile, aerobic, Gram-negative rod shaped bacterium .*Pseudomonas aeruginosa* name depicts properties of this bacteria, *Pseudomonas* means false unit, *aeruginosa* means copper rust this is based on its blue green color when it is cultured in laboratory pyoverdine and pyocyanin are the two metabolites on the basis of which they show blue-green color. In absence of pyocyanin, pyoverdine show yellow florescent color, Cyanin means blue, Verdine means green and Pyo means pus.

1.5.5.1. *Pseudomonas aeruginosa* infections

P. aeruginosa has resistance to large number of drugs which causes very difficulties but are not resistant to fluoroquinolones. *P. aeruginosa* is opportunist and hospital acquired infection and thus causes disease in low immunity person but does not affect healthy person. [15]

Septic shock: septic shock is mostly caused by this bacterium in patient with low immunity due to less amount of white blood cells

Gastrointestinal infection: these infections mostly occurs in new born.

Pneumonia: it occurs in cystic fibrosis patients.

Tissues and skin infections: it occurs when skin burns.

1.6 Role of Surface contamination in bacterial infections transmission

Bacteria form biofilm on different surfaces this biofilm show resistance to various antibiotics that increases the spread of infections so there is a need of modified surfaces to control bacterial population. [16] Bacteria have tendency to attach to any kind of surface after their attachment to a surface bacteria form colony in which a number of bacterial species get attached on surface of other bacteria and start growing this multilayer bacterial colony protected by extracellular polymeric matrix is called biofilm, after maturity of bacterial colony bacteria start dispersing into environment. [17]

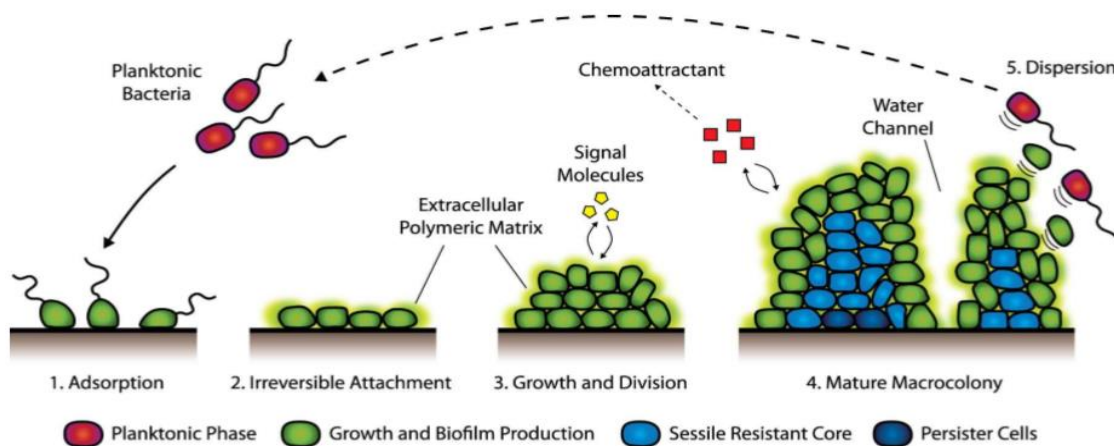


Figure 1.3 Bacterial infections through surfaces

Bacteria can reside on surfaces for longer period for example klebsiella species can reside on surface from 2 hours to 30 months and then from surfaces they are transmitted to person through contact with surface or the dispersal of bacteria from surface to environment.[18-21]

1.7 Hospitals Acquired Bacterial Infections

Hospitals are the major source for transmission of bacterial infections these needs to be addressed.[22]Hospitals, schools, ATM and other public places surfaces are contaminated with bacteria and most commonly hospitals[23] are the main cause of bacterial transmission from one person to another person. Sanitization, sterilization, disinfection help in control of germs but it is difficult to do all such practices on regular basis so surface must be made antibacterial in order to control bacterial infections. In hospitals due large scale use of antibiotics [24]and other health care related practices most common pathogens are antibiotic resistant.[25]

Hands of doctors and other health care workers are the major source of transmission of bacterial infections.

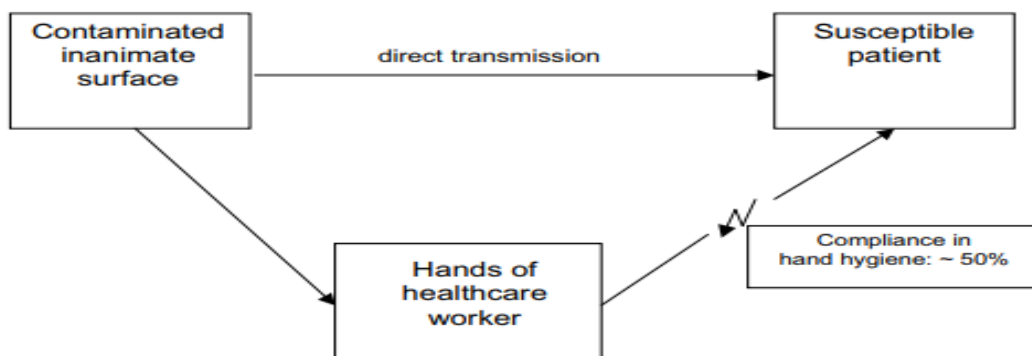


Figure 1.4 Role of hands in bacterial in bacterial infection transmission

1.8 Measures to control bacterial infections:

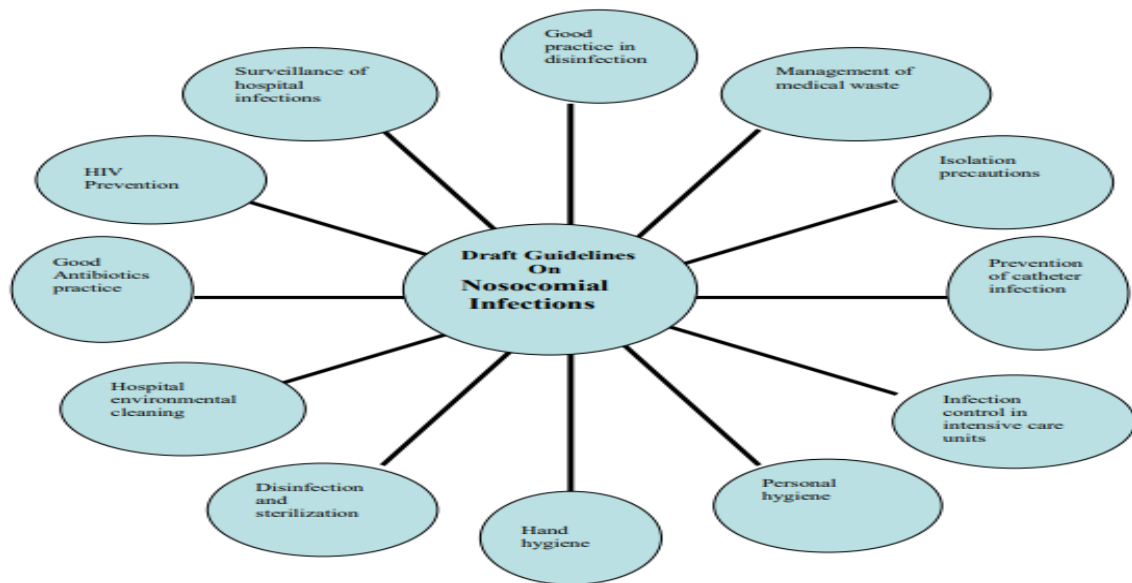


Figure 1.5 Measures to control bacterial infections

1.8.1.Prevention is better than cure, Skin is largest organ of humans and the diverse range of microorganism colonize our skin, disruption in balance between human and microorganism can cause serious infections and spread from one person to other, washing hands with sanitizer as hands are the most social part of our body and the major cause of germ spread sanitizer mostly contain alcohols, antimicrobial peptides or probiotic which can be living or dead as composition but sanitizer just kill the germs after direct contact. [26]

1.8.2.Sterilization: By the application of high pressure, temperature, heat and irradiation control of bacterial and other germs is termed as sterilization [27, 28] sterilization is the oldest known technique to control bacteria.

1.8.3.Disinfectants: They kill bacteria either by cell wall destruction or by disturbing the metabolism of bacteria, but they cannot kill the resistant bacteria and they kill bacteria present on nonliving objects. Most commonly used disinfectants[29] are Chlorine and Chlorine based disinfectants such as hypo-chlorites but they undergo oxidation and corrosion[30], Quaternary Ammonium based ionic liquids have been most commonly used as disinfectant , niacinamide and its derivatives are also good antimicrobial and can be used in disinfectant[31] but bacteria are becoming resistant to disinfectant[32]

1.8.4.Antibiotics are most commonly used for destroying bacteria inside living organisms.[33] Many antibiotics are being utilized to cure bacterial infections[34] but bacteria are gaining

resistance to these antibiotics day by day [35]there is a need to control these bacteria from there access route especially from public places.

1.8.5.Antibacterial surfaces: Public places like school, offices, hospitals are the most common routes for bacteria to be transmitted from one person to another and causing diseases in them it is very difficult to sanitize and disinfect these places on regular basis so there must be a solution to control bacterial infection from these places within less time and cost effectively without any further harmful effects, for centuries Silver, Copper, copper alloys, titanium, quaternary compounds are being utilized for making different most commonly used products and on surfaces due to antibacterial activity against most commonly occurring bacteria which help to control these infections.[36]

1.8.6.Antibacterial paint: To resolve issue of bacterial infection of public places antibacterial paint is a helpful, long lasting, easy way. With help of paint bacteria will be killed from atmosphere and will not be able to be transmitted to next host. Paint already synthesized are nanoparticles based paint but due to high cost and release of toxic nanoparticles limit the application of paint. Silver[37], Molybdenum, copper [38, 39]and Titanium [40-43]are some of the nanoparticles that due to their antibacterial activity have already been used in paint.

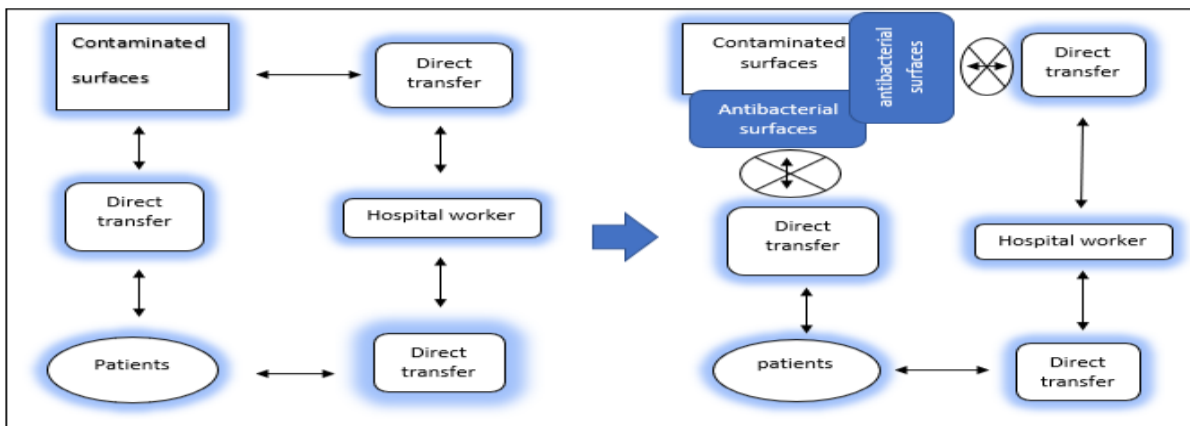


Figure 1.6 Control of infections by antibacterial surfaces

1.9 Ionic liquids and properties of ionic liquids:

Ionic liquids are molten salts that contain ions Ionic liquids have various properties due to which they can be utilized as an antibacterial additive in paints with the most useful of their antibacterial property due to toxic nature.

- Melting point:

Melting point of ionic liquids is less than 100⁰C and most of ionic liquids are liquid at room temperature.

- Viscosity:

Ionic liquids are more viscous as compare to other organic solvents due to van der Waal's forces of attraction and hydrogen bonding, their viscosity also depends on the chain length of alkyl group attached to cation.

- Density:

Ionic liquids are denser as compare to water.

- Solubility:

Cationic part of ionic liquid is hydrogen bond donor and anionic part is hydrogen bond acceptor so ionic liquids have both of donating and accepting properties, solubility of ionic liquid depends on anionic part and structure of cation, ionic liquids are soluble in most of the solvents.

- Thermal stability:

Highly thermal stable and can bear high temperature without being decomposed.

- Vapor pressure:

Ionic liquids have negligible vapor pressure and so does not contribute to air pollution.

- Antibacterial , Antibiofilm and Anticorrosive nature:

Bacteria form biofilm on different surfaces this biofilm show resistance to various antibiotics that increases the spread of infections so there is a need of antibacterial surface which can control bacterial population and ionic liquids have antibiofilm and anticorrosive properties due to which it can be used as antibacterial additive in paints. ionic liquids are also very toxic so have antibacterial property.[44]

Chapter 2

2. LITERATURE REVIEW

Different papers have been published to draw attention towards the problem of bacterial infections which are spreading around the world day by day and causing worse effects on human health along with an economic burden on a country[45, 46].

Annually millions of people worldwide are affected by bacterial infections most of these infections are antibiotic resistant in hospitals most of the bacterial diseases are treated with antibiotics so their regular use kills some bacteria with the survival of antibiotic resistant bacteria which then spread to next host causes diseases in the healthy person. Most of antibacterial surfaces contain copper and other inorganic nanoparticles such as silver, zinc, chlorides, Titanium, Quaternary ammonium polymer and antibiotics as an antibacterial agent but these coatings cause emission of the compounds which are bioactive and their emission into atmosphere cause health problems to not only humans but also to beneficial microorganisms and live stocks [47, 48]

2.1. Nanoparticles based antibacterial paint

Khaydarove *et al* synthesized silver nanoparticles by electrochemical method and utilized it in paint in water bodies to kill bacteria and fungus they observed that smaller the size of silver nanoparticle the more it has antibacterial property size distribution of their silver nanoparticles was 2 to 20 nm and average size was 7nm and minimum inhibitory concentration (MIC) mg/ml demerits of using silver in water based paints are cytotoxicity which increases as nanoparticles agglomerate.[49]

Strains	MIC mg/l
E. coli	3
B. subtilis	19
S. aureus	2

Table 2.1 Minimum Inhibitory Concentration of Silver Nanoparticles for water based paint Silver and gold nanoparticles embedded in alkylated resin have been used by Kumar *et al* in research as an antibacterial paint and synthesized by autooxidation or drying process S. aureus

and E.coli were tested for antibacterial activity of these nanoparticles multidrug resistant bacterial strains were not considered in this research. size of Ag Np were 12-14 nm and larger sized particles were 10-30 nm while size of Au Np were 11-25 nm overnight incubation kills bacteria on Ag Np and Au Np based paint. [50]

Silver vanadate nanostructures have been used in water based paint as an antibacterial additive by R.D. Holtz spherical silver nanoparticles size was 5 to 40 nm, their MIC values for different strains microgram per milliliter were:-

Strains	MIC $\mu\text{g/ml}$
Enterococcus faecalis	5.00
Staphylococcus aureus	3.15
MRSA	3.15
Salmonella enterica Typhimurium	3.15
Escherichia coli	1.00

Table 2.2 Minimum Inhibitory Concentration of Silver vanadate based paint

Silver vanadate based paint show 4mm zone of inhibition, although there is no agglomeration of silver nanoparticles but still there is a problem of leaching of silver nanoparticles into atmosphere. [51]

Most work done so far on antibacterial paint is on nanoparticle based paint, silver nanoparticles have an antibacterial property and have been utilized in paint industry as antibacterial additive in antibacterial paint but due to high cost and due to release of these nanoparticles which causes cytotoxic and genotoxic effects on human health their use is dangerous[52, 53]

Karthikeyan Krishnamoorthy et al synthesized Alkyl resin binded Molybdenum oxide (MoO_3) nanoplates by ball milling process and these nanoparticles were used in antibacterial paint examination that was not based on aqueous environment. MoO_3 based paint show time dependent antibacterial activity and show resistance to S. aureus 91%, P. aeruginosa 88%, K. pneumoniae 90% and E.coli 91% after 48 hours of incubation so 48 hours were necessary for showing the maximum antibacterial activity of these nanoparticles.[54]

Strains	MIC $\mu\text{g/ml}$
S. aureus	16
P. aeruginosa	8
K. pneumoniae	32
E.coli	8

Table 2.3 Minimum Inhibitory Concentration of molybdenum oxide based paint

Combination of nanoparticles have also been used in paint industry such as titanium dioxide and copper combinedly have been utilized as antibacterial additive in paint this combination have been employed to decrease the release of nanoparticles into atmosphere but even though copper releases into atmosphere[55]

Copper and copper oxide have also been utilized in paint industry due to antibacterial property but the problem is same the release of copper ion into atmosphere which causes toxic effect to humans[56]

Zinc oxide have an antibacterial property and was utilized in paint industry by Ying chen *et al*, hydrogen bond formation of zinc oxide over silica surface was formed by hydrothermal process to avoid the agglomeration of nanoparticles and to reduce their size. Characterization techniques SEM and TEM show particle size of 3 -8 nanometer.

MIC mg/ml	E.coli
ZnO	20
ZnO-SiO ₂ pH 5	1.60
ZnO-SiO ₂ pH 7	2.14

Table 2.4 Minimum Inhibitory Concentration of zinc oxide based paint

With 8% ZnO-SiO₂ pH 7 in coating antibacterial activity was 90.4 %.[57]

Most of review articles have been published are on hospital acquired infections control with help of antibacterial coatings C.P. Dune *et al* published a review article on the infection acquired in hospitals they that there is a need of another method to prevent infections in addition to use of disinfectant, cleaning and antibiotics and found antimicrobial coating to be an effective method for this purpose European commission form a the network AMiCI to research on the use of antimicrobial coating in prevention of healthcare acquired infections, their composition , environmental impact, new cleaning processes and antimicrobial resistance.[58]

M.P. Muller *et al* reviewed after selection 11 studies on copper, organo-silane, metal-alloy and silver coated surfaces and their antibacterial effect and the result of review was that copper surfaces harbor less bacteria as compared to non-copper surfaces [59]

A. Abbaszadegan *et al* work on silver nanoparticles coated with ionic liquids, ionic liquids they used were pyridinium and imidazolium with 12 and 18 alkyl chain length. Silver nanoparticles have antibacterial activity but also are cytotoxic and aggregate after some time interval with reducing antibacterial activity, to reduce cytotoxicity of silver nanoparticles they coated it with ionic liquids and to avoid aggregation large alkyl chain of ionic liquids were used as alkyl chains and silver nanoparticles will have higher repulsion with increase of intermolecular distance resulting in decreasing aggregation.

Ag NP _s coating	Average size (nm)	MIC ₉₀	Cell viability
C ₁₈ Im	8.6 nm	8.1x10 ⁻⁹	102.099%
C ₁₂ Im	9.0 nm	7.1x10 ⁻⁹	106.613%
C ₁₈ py	6.71 nm	8.5x10 ⁻⁹	99.1489%
C ₁₂ py	18.49 nm	8.1x10 ⁻¹⁰	97.6678%

Table 2.5 Minimum Inhibitory Concentration of Imidazolium coated Silver Nanoparticles
Imidazolium coated silver nanoparticles have highest antibacterial activity against *E. faecalis* with lowest cytotoxic effects but this is costly to use silver nanoparticles along with ionic liquids.[60]

2.2. Ionic liquids antibacterial activity

K.M. Docherty *et al* synthesized and checked antimicrobial activity for six ionic liquids 1-Butyl-3-methyl imidazolium bromide, 1-Octyl-3-methyl imidazolium bromide, 1-hexyl-3-methyl imidazolium bromide, Butyl pyridinium bromide, hexyl pyridinium bromide, octyl pyridinium bromide against *E. coli*, *B. subtilis* and *S. aureus*. [61]

O.F. Doria *et al* synthesized different N Cinnamyl imidazole containing chain lengths of 1, 6, 8 and 10 carbon and studied their antibacterial activity in terms of minimum inhibitory concentration against *E. coli*, *P. aeruginosa*, *S. pyogenes*, *S. aureus*, *S. epidermidis*. [62]

H. Hajfarajollah *et al* checked antibacterial and antiadhesive properties of butyl[BMIM]NO₃, [BMIM]SCN, [BMIM]MeSO₃, [BMIM]PF₆, [BMIM]HSO₄, [BMIM]BF₄ and [BMIM]Tf₂N among these ionic liquids of same chain length [BMIM]HSO₄ and [BMIM]Tf₂N were most

antibacterial not all of them were antiadhesive but most of them show antiadhesive property [63]

S Anvari *et al* Studied antibacterial and antiadhesive activity of various ionic liquids of pyridinium and imidazolium with hexyl and octyl chain with different anions against strains of *B. subtilis*, *E. coli*, *K. pneumoniae*, *S. aureus* and *S. typhimurium* and found that octyl chain imidazolium and pyridinium have high antibacterial activity as compare to hexyl chain ionic liquids .[64]

Z. Zheng *et al* synthesized Different 1-alkyl-3-vinyl imidazolium bromide monomer and polymer checked the antibacterial activity against *E. coli* and *S. aureus* and found that antibacterial activity has direct relation with alkyl chain length found no correlation between monomer and polymer [65]

J.Pernak *et al* synthesized series of ionic liquids 3-alkoxymethyl-1-methyl imidazolium chloride, tetrafluoroborate and hexafluorophosphate containing 3 to 16 alkyl chain. And studied the antibacterial activity of these ionic liquids against cocci, rods and Fungi and found result that ionic liquids with 10,11,12 and 14 carbon atom in alkoxy group show high antibacterial activity. [66]

D.Demberelnyamba *et al* for disinfectant use synthesized 3 series 1 alkyl-3-methylimidazolium chloride and bromide, 1alkyl-2-methyl-3-hydroxyethyl imidazolium chloride, N-alkyl N-hydroxy ethyl pyrrolidinium and checked their MIC value against salmonella typhimurium, *S. aureus*, *B. subtilis*, *E. coli*, *candida albicans* and found high antibacterial activity for longer chain imidazolium and hydroxy imidazolium. [67]

Phosphonium based ionic liquids have been synthesized A.C. Rosłonkiewicz anions used were halide, bis(tri-fluoromethanesulphonyl) imide, trifluoromethanesulphonate, dicynamide, nitrate, tetrafluoroborate with alkyl trihexyl cation with pentyl to decyl groups show good antibacterial activity against cocci.[68]

2.3. Drug derived ionic liquids and their antibacterial activity

N. Iwai synthesized imidazolium, pyrrolidinium and piperidinium with propargyl and silyl alkyl groups of different chain length and studied their antibacterial activity against *E. coli*, *B. subtilis*, *S. aureus*. They found that 3-pentylpropargyl and silyl alkyl show good antibacterial properties. [69]

Quaternary ammonium lactate ionic liquids, Didecylmethyl ammonium (DDA) and benzalkonium (BA) lactates were synthesized by J.Cybulsk *et al* their antibacterial activity was found to be more as compare to Quaternary ammonium chloride against streptococcus mutans but have oral toxicity.[70]

BA and DDM ammonium with anions saccharinate and acesulfamate were synthesized by W.L.Hough-Troutman *et al* although they were antibacterial but have oral toxicity and their MIC value was much higher as compare to chloro derivatives[71]

J. cybulski *et al* synthesized BA and DDM ammonium ionic liquids with anions mendalates and proline, DDM proline was most antibacterial and antifungal[72]

F. Walkiewicz *et al* synthesized azolate based tetraammonium ionic liquids, Anions used were 4-nitroimidazolate [4-NO₂Im], Benzotriazolate [Bt], 2-methyl-4-nitroimidazolate [2-Me-4-NO₂Im], 1,2,4-triazolate[Tr] shown in fig. 2.1 and cation used were hexadecyltrimethylammonium [CTA], domiphen [DOM], DDA and BA. shown in fig. 2.1 and found good antibacterial activity for these ionic liquids.[73]

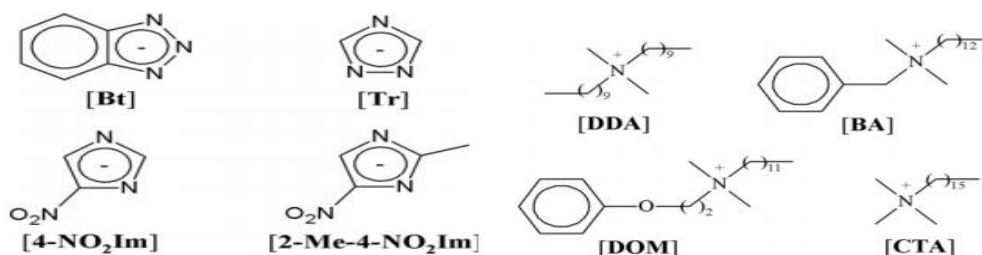


Figure 2.1 azolate based tetraammonium ionic liquids structures

K.N. Ibsen have synthesized ionic liquids based on combination of choline and geranate and report that it is less toxic and more effective as compare to either of the antibiotic alone they treat E.coli with CAGE several times and found it to be powerful antibacterial agent against infections when concentration was 25 mM. [74]

R.J.V.Ferraz worked on drug derived ionic liquids and their antibacterial and antitumor properties ampicillin, Amoxicillin, penicillin G based ionic liquids were synthesized by ion exchange method. These drug derived ionic liquids show good antibacterial properties [75]

Paints available in market

BioCote paints are available and they utilize silver as an antibacterial additive.

Dulux water based acrylic paint is also an antibacterial paint.

Sherwin-William introduces a paint which according to them can kill germs of hospitals the company claims that bacteria are killed within the exposure limit of 2 hours but the paint has a side effect on human health it contains quaternary ammonium compounds as bioactive agent.[76, 77]

2.4. Research work aims

- This research study aims at resolving issue of bacterial infection at hospitals, schools, offices, homes and industries.
- This study is worth investigating as Ionic liquids have been synthesized and used in paint industry, ionic liquids based paint provide protection from bacteria and help to control infections spread.
- Different characterization techniques used for the confirmation of product formation were :Thin layer chromatography, Infra-red spectrometry and Nuclear magnetic resonance spectrometry.
- Determination of Antibacterial activity of ionic liquids
- Formulation of antibacterial paint based on ionic liquids.

Chapter 3

3. EXPERIMENTAL

This chapter includes synthesis of different ionic liquids in lab ,at first step bromide type ionic liquids were synthesized then bromide anion was replaced with different anions, that were Methanesulphonate $[\text{CH}_3\text{SO}_3]^-$,Dichloroacetate $[\text{CHCl}_2\text{CO}_2]^-$,Tetrafluoroborate $[\text{BF}_4]^-$,Bis(trifluoromethane-sulfonyl)imide $[\text{Tf}_2\text{N}]^-$,Hydrogen sulphate $[\text{HSO}_4]^-$.

3.1 Solvents and chemicals

All solvents were dried with help of distillation assembly different solvents used were: Methanol (CH_3OH), Chloroform (CHCl_3), Acetonitrile (CH_3CN), n-Hexane, Ethyl acetate and Distilled water.

Chemicals were:1-Methyl imidazole (I), Pyridine(II), Tri-octyl phosphine(III), Diethyl amine(IV), Butyl Bromide(V), Octyl bromide(VI), Methane sulphonic acid(VII), Dichloroacetic acid (VIII), potassium hydrogen sulphate, Lithium Bis(trifluoromethane-sulfonyl)imide, sodium tetrafluoroborate and Sodium hydroxide(IX).

3.2 Apparatus and Glassware

Weighing balance, Vacuum oven, Vacuum pump, Fume hood, Hot plates, Nitrogen cylinder, Drying oven, pH papers and pH meter, Filter paper , Rotary Evaporator, Clamps and stands, TLC plates.

Beakers, conical flasks, 2 neck and single neck Round bottom flasks, Condenser, Rubber stoppers, Magnetic stirrer, Glass vials, Reagent bottles, Distillation assembly, Spatula, Pipettes, Thermometer, Oil bath, Measuring cylinder, Nitrogen balloons, Funnel, Syringes, Eppendorf tubes, Capillaries.

3.3 Experimental procedure

Different anions used were

- Sodium Methane sulphonate $\text{Na}[\text{CH}_3\text{SO}_3]$ (X)
- Lithium Bis(trifluoromethane-sulfonyl)imide $\text{Li}[\text{Tf}_2\text{N}]$ (XI)
- Sodium Dichloroacetate $\text{Na}[\text{CHCl}_2\text{CO}_2]$ (XII)
- Sodium Tetrafluoroborate $\text{Na}[\text{BF}_4]$ (XIII)

- Potassium Hydrogen sulphate $K[HSO_4]$ (XIV)

Sodium salt of Methane sulphonate and Dichloroacetate were synthesized while salts of Bis(trifluoromethane-sulfonyl)imide, Tetrafluoroborate and Hydrogen sulphate were purchased.

Different cations used were

- 1-Octyl-3-methylimidazolium bromide(XV)
- 1-Butyl- 3-methylimidazolium bromide(XXI)
- 1-Octyl pyridinium bromide (XXVII)
- 1-Butyl pyridinium bromide(XXXIII)
- 1-Butyl tri octyl phosphonium bromide(XXXIX)
- Diethyl dibutyl ammonium bromide(XLV)

All cations were synthesized

Synthesis of ionic liquids

3.3.1. Synthesis of Sodium Methanesulphonate (X)

3.3.2. Synthesis of Sodium Dichloroacetate (XII)

3.3.3. 1-Methyl-3-octylimidazolium bromide Synthesis $[C_8mim]Br$ (XV)

3.3.4. 1-Methyl-3-octylimidazolium Methane sulphonate $[C_8mim][CH_3SO_3]$ (XVI)

Synthesis

3.3.5. 1-Methyl-3-octylimidazolium Bis(trifluoromethane-sulfonyl)imide $[C_8mim][Tf_2N]$ (XVII) Synthesis

3.3.6. 1-Methyl-3-octylimidazolium Dichloroacetate $[C_8mim][CHCl_2CO_2]$ (XVIII) Synthesis

3.3.7. 1-Methyl-3-octylimidazolium Tetrafluoroborate $[C_8mim][BF_4]$ (XIX) Synthesis

3.3.8. 1-Methyl-3-octylimidazolium Hydrogen sulphate $[C_8mim][HSO_4]$ (XX) Synthesis

3.3.9. 1-Methyl- 3-butylimidazolium bromide Synthesis $[C_4mim]Br$ (XXI)

3.3.10. 1-Methyl- 3-butylimidazolium Methane sulphonate $[C_4mim][CH_3SO_3]$ (XXII) Synthesis

- 3.3.11. 1-Methyl- 3-butylimidazolium Bis(trifluoromethane-sulfonyl)imide[C₄mim][Tf₂N] (XXIII) Synthesis
- 3.3.12. 1-Methyl- 3-butylimidazolium Dichloroacetate [C₄mim][CHCl₂CO₂] (XXIV) Synthesis
- 3.3.13. 1-Methyl- 3-butylimidazolium Tetrafluoroborate [C₄mim][BF₄] (XXV) Synthesis
- 3.3.14 1-Methyl- 3-butylimidazolium Hydrogen sulphate [C₄mim][HSO₄] (XXVI) Synthesis
- 3.3.15 Octyl pyridinium bromide [C₈py]Br(XXVII) Synthesis
- 3.3.16. Octyl pyridinium Methane sulphonate [C₈py][CH₃SO₃] (XXVIII) Synthesis
- 3.3.17. Octyl pyridinium Bis(trifluoromethane-sulfonyl)imide [C₈py][Tf₂N] (XXIX)Synthesis
- 3.3.18. Octyl pyridinium Dichloroacetate [C₈py][CHCl₂CO₂]] (XXX)Synthesis
- 3.3.19. Octyl pyridinium Tetrafluoroborate [C₈py][BF₄]] (XXXI)Synthesis
- 3.3.20. Octyl pyridinium Hydrogen sulphate [C₈py][HSO₄]] (XXXII)Synthesis
- 3.3.21. Butyl pyridinium bromide [C₄py]Br] (XXXIII) synthesis
- 3.3.22. Butyl pyridinium Methane sulphonate [C₄py][CH₃SO₃] (XXXIV) Synthesis
- 3.3.23. Butyl pyridinium Bis(trifluoromethane-sulfonyl)imide [C₄py][Tf₂N] (XXXV) Synthesis
- 3.3.24. Butyl pyridinium Dichloroacetate [C₄py][CHCl₂CO₂] (XXXVI) Synthesis
- 3.3.25. Butyl pyridinium Tetrafluoroborate [C₄py][BF₄] (XXXVII) Synthesis
- 3.3.26. Butyl pyridinium Hydrogen sulphate [C₄py][HSO₄] (XXXVIII) Synthesis
- 3.3.27. Tri-octyl mono-butyl phosphonium bromide [P_{4 8 8 8}]Br (XXXIX) Synthesis
- 3.3.28. Tri-octyl mono-butyl phosphonium Methane sulphonate [P_{4 8 8 8}][CH₃SO₃] (XL) Synthesis
- 3.3.29. Tri-octyl mono-butyl phosphonium Bis(trifluoromethane-sulfonyl)imide [P_{4 8 8 8}][Tf₂N] (XLI) Synthesis
- 3.3.30. Tri-octyl mono-butyl phosphonium Dichloroacetate [P_{4 8 8 8}][CHCl₂CO₂] (XLII) Synthesis

3.3.31. Tri-octyl mono-butyl phosphonium Tetrafluoroborate [P_{8 8 8}][BF₄] (XLIII) Synthesis

3.3.32. Tri-octyl mono-butyl phosphonium Hydrogen sulphate [P_{8 8 8}][HSO₄] (XLIV) Synthesis

3.3.33. Diethyl dibutyl ammonium bromide [N_{2 2 4 4}]Br (XLV) Synthesis

3.3.34. Diethyl dibutyl ammonium Methane sulphonate [N_{2 2 4 4}][CH₃SO₃] (XLVI) Synthesis

3.3.35. Diethyl dibutyl ammonium Bis(trifluoromethane-sulfonyl)imide (XLVII)

[N_{2 2 4 4}][Tf₂N] Synthesis

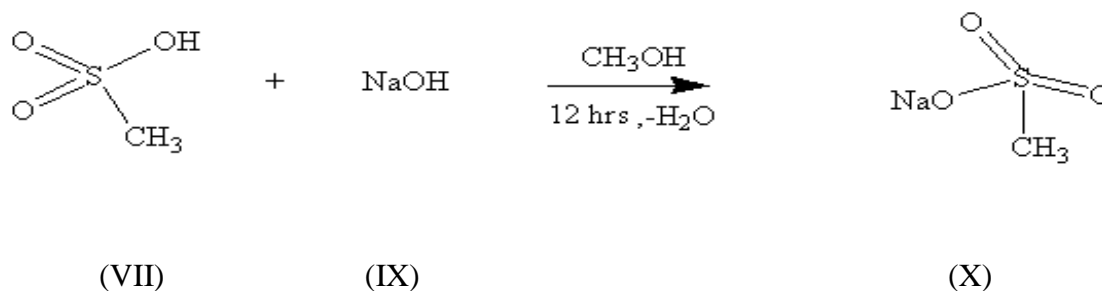
3.3.36. Diethyl dibutyl ammonium Dichloroacetate [N_{2 2 4 4}][CHCl₂CO₂] (XLVIII) Synthesis

3.3.37. Diethyl dibutyl ammonium Tetrafluoroborate [N_{2 2 4 4}][BF₄] (IL)Synthesis

3.3.38. Diethyl dibutyl ammonium Hydrogen sulphate [N_{2 2 4 4}][HSO₄] (L) Synthesis

3.3.1. Synthesis of Sodium Methanesulphonate

Sodium Methanesulphonate was obtained when Methanesulphonic acid (2 g, 20.8 mmol) was neutralized with sodium hydroxide (0.8 g, 20 mmol) in methanol (60ml) (scheme 3.1). Although neutralization occur instantaneously even though reaction mixture was stirred overnight, reaction completion was confirmed with help of pH paper. Methanol and water produced from reaction were rotary evaporated and product was kept in vacuum oven overnight at 50°C to completely dry the product, product obtained was white powder with 99% yield.

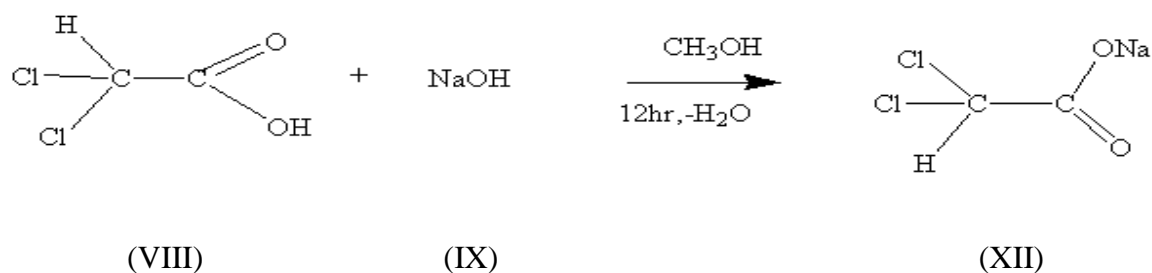


Scheme 3.1

3.3.2. Synthesis of Sodium Dichloroacetate

Sodium Dichloroacetate was synthesized from neutralization reaction of dichloroacetic acid (2g, 15.6mmol) with sodium hydroxide (0.62 g, 15.5mmol) in 60ml methanol (scheme 3.2). Reaction mixture was stirred in methanol overnight, reaction completion was confirmed with

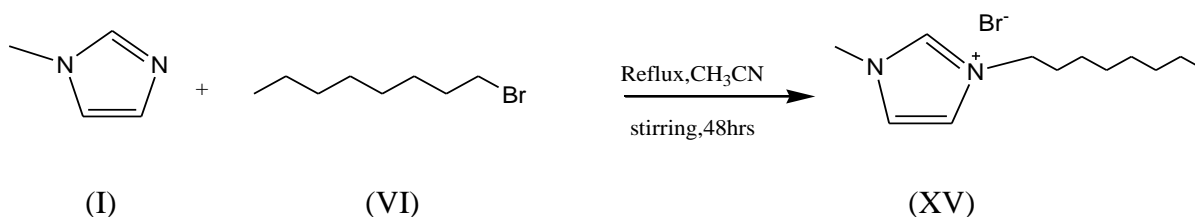
help of pH paper. Water produced during neutralization reaction and methanol were rotary evaporated, product was completely dried in vacuum oven overnight at 50°C to obtain white powder of sodium dichloroacetate with 99% yield.



Scheme 3.2

3.3.3. 1-Methyl-3-octylimidazolium bromide synthesis

1-Methyl-3-octylimidazolium bromide was synthesized by reacting 1 Methyl imidazole (5 g, 60 mmol) with octyl bromide (11.74 g, 61 mmol) in acetonitrile (60ml) (scheme 3.3). Reaction mixture was refluxed for 48 hours to obtain maximum yield of product reaction completion was confirmed with help of TLC, solvent was rotary evaporated, reactants were decanted to obtain pure product, product obtained was further dried with vacuum oven for 12 hours at 50°C product obtained as a yellow oily liquid with 81% yield.

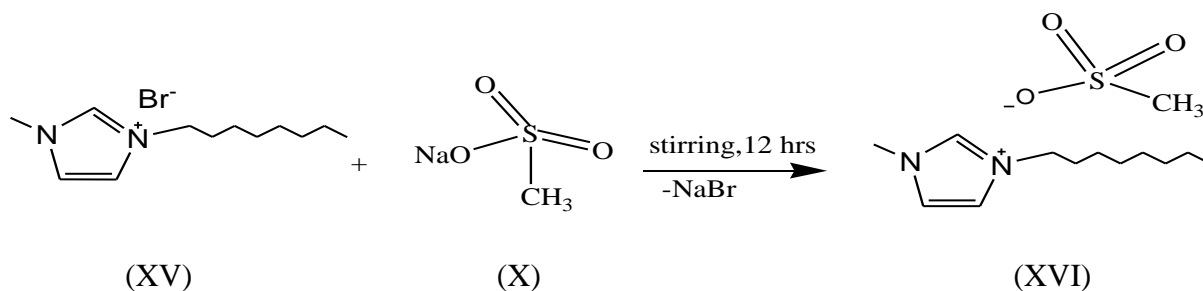


Scheme 3.3

3.3.4. 1-Methyl-3-octylimidazolium methanesulphonate synthesis

Metathesis reaction of 1-Methyl-3-octylimidazolium bromide (2.75 g, 10 mmol) and sodium methanesulphonate (4 g, 11.76 mmol) results in the synthesis of 1-Methyl-3-octylimidazolium methanesulphonate in methanol (60ml). Reaction mixture was stirred overnight at room temperature (Scheme 3.4). After completion of reaction solvent was evaporated with rotary evaporator and sodium bromide was separated with help of solvent extraction. Several fractions of chloroform and ethyl-acetate were collected by filtration containing product excluding

sodium bromide on filter paper solvent were evaporated to obtain dry product, product was further dried at 50°C in vacuum oven with yield of 71%.

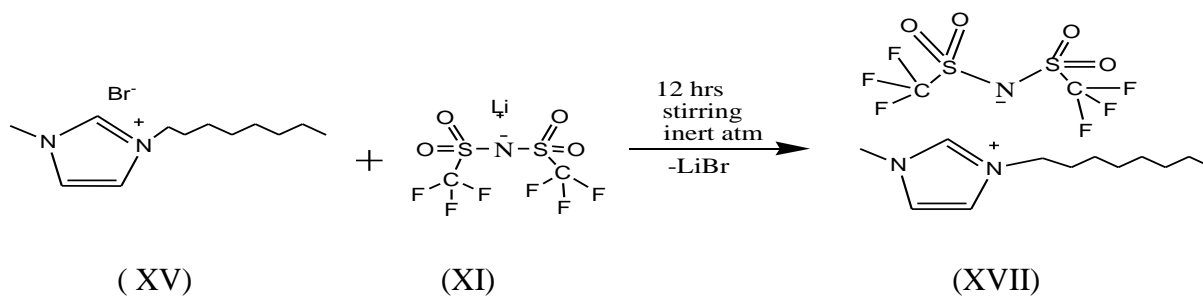


Scheme 3.4

3.3.5. 1-Methyl-3-octyl-imidazolium Bis(trifluoromethane-sulfonyl)imide

[C₈mim][Tf₂N] synthesis

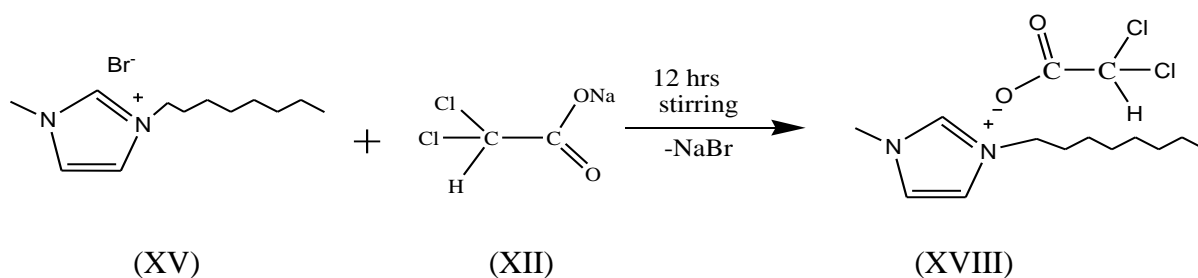
[C₈mim]Br (0.3 g, 1mmol) was dissolved in to form a solution and Li[Tf₂N] (0.313 g, 1.1mmol) solution was prepared in 2neck RB flask and was evacuated to remove air and an inert atmosphere was created in the RB flask then [C₈mim]Br solution was added into RB flask. The reaction mixture in methanol (60ml) was stirred(Scheme 3.5) at room temperature for overnight after reaction completion methanol was evaporated and LiBr was removed with help of solvent extraction and filtration. Solvent was evaporated to obtain pure product which was further completely dried in vacuum oven over night at 40°C with yield 75%.



Scheme 3.5

3.3.6. 1-Methyl-3-octylimidazolium dichloroacetate [C₈mim][CHCl₂CO₂] synthesis

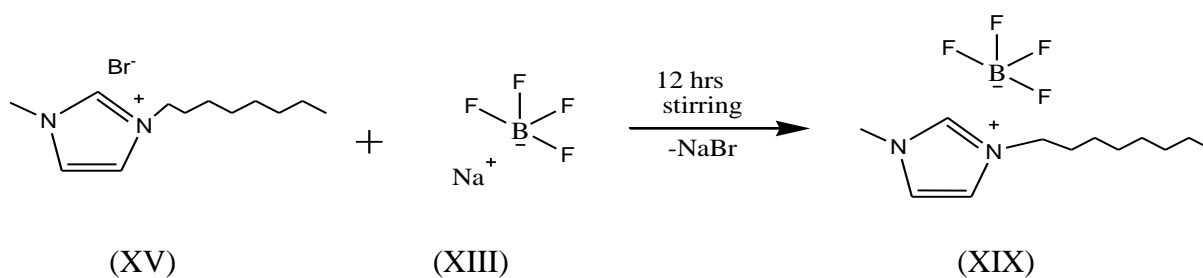
[C₈mim]Br (0.5 g , 12 mmol) solution was slowly added into Na[CHCl₂CO₂] (0.3 g, 2 mmol) solution and stirred overnight in acetonitrile (60ml) at room temperature to obtain product [C₈mim][CHCl₂CO₂] (scheme 3.6). Product was separated through filtration and solvent was evaporated , remaining NaBr was separated with solvent extraction and filtration, filtrate was dried to obtain pure product with 96% yield.



Scheme 3.6

3.3.7. 1-Methyl-3-octylimidazolium tetrafluoroborate[C₈mim][BF₄] synthesis

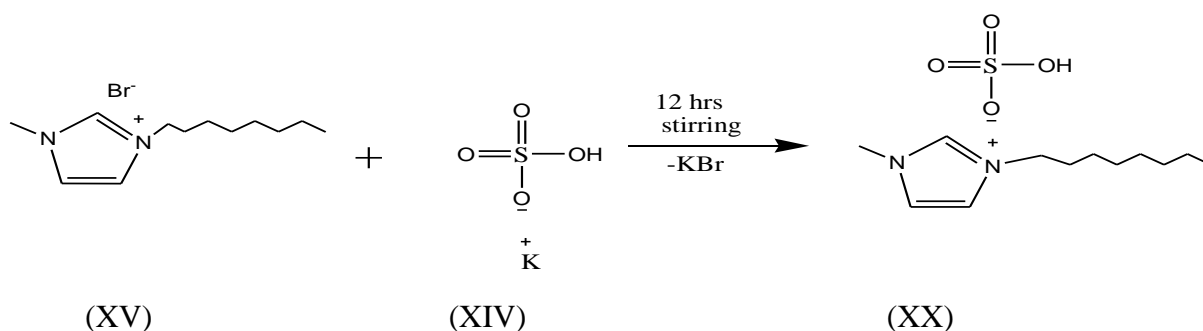
[C₈mim]Br (0.75 g ,2.72 mmol) solution was slowly added into evacuated solution of Na[BF₄](0.3 g, 2.7 mmol) and stirred in acetonitrile(60ml) overnight at room temperature in inert atmosphere to obtain product [C₈mim][BF₄] (scheme 3.7). NaBr was separated through filtration, solvent extraction and again filtration, Final product was dried with rotary evaporator and vacuum oven product yield was 70%.



Scheme 3. 7

3.3.8. 1-Methyl-3-octylimidazolium hydrogen sulphate[C₈mim][HSO₄] synthesis

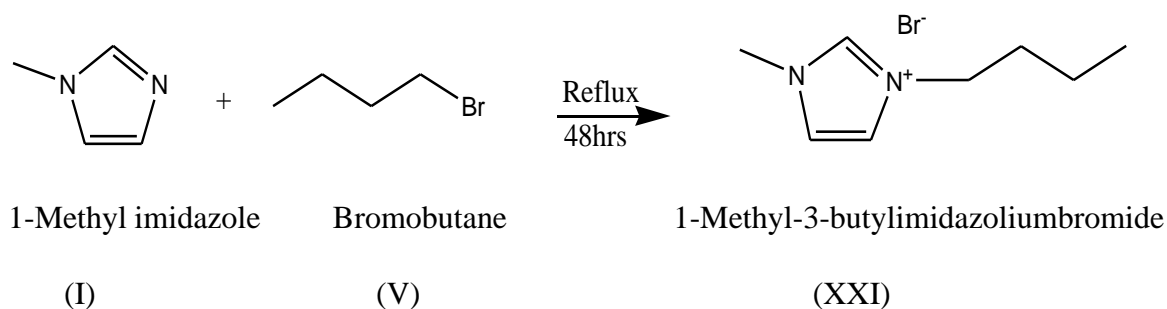
[C₈mim]Br (0.5 g, 1.8 mmol) solution in distilled water was added slowly into solution of K[HSO₄] (.25 g, 1.8 mmol) in distilled water[30][7] and stirred overnight at room temperature to obtain product [C₈mim][HSO₄] (scheme 3.8), solvent was rotary evaporated, KBr was separated through solvent extraction followed by filtration. Product was vacuum dried to obtain completely dried product with 73% yield.



Scheme 3.8

3.3.9.1 1-Methyl- 3-butylimidazolium bromide synthesis

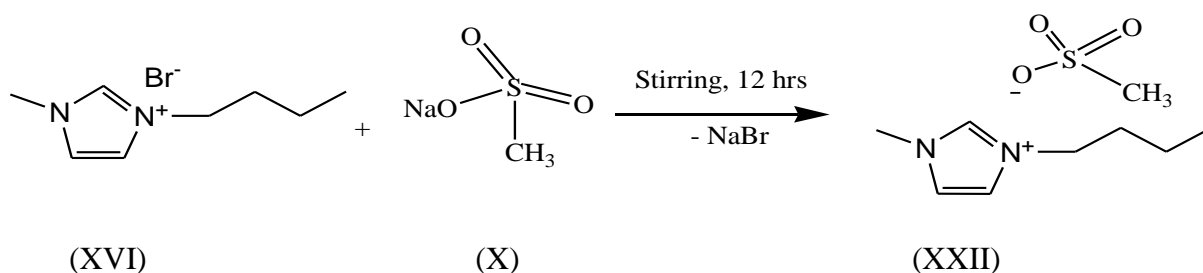
1 methyl imidazole (5g,60mmol) was reacted with butyl bromide(8.36 g, 61 mmol) in acetonitrile (60ml) to obtain 1-Methyl- 3-butylimidazolium bromide (scheme 3.9), reaction mixture was refluxed and stirred for 48 hours to obtain maximum yield of product. Completion of reaction was confirmed with help of TLC, after reaction completion solvent was evaporated with help of rotary evaporator, reactants were decanted. Then product was dried in vacuum oven for 12 hours at 50°C. Product obtained as yellow oily liquid with 92% yield.



Scheme 3.9

3.3.10. 1-Butyl-3-methylimidazolium methanesulphonate synthesis

1-Butyl-3-methylimidazolium methanesulphonate was synthesized with help of metathesis reaction of 1-Butyl-3-methylimidazolium bromide (2.41 g, 11 mmol) with sodium methanesulphonate (1.3 g, 10 mmol). Reaction mixture was stirred overnight at room temperature in methanol (scheme 3.10). Sodium bromide was removed from product with help of solvent extraction followed by filtration. Chloroform and ethyl-acetate were used for solvent extraction of product from sodium bromide. Several fractions of these solvents containing product were collected through filtration then solvent was rotary evaporated to obtain pure product which was further completely dried in vacuum oven over night at 50°C product yield was 78%.

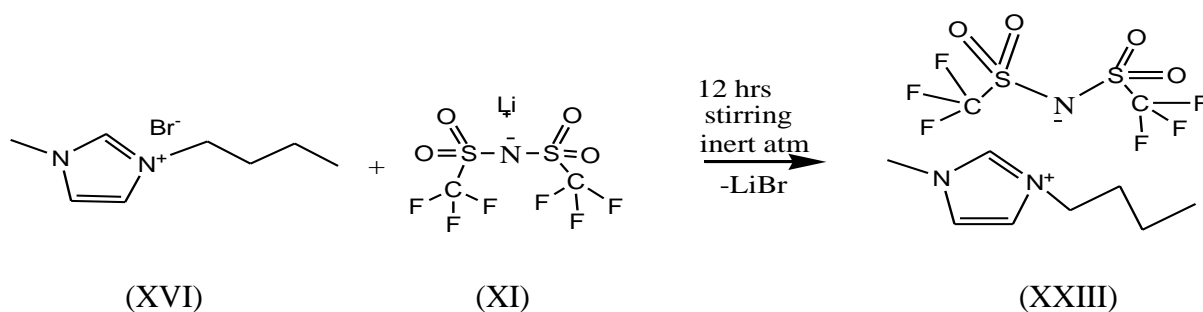


Scheme 3.10

3.3.11. 3-Butyl-1-methylimidazolium Bis(trifluoromethane-sulfonyl)imide

[C₄mim][Tf₂N] synthesis

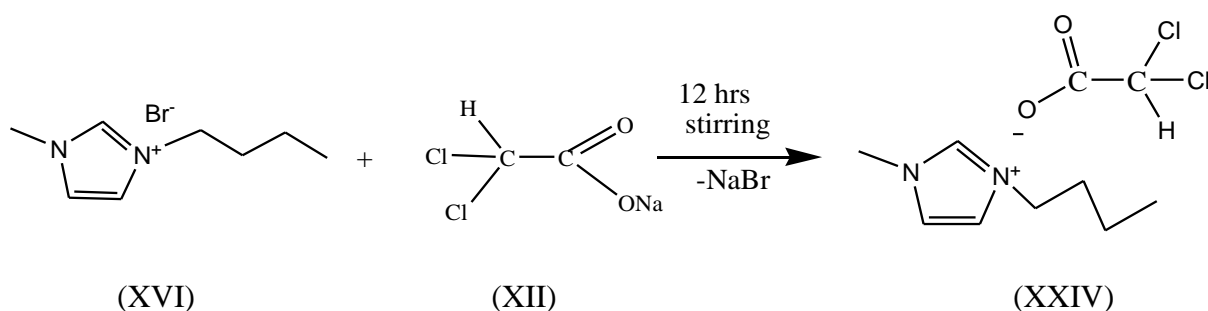
Solution of LiTf₂N (0.313 g, 1 mmol) in 2 neck round bottom flask was evacuated with help of vacuum pump and an inert atmosphere was created into flask then 3-Butyl-1-methylimidazolium bromide (0.3 g, 1 mmol) solution was added into flask. Two reactants were kept on stirring for overnight under inert atmosphere in methanol (60ml) (Scheme 3.11). After product formation methanol was evaporated and lithium bromide (LiBr) was separated with help of solvent extraction and filtration for which chloroform was used, chloroform was rotary evaporated. Product formed was dried in vacuum oven resulted into 78% yield.



Scheme 3.11

3.3.12. 3-Butyl-1-methylimidazolium dichloroacetate [C₄mim][CHCl₂CO₂] synthesis

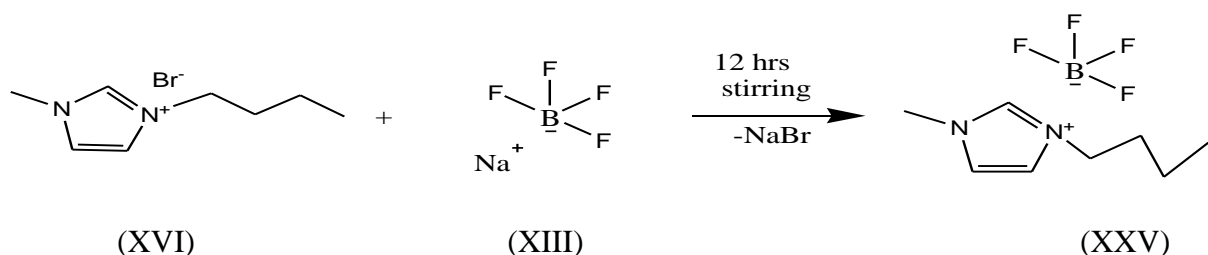
[C₄mim]Br (0.44 g, 2 mmol) solution was slowly added into solution of Na[CHCl₂CO₂] (0.3g, 2mmol) and stirred overnight in (acetonitrile 60ml) to obtain Product [C₄mim][CHCl₂CO₂] (Scheme 3.12) . NaBr was filtered acetonitrile was evaporated to obtain product, remaining NaBr was removed with solvent extraction and filtration, filtrate was dried to obtain pure and dried product with 85 % yield.



Scheme 3.12

3.3.13. 1-Methyl-3-butylimidazolium tetrafluoroborate [C₄mim][BF₄] synthesis

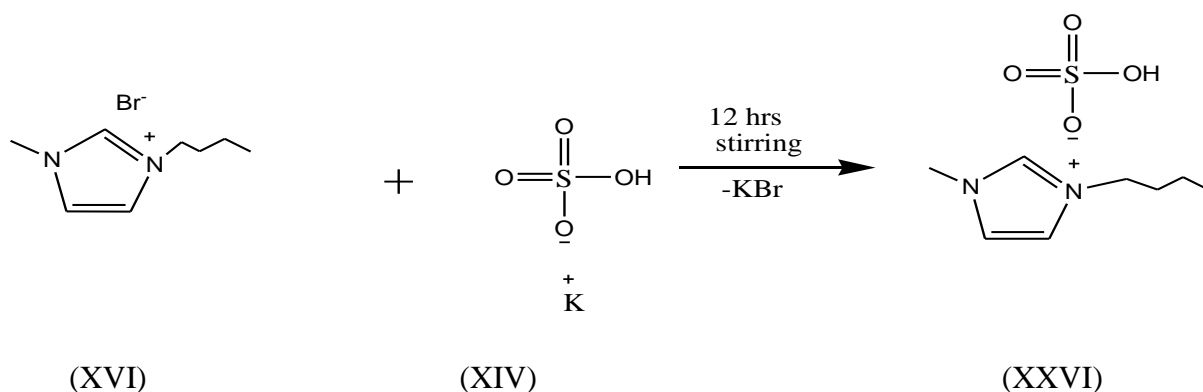
Solutions of [C₄mim]Br (0.59 g, 2.6 mmol) and Na[BF₄] (0.3g ,2.7 mmol) in acetonitrile (60ml) at room temperature for 12 hours in inert atmosphere (scheme 3.13). NaBr was separated as residue on filter paper and product was passed as filtrate, filtrate was dried through rotary evaporator to obtain product remaining NaBr was further removed with solvent extraction technique, solvent was evaporated, and product was vacuum dried product yield was 70 % .



Scheme 3.13

3.3.14. 1-Methyl-3-butylimidazolium hydrogen sulphate [C₄mim][HSO₄] synthesis

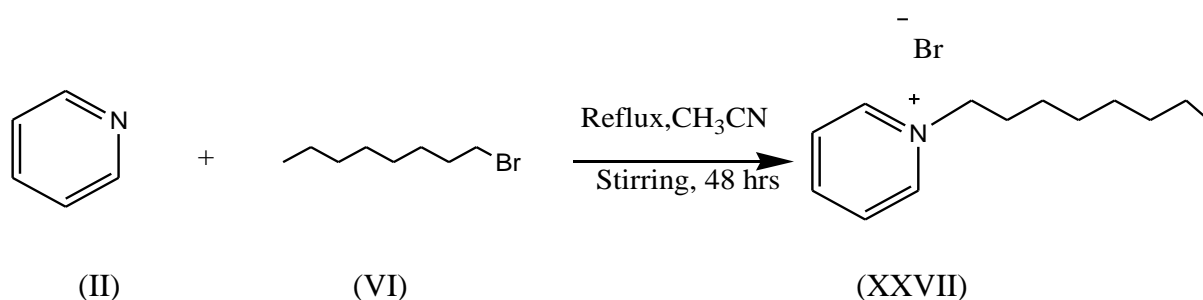
[C₄mim]Br (0.48 g ,2.1 mmol) solution in distilled water was added slowly into solution of K[HSO₄] (0.3 g, 2.2 mmol) in distilled water and stirred overnight at room temperature to obtain product [C₄mim][HSO₄] (scheme 3.14), solvent was rotary evaporated, KBr was separated through solvent extraction followed by filtration. Product was vacuum dried to obtain completely dried product with 75% yield.



Scheme 3.14

3.3.15 Octyl pyridinium bromide synthesis

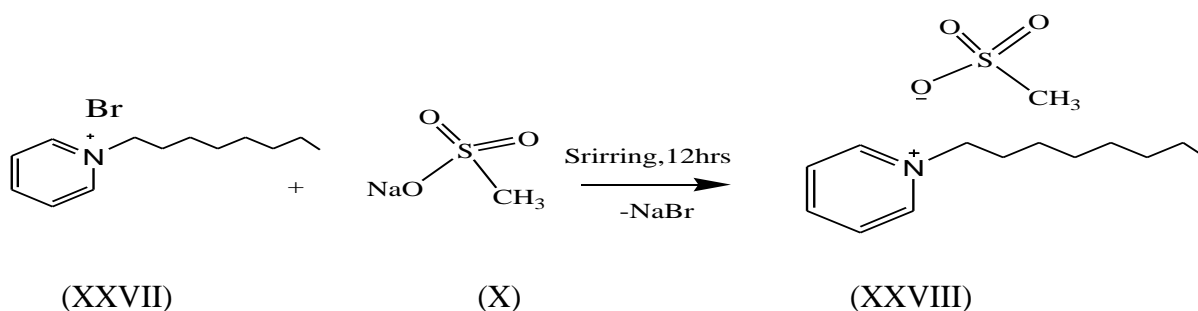
Octyl pyridinium bromide was obtained by reacting pyridine (5 g, 63 mmol) with octyl bromide (12.28 g, 63.2 mmol) in acetonitrile (60 mL). Reactants were refluxed for 48 hours to obtain maximum yield of product (scheme 3.15). After reaction completion confirmation with TLC solvent was evaporated through rotary evaporator, reactants were decanted to obtain brown colored crystalline product. Then product was completely dried in vacuum oven at 50°C for 12 hours yield was 95%.



Scheme 3.15

3.3.16 Octyl pyridinium methanesulphonate synthesis

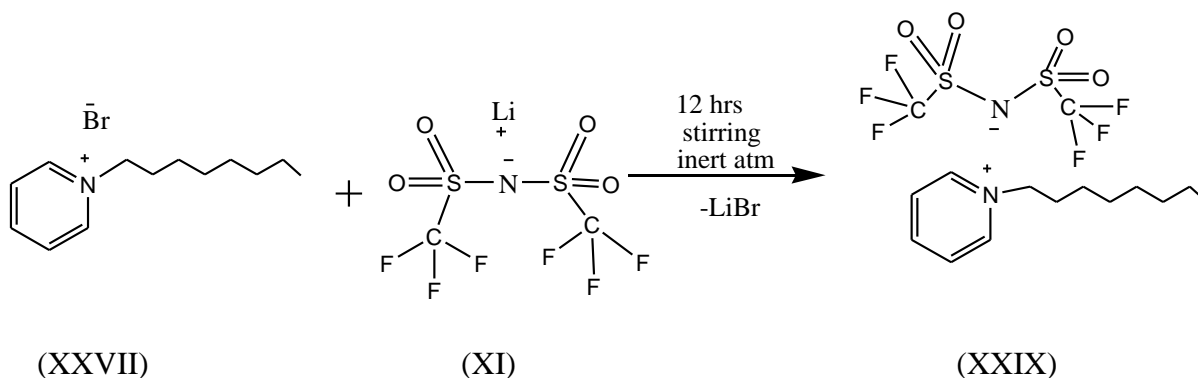
40 ml solution of Octyl pyridinium bromide (0.57 g, 2 mmol) in methanol was slowly added into 40ml solution of sodium methanesulphonate (0.25 g, 2.1 mmol), the reaction mixture was stirred overnight at room temperature to obtain Octyl pyridinium methanesulphonate (scheme 3.16). Sodium bromide was removed from product with help of solvent extraction followed by filtration, fractions of chloroform and ethyl acetate containing product were evaporated and vacuum dried in order to obtain pure and dried product with 73% yield.



Scheme 3.16

3.3.17. Octyl pyridinium Bis(trifluoromethane-sulfonyl)imide [C₈py][Tf₂N] synthesis

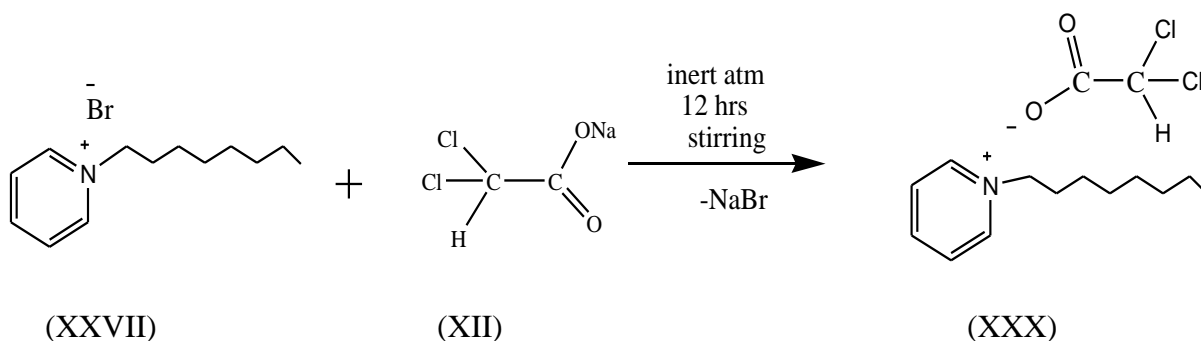
30 ml solution of [C₈py]Br (0.3 g, 1.1 mmol) in methanol was slowly added into evacuated 30ml Li[Tf₂N] (0.311 g 1.1 mmol) methanol solution, Inert atmosphere was created, and reaction mixture was stirred for overnight (scheme 3.17). Methanol was evaporated and LiBr was separated from product by solvent extraction followed by filtration. Filtrate containing product and solvent was passed through rotary evaporator to evaporate solvent remaining pure and dried product, product was further completely dried in vacuum oven over night at 40°C product yield was 75%.



Scheme 3.17

3.3.18. Octyl pyridinium dichloroacetate [C₈py] [CHCl₂CO₂] synthesis

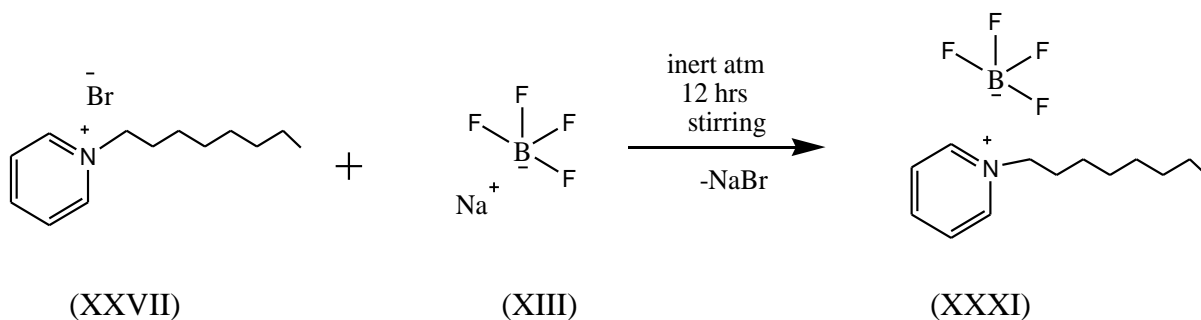
Octyl pyridinium dichloroacetate was synthesized when Octyl pyridinium bromide (0.54 g, 1.9 mmol) solution was slowly added into solution of sodium dichloroacetate (0.3 g, 2 mmol) in acetonitrile (60ml) and stirred overnight at room temperature (scheme 3.18). NaBr was separated by filtration and solvent was evaporated, any remaining NaBr was further removed with help of solvent extraction and filtration, product formed was completely dried in vacuum oven overnight, yield was 90%.



Scheme 3. 18

3.3.19. Octyl pyridinium tetrafluoroborate [C_8py][BF_4] synthesis

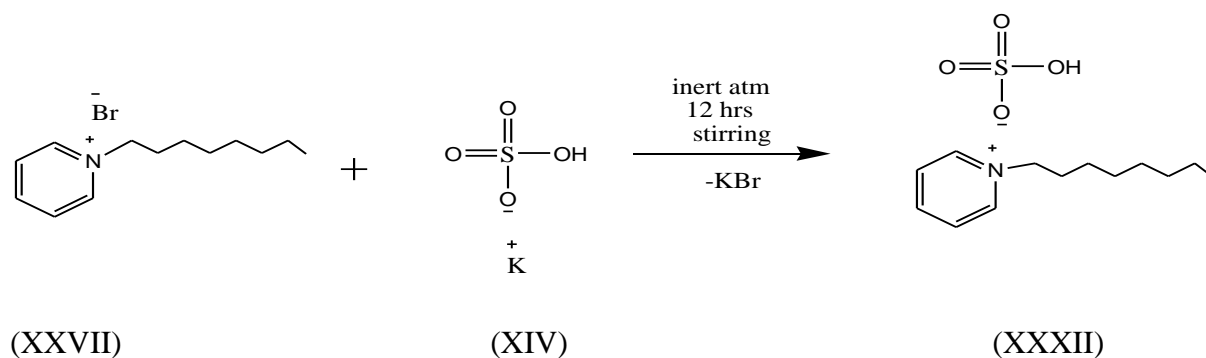
30ml solution of [C_8py] Br (0.7 g, 2.5 mmol) was added in to evacuated 30ml solution of $Na[BF_4]$ (0.3g, 2.7mmol) and stirred overnight under nitrogen atmosphere at room temperature to obtain [C_8py] $[BF_4]$ (scheme 3.19). $NaBr$ was filtered and solvent was evaporated product formed was dried in vacuum oven overnight, yield was 70%.



Scheme 3.19

3.3.20. Octyl pyridinium hydrogen sulphate [C_8py][HSO_4] synthesis

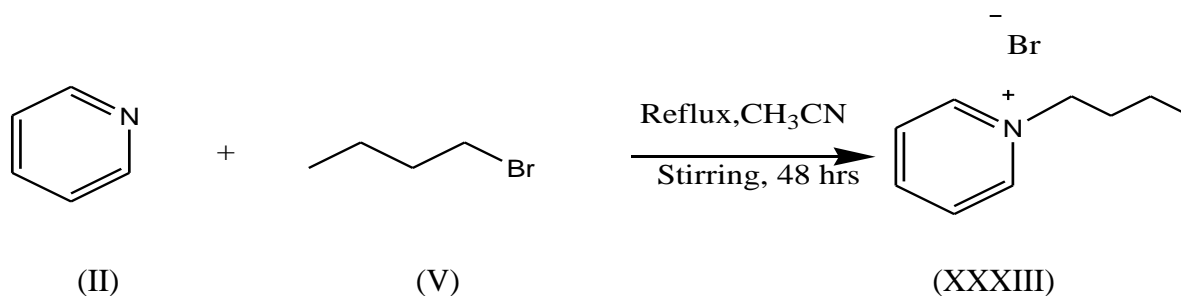
Distilled water was used to form solution of Octyl pyridinium bromide [C_8py] Br and potassium hydrogen sulphate $K[HSO_4]$. Solution of [C_8py] Br (0.6 g, 2.3 mmol) was slowly added in to $K[HSO_4]$ (0.3 g, 2.2 mmol) solution and stirred overnight at room temperature to obtain product [C_8py] $[HSO_4]$ and KBr (scheme 3.20). Water was evaporated, KBr was separated by solvent extraction, solvent was evaporated, and product was vacuum dried to obtain completely dried product with 75% yield.



Scheme 3.20

3.3.21. Butyl pyridinium bromide synthesis

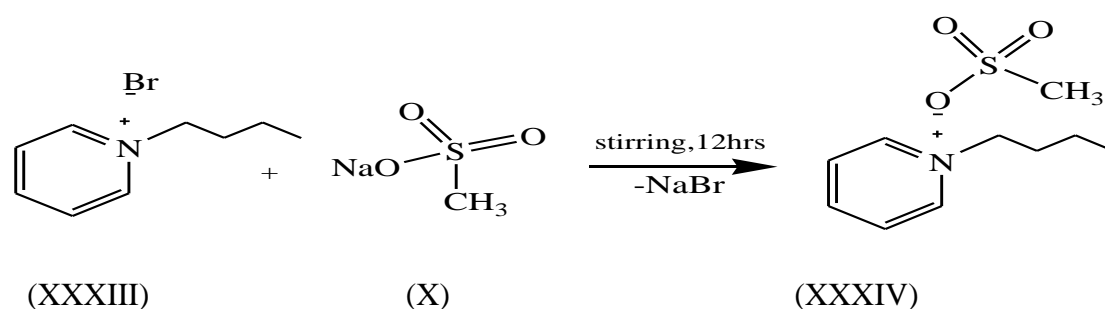
Pyridine (5g , 63.3 mmol) was reacted with butyl bromide (8.66g ,63.3 mmol) in acetonitrile (60ml) to obtain Butyl pyridinium bromide). Reaction mixture was refluxed and stirred for 48 hours to obtain maximum yield of product (scheme 3.21). After confirmation of reaction completion with help of TLC reaction was stopped ,solvent was rotary evaporated ,reactants were decanted to obtain brown colored liquid product. Product was further dried in vacuum oven for 12 hours at 50°C, yield was 93%.



Scheme 3.21

3.3.22. Butyl pyridinium methanesulphonate synthesis

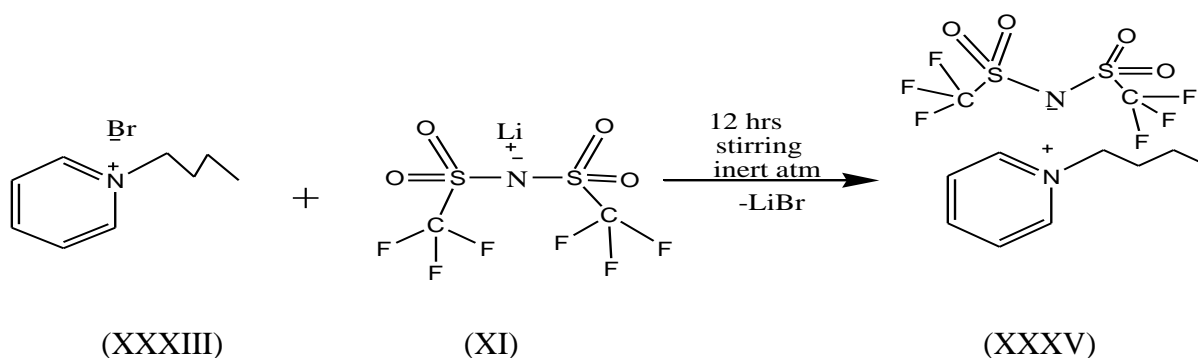
Butyl pyridinium bromide (0.9 g, 4 mmol) and sodium methanesulphonate (0.5 g, 4.2 mmol) were stirred overnight at room temperature methanol (80ml) to obtain Butyl pyridinium methanesulphonate (scheme 3.22). After reaction completion, solvent was rotary evaporated and sodium bromide was solvent extracted with help of ethyl-acetate and chloroform. Several fractions of solvent were collected through filtration containing product and remaining sodium bromide on filter paper. Fractions of solvent were evaporated, and product was vacuum dried to obtain pure dried product, yield was 91%.



Scheme 3.22

3.3.23. Butyl pyridinium Bis(trifluoromethane-sulfonyl)imide [C₄py] [Tf₂N] synthesis

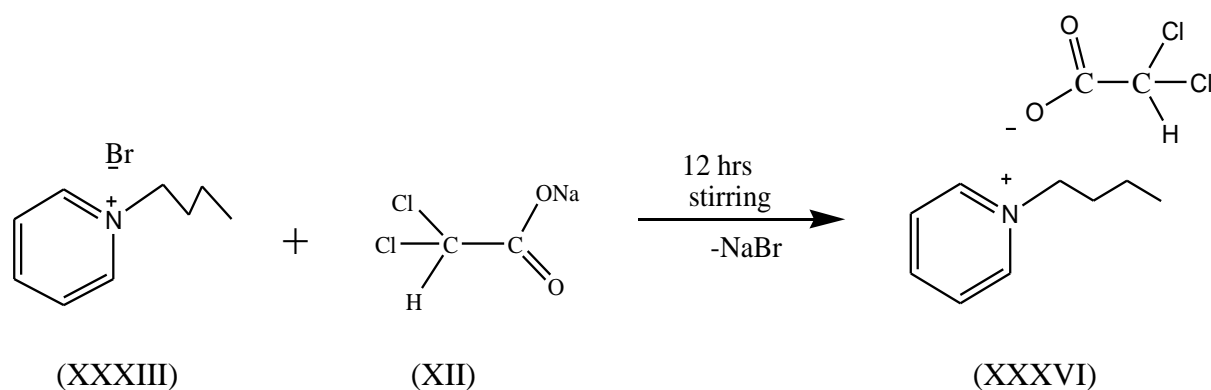
Li[Tf₂N] (0.3 g, 1 mmol) solution in methanol (30ml) was formed in 2 neck RB flasks, was evacuated then inert atmosphere was created, [C₄py]Br (0.39 g, 1.8 mmol) solution in methanol (30ml) was added and stirred overnight to form [C₄py] [Tf₂N] (scheme 3.23). Methanol was evaporated, LiBr with solvent extraction and filtration was separated from product. Solvent was rotary evaporated to obtain pure product, product was further dried in vacuum oven at 40°C overnight, yield was 75%.



Scheme 3.23

3.3.24. Butyl pyridinium dichloroacetate [C₄py][CHCl₂CO₂] synthesis

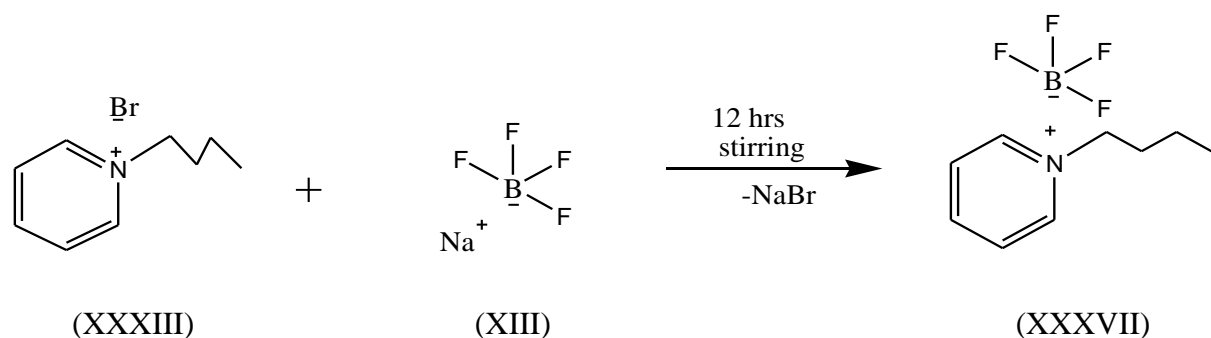
[C₄py]Br (0.4 g, 1.8 mmol) and Na[CHCl₂CO₂] (0.3 g, 2 mmol) solutions were prepared in acetonitrile (60ml). [C₄py][CHCl₂CO₂] was synthesized when [C₄py]Br solution was slowly added into Na[CHCl₂CO₂] solution and stirred overnight at room temperature (scheme 3.24). After product formation NaBr was separated from solvent through filtration, solvent was rotary evaporated, further NaBr was separated with solvent extraction followed by filtration. Product was completely dried in vacuum oven overnight, yield was 90%.



Scheme 3.24

3.3.25. Butyl pyridinium tetrafluoroborate[C₄py][BF₄] synthesis

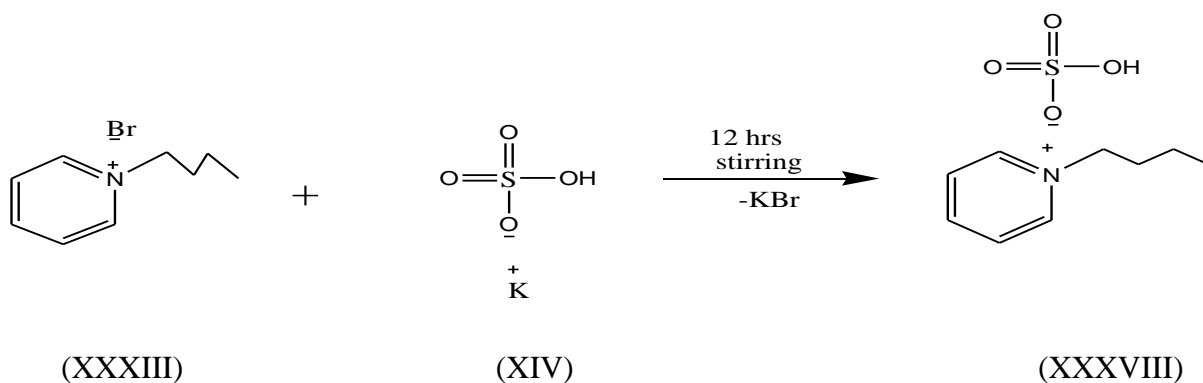
[C₄py]Br (0.59g, 2.7 mmol) was slowly added into evacuated Na [BF₄] (0.3 g, 2.75 mmol) and reaction mixture was stirred in acetonitrile (60ml) overnight in inert atmosphere to obtain [C₄py][BF₄] (scheme 3.25). NaBr was removed through solvent extraction and filtration, solvent was evaporated, and product was completely dried in vacuum oven overnight, yield was 88%.



Scheme 3.25

3.3.26. Butyl pyridinium hydrogen sulphate [C₄py][HSO₄] synthesis

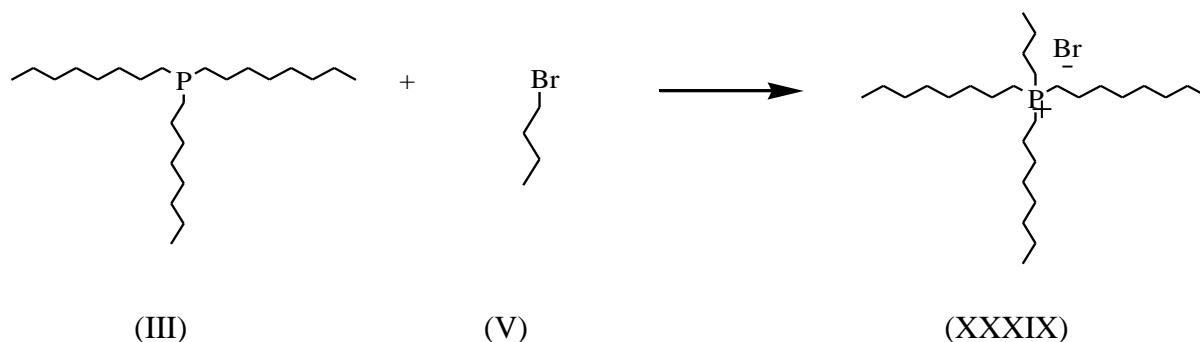
Butyl pyridinium bromide [C₄py]Br (0.4 g, 1.8 mmol) and potassium hydrogen sulphate K[HSO₄] (0.3g, 2.2mmol) were added into 30ml distilled water separately to form solution, then [C₄py]Br solution was slowly added into K[HSO₄] solution and stirred overnight at room temperature to form product [C₄py][HSO₄] and KBr (scheme 3.26). Water was rotary evaporated, KBr was removed with help of solvent extraction and filtration, solvent was rotary evaporated to obtain product which was further completely dried in vacuum oven, yield was 93%.



Scheme 3.26

3.3.27. Mono-butyl tri-octyl phosphonium bromide synthesis

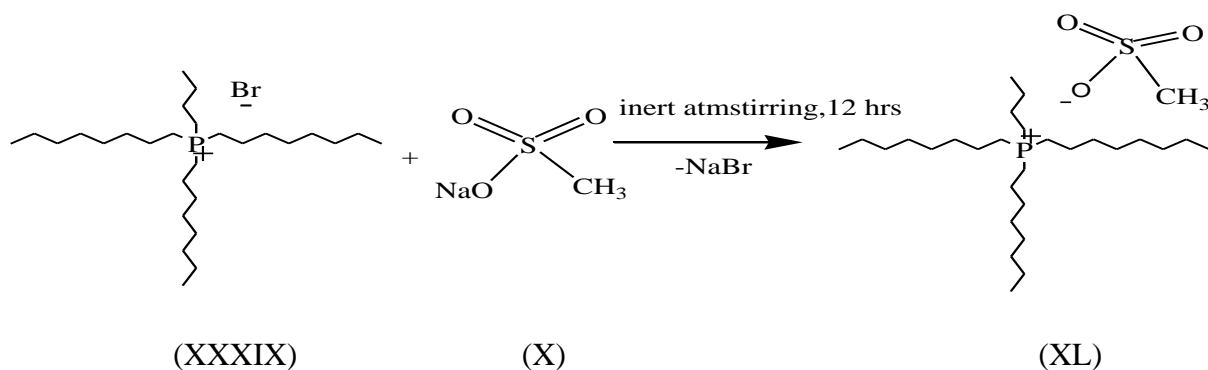
Tri-octyl phosphine (5g, 13.5mmol , 6.02ml) was reacted with butyl bromide (1.85g, 13.5mmol) to obtain Mono-butyl tri-octyl phosphonium bromide .Reaction was neat, reactants were evacuated with help of vacuum pump to remove air then refluxed and stirred under inert atmosphere for 24 hours at 120 °C to obtain maximum yield of product (scheme 3.27). Reaction completion was confirmed with help of TLC , product was decanted to remove unreacted materials product obtained was dark yellow oily liquid and was dried in vacuum oven for 12 hours at 50°C, yield was 91%.



Scheme 3.27

3.3.28. Mono-butyl tri-octyl phosphonium methanesulphonate synthesis

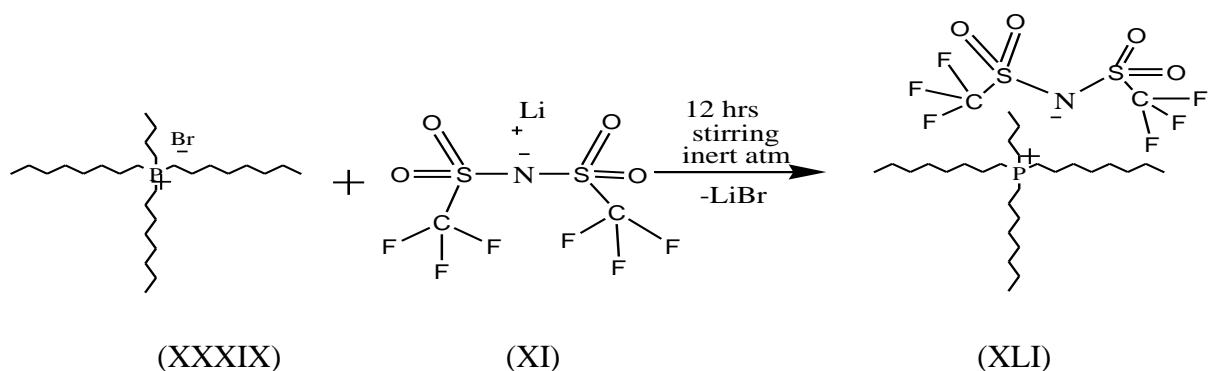
Solution of Mono-butyl tri-octyl phosphonium bromide (1 g, 1.9 mmol) in methanol (40ml) was slowly added into solution of sodium methanesulphonate (0.23g, 1.9 mmol) in methanol (40ml) and stirred overnight at room temperature to obtain Mono-butyl tri-octyl phosphonium methanesulphonate (scheme 3.28). After product formation methanol was evaporated and sodium bromide side was separated with help of several fractions of chloroform and ethyl acetate. Solvents were rotary evaporated and vacuum dried in order to obtain product in pure and dried form, yield was 73%.



Scheme 3.28

3.3.29. Butyl-tri-octyl phosphonium Bis(trifluoromethane-sulfonyl)imide [P₄₈₈₈][Tf₂N] synthesis

Butyl-tri-octyl phosphonium bromide [P₄₈₈₈]Br (1 g, 1.9 mmol) was dissolved in methanol (30ml) to form a solution then Bis(trifluoromethane-sulfonyl)imide Li[Tf₂N] (0.5g, 1.8 mmol) was taken in 2 neck RB flask methanol (30ml) was added to form its solution and it was evacuated to remove any air then inert atmosphere was created. [P₄₈₈₈]Br solution was added into evacuated solution of Li[Tf₂N] the reaction mixture was stirred overnight at room temperature under nitrogen atmosphere (scheme 3.29). Product [P₄₈₈₈][Tf₂N] and LiBr were dried from methanol in rotary evaporator and then LiBr was separated from product with the help of solvent extraction followed by filtration. Filtrate containing product was rotary dried and then completely dried in vacuum oven overnight at 40°C, yield was 83%.

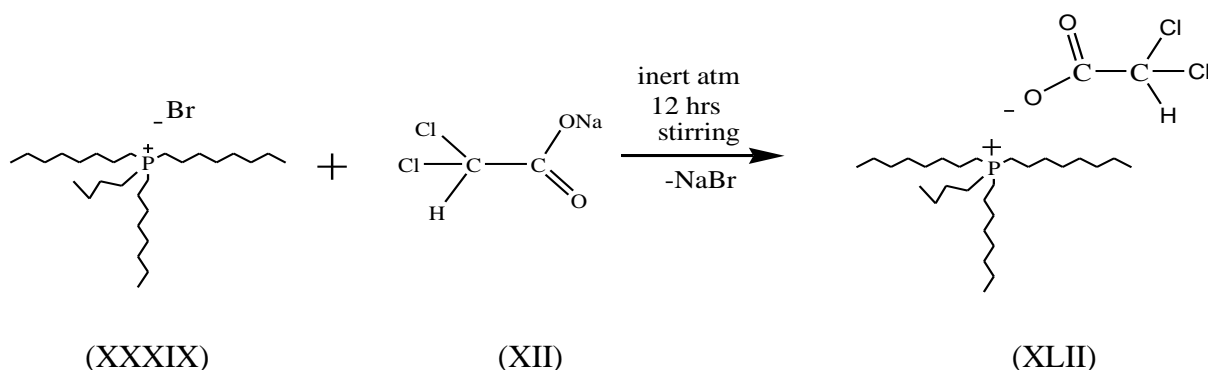


Scheme 3.29

3.3.30. Butyl-Tri-octyl phosphonium dichloroacetate [P₄₈₈₈][CHCl₂CO₂] synthesis

Na[CHCl₂CO₂] (0.3 g, 2 mmol) solution was added into evacuated solution of [P₄₈₈₈]Br (1 g, 1.9 mmol), under inert atmosphere and room temperature reaction mixture in acetonitrile (80ml) was stirred overnight to obtain product (scheme 3.30). NaBr formed was filtered,

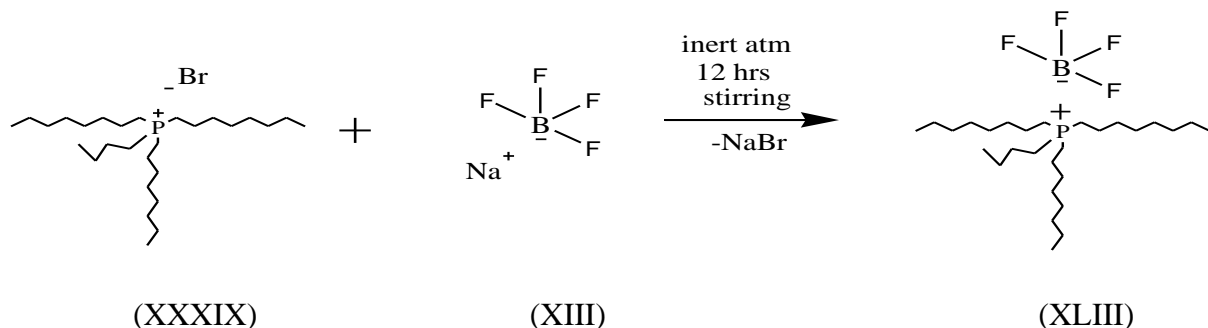
solvent was evaporated. Pure product was obtained by further solvent extraction and filtration followed by complete drying in vacuum oven overnight, yield was 85%.



Scheme 3.30

3.3.31. Tri-octyl mono-butyl phosphonium tetrafluoroborate [P_{4888}][BF_4] synthesis

$[P_{4888}]Br$ (1 g, 1.9 mmol) was dissolved in acetonitrile (30ml) and $Na[BF_4]$ (0.2g, 1.8mmol) was also dissolved into acetonitrile (30ml). $[P_{4888}]Br$ solution was added into evacuated $Na[BF_4]$ solution and stirred overnight at room temperature under nitrogen atmosphere to obtain $[P_{4888}][BF_4]$ (scheme 3.31). $NaBr$ was separated and solvent was evaporated, product formed was completely dried in vacuum oven overnight, yield was 70%.

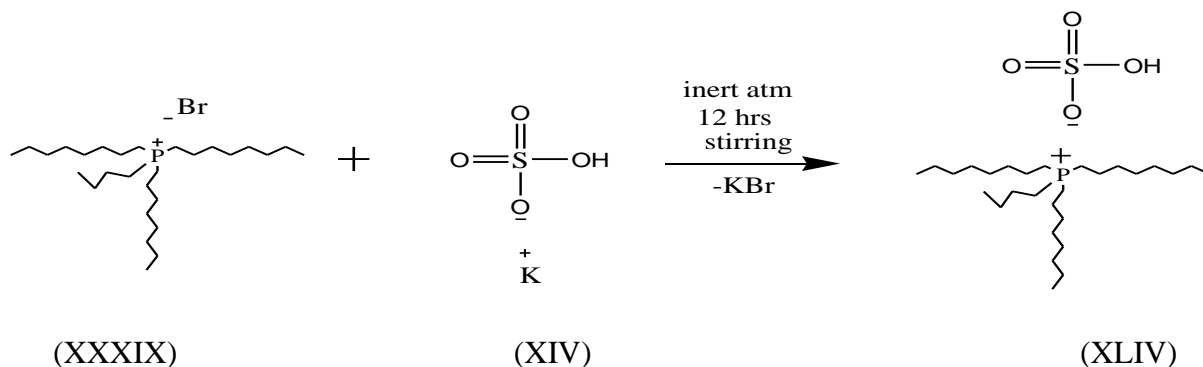


Scheme 3.31

3.3.32. Tri-octyl mono-butyl phosphonium hydrogen sulphate [P_{4888}][HSO_4] synthesis

Tri-octyl mono-butyl phosphonium bromide $[P_{4888}]Br$ (1g, 1.9mmol) was dissolved into distilled water (30ml) to form solution and potassium hydrogen sulphate $K[HSO_4]$ (0.2g, 1.4mmol) was also dissolved in distilled water (30ml) to obtain its solution. Then solution of $[P_{4888}]Br$ was added into $K[HSO_4]$ solution and stirred overnight to obtain product $[P_{4888}][HSO_4]$ (scheme 3.31). Product and KBr both are soluble in water, so water was evaporated on rotary evaporator and KBr was extracted from $[P_{4888}][HSO_4]$ by solvent extraction using chloroform followed by filtration, filtrate containing product and chloroform was evaporated

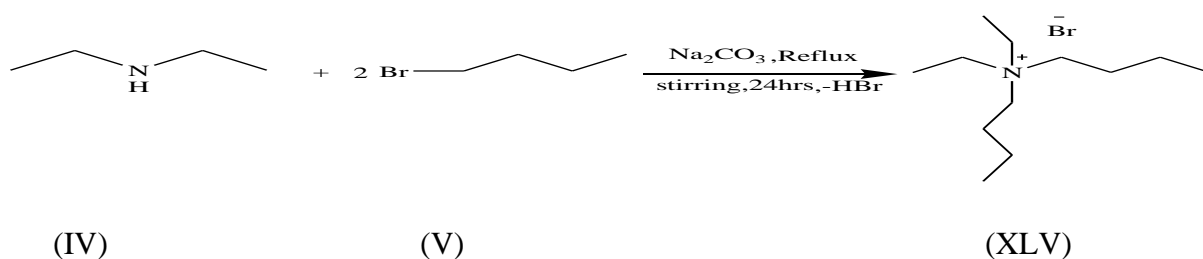
to obtain product, product was further completely dried in vacuum oven overnight, yield was 71%.



Scheme 3.32

3.3.33. Diethyl dibutyl ammonium bromide

Diethyl dibutyl ammonium bromide was synthesized by reacting diethylamine (2.5 g, 34mmol) with 2 molar equivalents bromobutane (9.36 g, 68mmol) in acetonitrile (60ml). 3 molar equivalents (10.8 g, 102mmol) of Sodium carbonate (Na_2CO_3) was taken as base. Reaction mixture containing reactants, solvent and base was evacuated with help of vacuum pump to remove air then stirred and refluxed under nitrogen atmosphere at 90°C for 24 hours to obtain the required product (scheme 3.33). Completion of reaction was confirmed with TLC, solvent was rotary evaporated, unreacted material was decanted, base was filtered to obtain pure product, pure crystalline product was obtained and dried in vacuum oven for 12 hours at 50°C , yield was 93%.

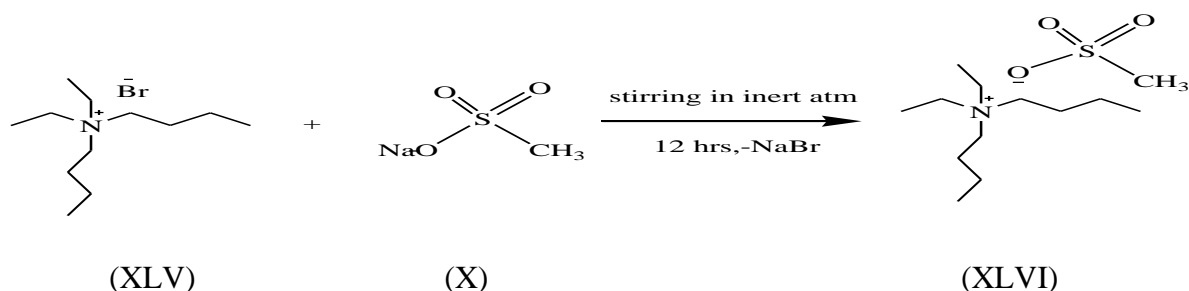


Scheme 3.33

3.3.34. Diethyl dibutyl ammonium methanesulphonate synthesis

Diethyl dibutyl ammonium bromide (1g, 3.7 mmol) solution in methanol (40ml) was added into sodium methanesulphonate (0.44 g, 3.6 mmol) methanol solution (40ml) and stirred overnight at room temperature to obtain Diethyl dibutyl ammonium methanesulphonate

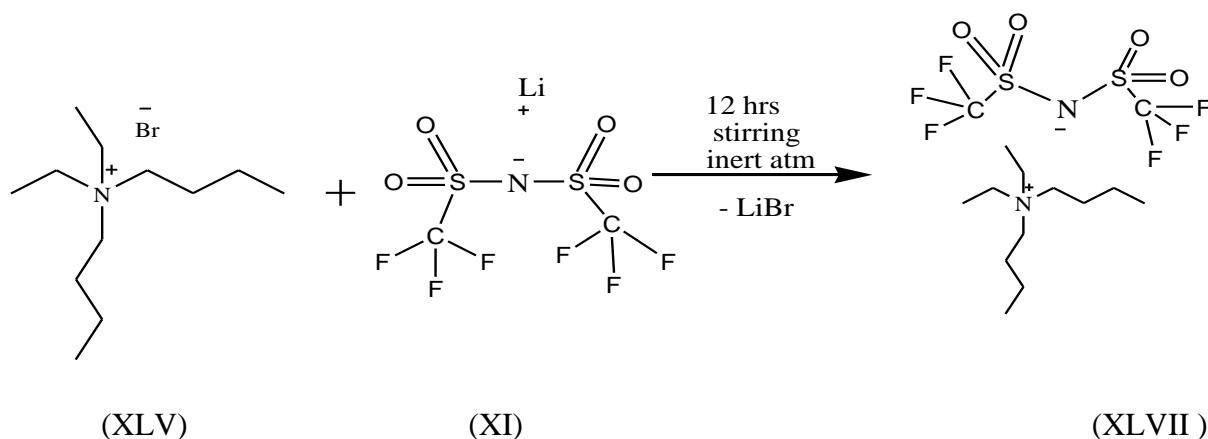
(scheme 3.34). Methanol was evaporated, Sodium bromide was solvent extracted, solvents were rotary evaporated and product was completely dried in vacuum oven, yield was 76%.



Scheme 3. 34

3.3.35. Diethyl dibutyl ammonium Bis(trifluoromethane-sulfonyl)imide [$N_{2,2,4,4}$][Tf₂N] synthesis

[$N_{2,2,4,4}$]Br (0.5 g, 1.8 mmol) solution in methanol (30ml) was added into evacuated solution of Li[Tf₂N] (0.5 g, 1.8 mmol) in methanol (30ml) and stirred overnight under inert atmosphere at room temperature (scheme 3.35). Product [$N_{2,2,4,4}$][Tf₂N] and LiBr were dried in rotary evaporator to evaporate methanol then LiBr was separated with solvent extraction and filtration, filtrate containing product was dried from solvent to obtain pure and dried product, yield was 78%.

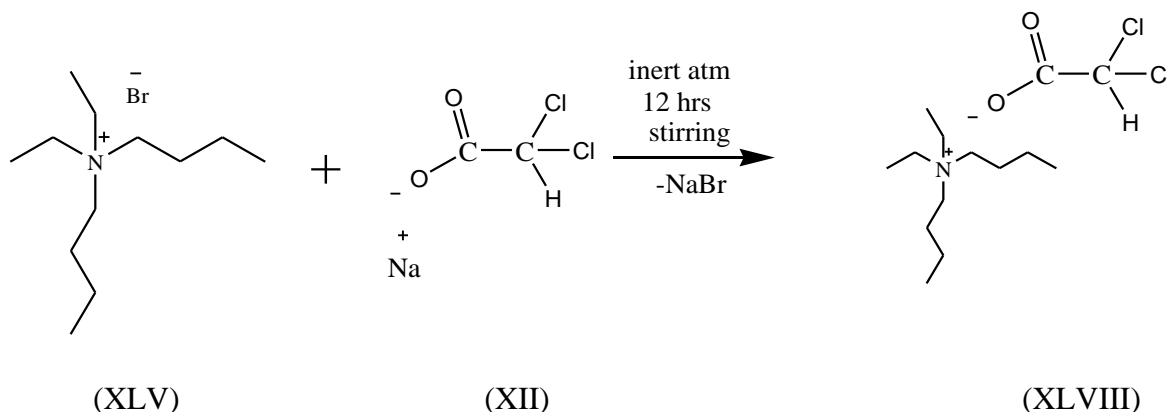


Scheme 3.35

3.3.36. Diethyl dibutyl ammonium dichloroacetate [$N_{2,2,4,4}$][CHCl₂CO₂] synthesis

Diethyl dibutyl ammonium dichloroacetate [$N_{2,2,4,4}$][CHCl₂CO₂] was obtained when Na[CHCl₂CO₂] (0.28g, 1.8 mmol) solution in acetonitrile (40ml) was added into evacuated solution of [$N_{2,2,4,4}$]Br (0.5 g, 1.8 mmol) in acetonitrile (40ml) and reaction mixture was stirred under nitrogen atmosphere at room temperature overnight (scheme 3.36). NaBr was filtered

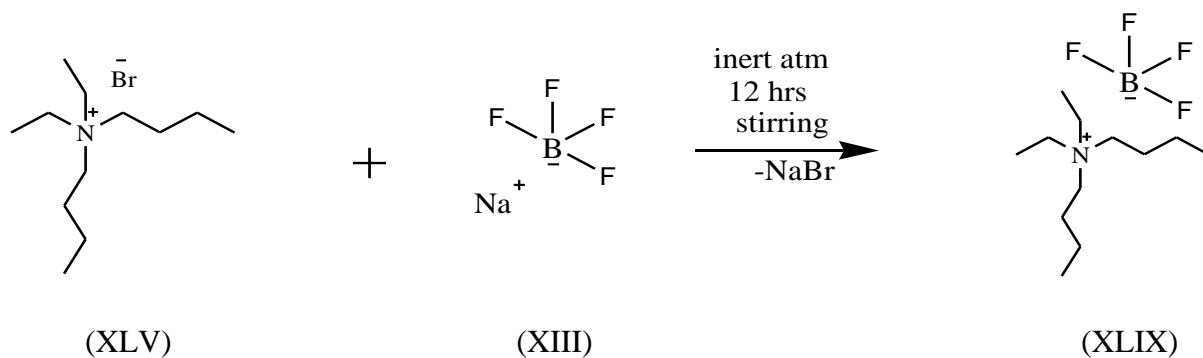
solvent was dried further solvent extraction was done to obtain pure product which was dried completely, yield was 83%.



Scheme 3.36

3.3.37. Diethyl dibutyl ammonium tetrafluoroborate $[\text{N}_{2,2,4,4}][\text{BF}_4]$ synthesis

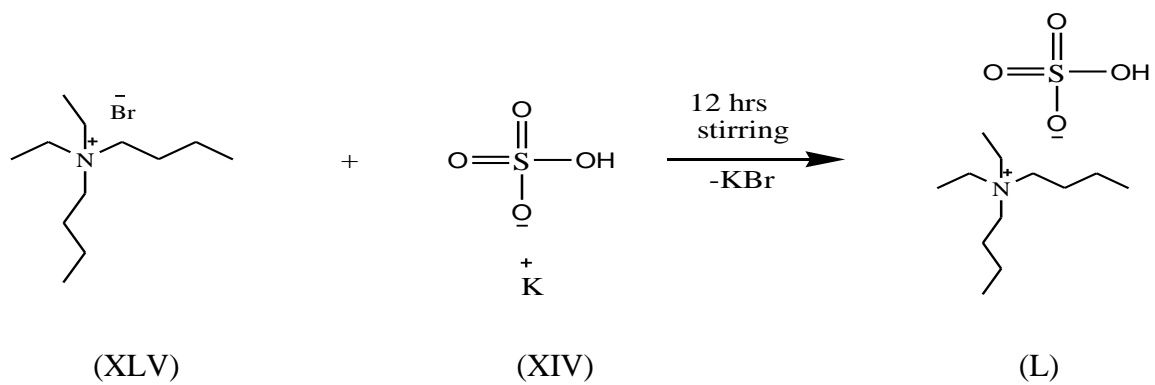
Diethyl dibutyl ammonium tetrafluoroborate $[\text{N}_{2,2,4,4}][\text{BF}_4]$ was synthesized by stirring solutions of Diethyl dibutyl ammonium bromide $[\text{N}_{2,2,4,4}]\text{Br}$ (1 g, 3.7 mmol) and sodium tetrafluoroborate $\text{Na}[\text{BF}_4]$ (0.4g, 3.6 mmol) in acetonitrile (80ml) under inert and evacuated atmosphere for overnight at room temperature (scheme 3.37). Sodium bromide was filtered solvent was evaporated and product was completely dried in vacuum oven overnight, yield was 75%.



Scheme 3.37

3.3.38. Diethyl dibutyl ammonium hydrogen sulphate $[\text{N}_{2,2,4,4}][\text{HSO}_4]$ synthesis

$[\text{N}_{2,2,4,4}]\text{Br}$ (1 g, 3.7 mmol) solution in distilled water (30ml) was added slowly into solution of $\text{K}[\text{HSO}_4]$ (0.5, 3.6 mmol) in distilled water (30ml) and stirred overnight at room temperature to obtain product $[\text{N}_{2,2,4,4}][\text{HSO}_4]$ (scheme 3.38), solvent was rotary evaporated, KBr was separated through solvent extraction followed by filtration. Product was vacuum dried to obtain completely dried product, yield was 73%.



Scheme 3.38

Chapter 4

4. RESULT AND DISCUSSION

Different ionic liquids which were synthesized in lab were characterized with help of characterization techniques at different levels during and after their synthesis, in this chapter these characterization techniques are discussed in detail.

4.1 Thin layer chromatography (TLC)

4.2 Attenuated Total Reflection-Fourier Transformation Infrared spectroscopy(ATR-FTIR)

4.3 Nuclear magnetic resonance spectroscopy(NMR)

4.1 Thin layer chromatography (TLC)

Principle:

TLC consist of two phases mobile phase and stationary phase; mobile phase is liquid as it has to travel over stationary phase which is solid these two phases help to partition different compounds on the basis of their solubilities and adsorption.

During TLC different spots of different compounds moves relatively to each other and if a spot is mixture of different compounds then a number of spots appear at the different distances.

Technique:

TLC was performed during reaction a number of times in order to check for the progress of reaction and to check for the completion of reaction.

Reactants were diluted with volatile solvent. In a beaker small amount of nonpolar solvent or mixture of solvents consisting of polarity needed for reaction type was taken. On silica gel TLC plate a line was drawn spot of reactants were placed with help of capillary line another spot consisting of reaction mixture was placed on line .Then this TLC plate was placed inside beaker and beaker was covered with lid solvent travelled over plate.

Observation with UV lamp:

Plate was removed and solvent distance was marked then spots were observed under UV light, spots were labelled and these marked spots were compared to check reaction progress and completion.

Iodine chamber :

In iodine chamber TLC plates were placed for a period of time until dark yellow or brown colored spots were appeared spots were compared to observe product formation, these spots were labelled for later observations.

4.2. Attenuated Total Reflection-Fourier Transformation Infrared spectroscopy (ATR-FTIR)

Basic principle:

Basic principle of IR spectroscopy is the interaction of radiation in IR region with molecule causing the covalent bond to vibrate these vibrations constitute of bending and stretching vibrations. IR spectrum has two regions functional group region lying in 4000 to 1000 cm^{-1} and fingerprint region lying in 1000 to 400 cm^{-1} . IR spectrum helps to find different functional groups present in a molecule for interpreting structure of molecule.

Stretching vibration changes the bond length it may be symmetric when all bonds changes bond length at same time and asymmetric when bonds moves in such a way that bond length of one increases and bond length of other bond decreases at same time.

Bending vibrations changes the bond angle of the molecule, Bending may be scissoring type when two bonds move like scissor to increase or decrease the bond angle , in rocking type bonds move like pendulum of clock, wagging is back and forth movement of V sign and twisting is movement of bonds that looks like they are walking.

Samples were placed on BRUKER ALPHA platinum ATR without any sample preparation and spectra of synthesized products were obtained by ATR-FTIR which are shown below:-

4.2.1. FT-IR analysis of 1-Methyl-3-octylimidazolium bromide [C₈mim]Br

FT-IR for 1-Methyl-3-octylimidazolium bromide is shown in Figure 4.1. At 3120 cm^{-1} band appeared is due to aromatic CH stretching vibrations, 2924 cm^{-1} and 2854 cm^{-1} peaks are stretching vibrations of CH for aliphatic sp^3 CH_2 and CH_3 respectively. A band appearing at 1650 cm^{-1} show C=N stretching vibrations of imidazolium ring, Band at 1569 cm^{-1} show

stretching vibration of C=C and bending vibrations for CH₂ are at 1463 cm⁻¹ strong peak at 1165 cm⁻¹ appear due to stretching vibration of C-N of imidazolium ring. At 752 cm⁻¹ peak appearance indicates presence of long chain CH₂ octyl group.

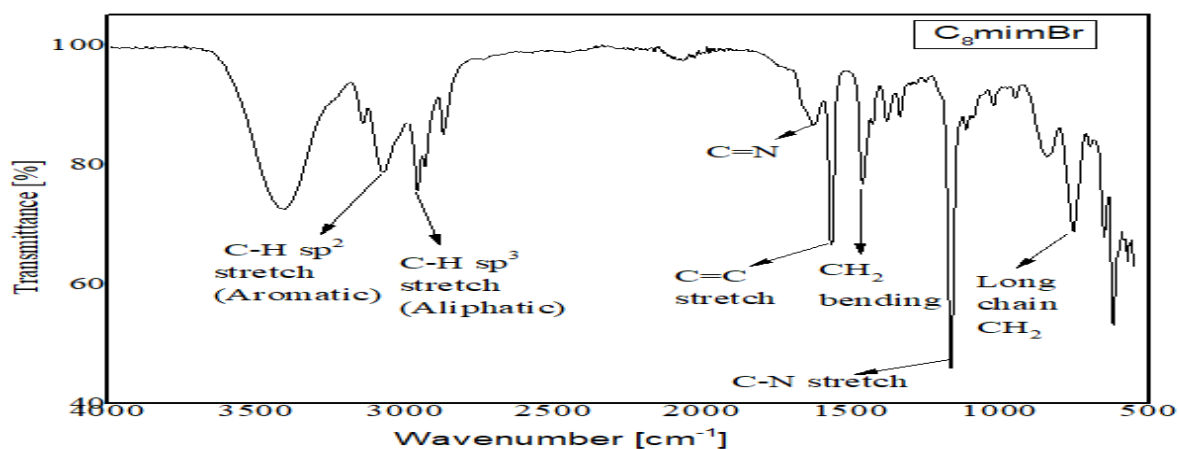


Figure 4.1 FTIR spectrum of [C₈mim]Br

4.2.2. FT-IR analysis of 1-Methyl-3-octylimidazolium methane sulphonate [C₈mim][MeSO₃]

The FTIR analysis of [C₈mim][MeSO₃] is shown in Figure 4.2. Formation of 1-Methyl-3-octylimidazolium methane sulphonate was indicated by FT-IR due to band appearance at 1040 cm⁻¹ this characteristic band appear due to exchange of anion .

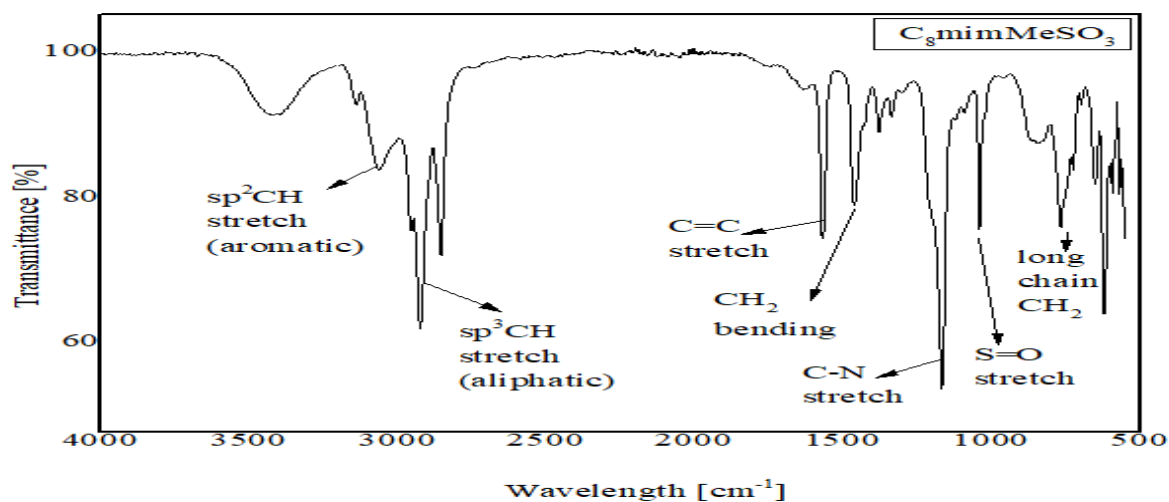


Figure 4.2 FTIR spectrum of [C₈mim][MeSO₃]

At 3120 cm⁻¹ band appeared is due to aromatic CH stretching vibrations, 2924 cm⁻¹ and 2854 cm⁻¹ peaks are stretching vibrations of CH for aliphatic sp³ CH₂ and CH₃ respectively. Band at 1569 cm⁻¹ show stretching vibration of C=C and bending vibrations for CH₂ are at 1463 cm⁻¹

strong peak at 1166 cm^{-1} appear due to stretching vibration of C-N of imidazolium ring. S=O stretch appears at 1040 cm^{-1} . At 767 cm^{-1} peak appearance indicates presence of long chain CH_2 octyl group.

4.2.3. FT-IR analysis of 1-Methyl-3-octylimidazolium Bis(trifluoromethanesulfonyl) imide [C_8mim][Tf_2N]

1-Methyl-3-octylimidazolium Bis(trifluoromethane-sulfonyl)imide [C_8mim][Tf_2N] formation was indicated by FT-IR shown in 4.3 due to appearance of peaks at 1358 cm^{-1} indicating asymmetric stretching vibration of S=O and at 1180 cm^{-1} symmetric stretching vibration of S=O.

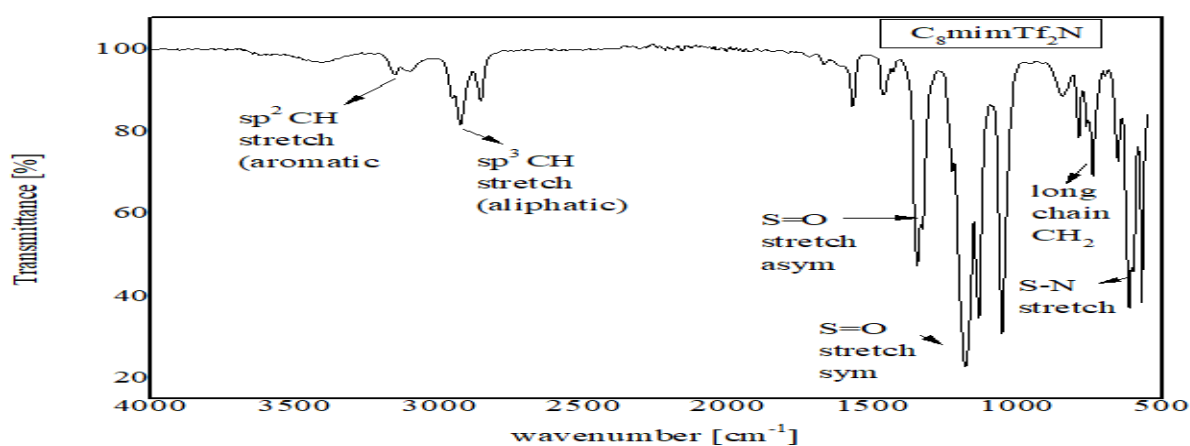


Figure 4.3 FTIR spectrum of [C_8mim][Tf_2N]

Band at 2929 cm^{-1} and 2854 cm^{-1} indicate stretching vibrations of aliphatic CH_2 and CH_3 respectively. Band at 1569 cm^{-1} show stretching vibration of C=C and bending vibrations for CH_2 are at 1463 cm^{-1} . At 739 cm^{-1} peak appearance indicates presence of long chain CH_2 of octyl group.

4.2.4. FT-IR analysis of 1-Methyl-3-octylimidazolium dichloroacetate [C_8mim][CHCl_2CO_2]

FT-IR analysis of 1-Methyl-3-octylimidazolium dichloroacetate in fig.4.4 Band at 1571 cm^{-1} show stretching vibration of C=C and bending vibrations for CH_2 are at 1463 cm^{-1} , peak at 1165 cm^{-1} appear due to stretching vibration of C-N of imidazolium ring, at 740 cm^{-1} peak appearance indicates presence of long chain CH_2 octyl group.

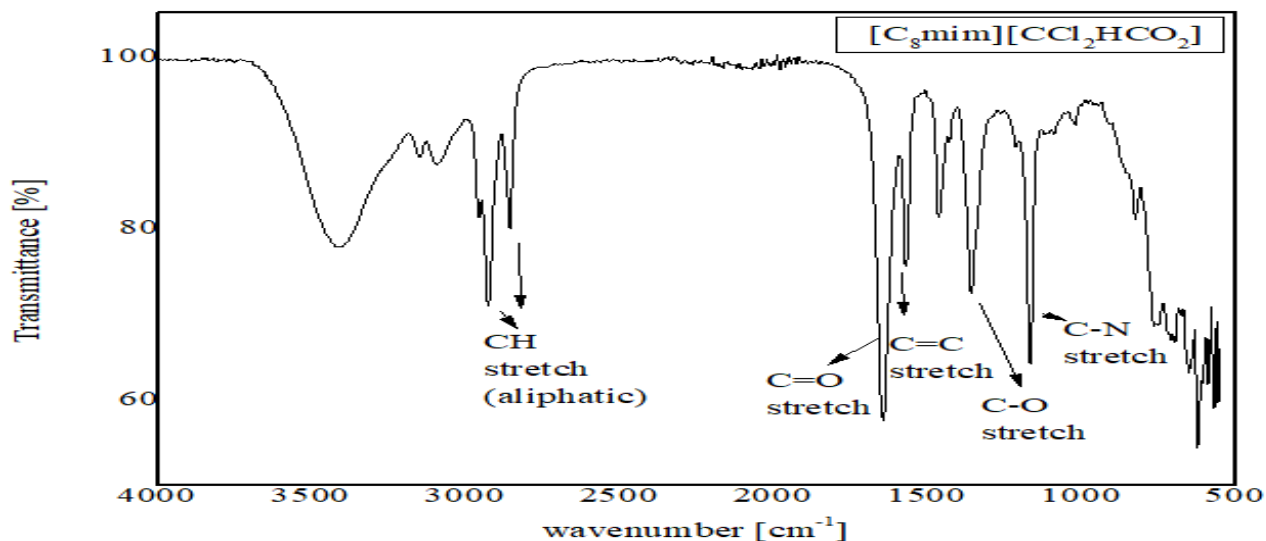


Figure 4.4 FTIR spectrum of [C₈mim][CHCl₂CO₂]

Band at 1644 cm⁻¹ indicate stretching vibration of C=O and band at 1358 cm⁻¹ shows stretching vibration for C-O these band indicated formation of 3-Octyl-1-methylimidazolium dichloroacetate [C₈mim][CHCl₂CO₂].

4.2.5. FT-IR analysis of 1-Methyl-3-octylimidazolium tetrafluoroborate [C₈mim][BF₄]

Strong band appearance at 1049 cm⁻¹ confirm presence of BF₄ anion so indicated formation of 1-Methyl-3-octylimidazolium tetrafluoroborate [C₈mim][BF₄] in fig. 4.5.

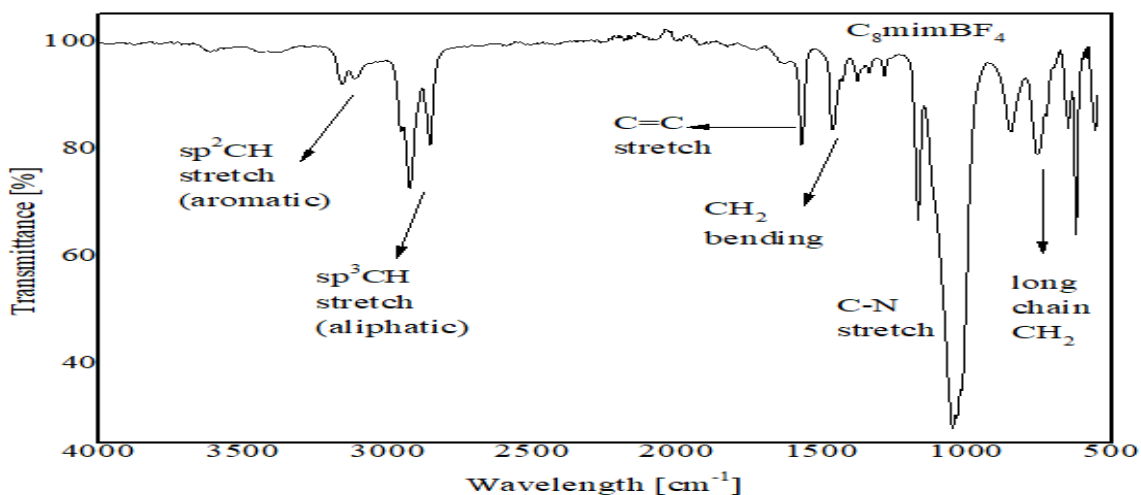


Figure 4.5 FTIR spectrum of [C₈mim][BF₄]

At 3120 cm⁻¹ band appeared is due to aromatic CH stretching vibrations, 2924 cm⁻¹ and 2854 cm⁻¹ peaks are stretching vibrations of CH for aliphatic sp³ CH₂ and CH₃ respectively. Band at 1569 cm⁻¹ show stretching vibration of C=C and bending vibrations for CH₂ are at 1463 cm⁻¹

strong peak at 1165 cm^{-1} appear due to stretching vibration of C-N of imidazolium ring. At 752 cm^{-1} peak appearance indicates presence of long chain CH_2 octyl group.

4.2.6. FT-IR analysis for 1-Methyl-3-Octylimidazolium hydrogen sulphate $[\text{C}_8\text{mim}][\text{HSO}_4]$

FT-IR for 1-Methyl-3-Octylimidazolium hydrogen sulphate $[\text{C}_8\text{mim}][\text{HSO}_4]$ is shown in figure. 4.6 At 3120 cm^{-1} band appeared is due to aromatic CH stretching vibrations, 2958 cm^{-1} and 2854 cm^{-1} peaks are stretching vibrations of CH for aliphatic $\text{sp}^3\text{ CH}_2$ and CH_3 respectively. Band at 1567 cm^{-1} show stretching vibration of C=C and bending vibrations for CH_2 are at 1463 cm^{-1} strong peak at 1165 cm^{-1} appear due to stretching vibration of C-N of imidazolium ring. At 752 cm^{-1} peak appearance indicates presence of long chain CH_2 of octyl group.

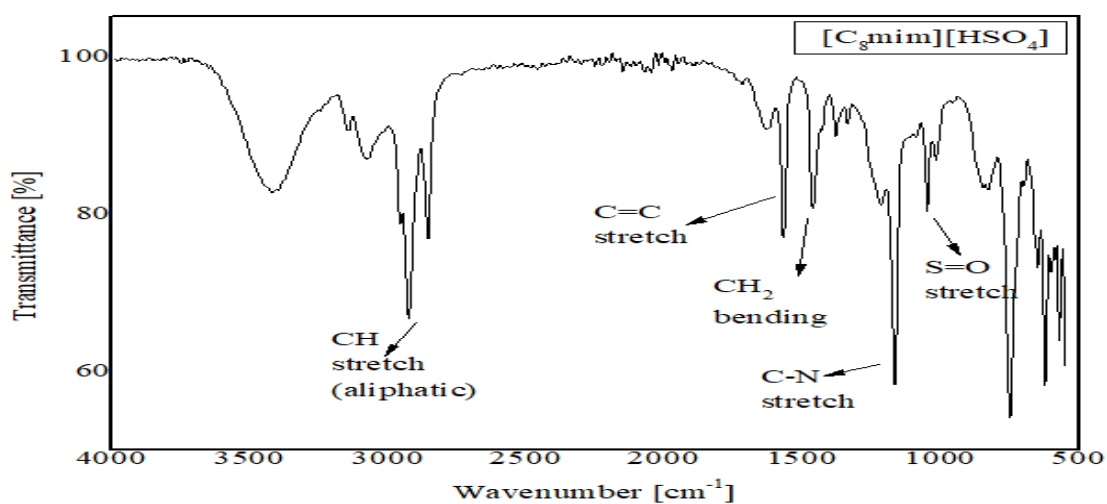


Figure 4.6 FTIR spectrum of $[\text{C}_8\text{mim}][\text{HSO}_4]$

Formation of 1-Methyl-3-Octylimidazolium hydrogen sulphate was indicated by FT-IR due to peak appearance of S=O at 1047 cm^{-1} .

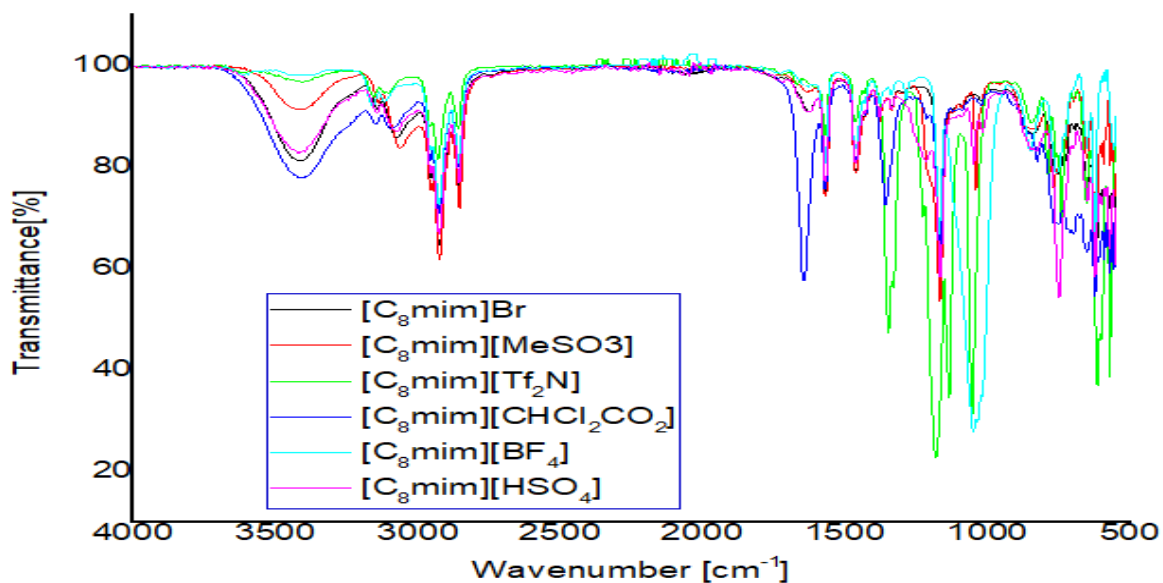


Figure 4.7 FTIR for comparison of different exchanged anions with [C₈mim]

4.2.7. FT-IR analysis for 1-Methyl-3-butylimidazolium bromide [C₄mim]Br

FT-IR for 1-Methyl-3-butylimidazolium bromide is shown in fig. 4.8 At 3120 cm⁻¹ band appeared is due to aromatic CH stretching vibrations, 2958 cm⁻¹ and 2854 cm⁻¹ peaks are stretching vibrations of CH for aliphatic sp³ CH₂ and CH₃ respectively. A band appearing at 1650 cm⁻¹ show C=N stretching vibrations of imidazolium ring, Band at 1567 cm⁻¹ show stretching vibration of C=C and bending vibrations for CH₂ are at 1463 cm⁻¹ strong, peak at 1165 cm⁻¹ appear due to stretching vibration of C-N of imidazolium ring. At 752 cm⁻¹ peak appearance indicates presence of long chain CH₂ of butyl group.

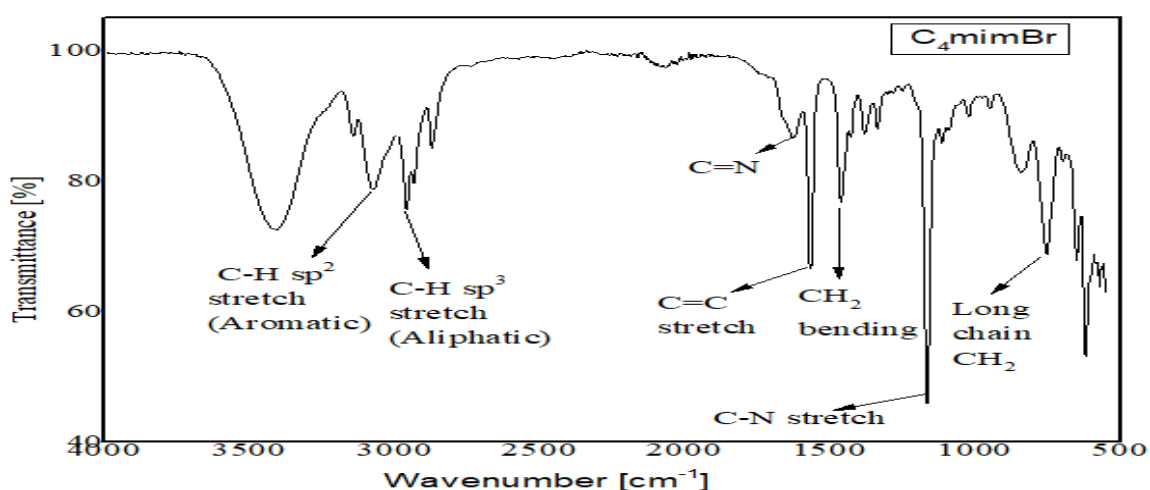


Figure 4.8 FT-IR spectrum [C₄mim]Br

4.2.8. FT-IR analysis of 1-Methyl-3-butylimidazolium methanesulphonate [C₄mim][MeSO₃]

1-Methyl-3-butylimidazolium methane sulphonate [C₄mim][MeSO₃] FT-IR is shown in fig.4.9 At 3120 cm⁻¹ band appeared is due to aromatic CH stretching vibrations, 2958 cm⁻¹ and 2854 cm⁻¹ peaks are stretching vibrations of CH for aliphatic sp³ CH₂ and CH₃ respectively. A band appearing at 1650 cm⁻¹ show C=N stretching vibrations of imidazolium ring, Band at 1567 cm⁻¹ show stretching vibration of C=C and bending vibrations for CH₂ are at 1463 cm⁻¹, strong peak at 1165 cm⁻¹ appear due to stretching vibration of C-N of imidazolium ring. At 752 cm⁻¹ peak appearance indicates presence of long chain CH₂ of butyl group.

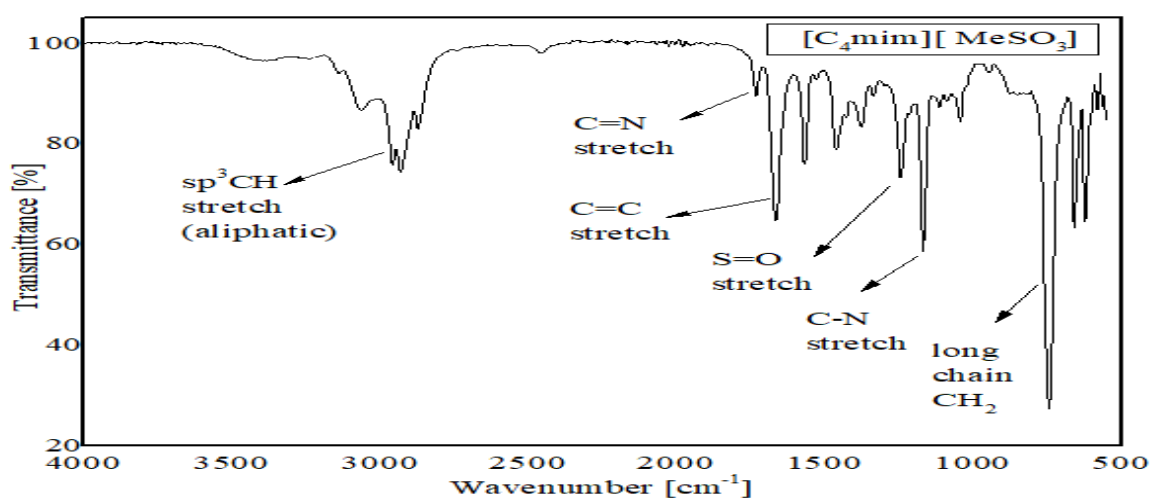


Figure 4.9 FT-IR spectrum of [C₄mim][MeSO₃]

Formation of 1-Methyl-3-butylimidazolium methane sulphonate was indicated by FT-IR due to peak appearance of S=O at 1200 cm⁻¹.

4.2.9. FT-IR analysis of 1-Methyl-3-butylimidazolium Bis(trifluoromethane-sulfonyl) Imide [C₄mim][Tf₂N]

1-Methyl-3-butylimidazolium Bis(trifluoromethane-sulfonyl)imide [C₈mim][Tf₂N] formation was indicated by FT-IR due to appearance of peaks at 1346 cm⁻¹ indicating asymmetric stretching vibration of S=O and at 1180 cm⁻¹ symmetric stretching vibration of S=O in fig. 4.10. Band at 2929 cm⁻¹ and 2854 cm⁻¹ indicate stretching vibrations of CH₂ and CH₃ respectively. Band at 1569 cm⁻¹ show stretching vibration of C=C and bending vibrations for CH₂ are at 1463 cm⁻¹ peak, at 1165 cm⁻¹ and at 740 cm⁻¹ peak appearance indicates presence of long chain CH₂ butyl group.

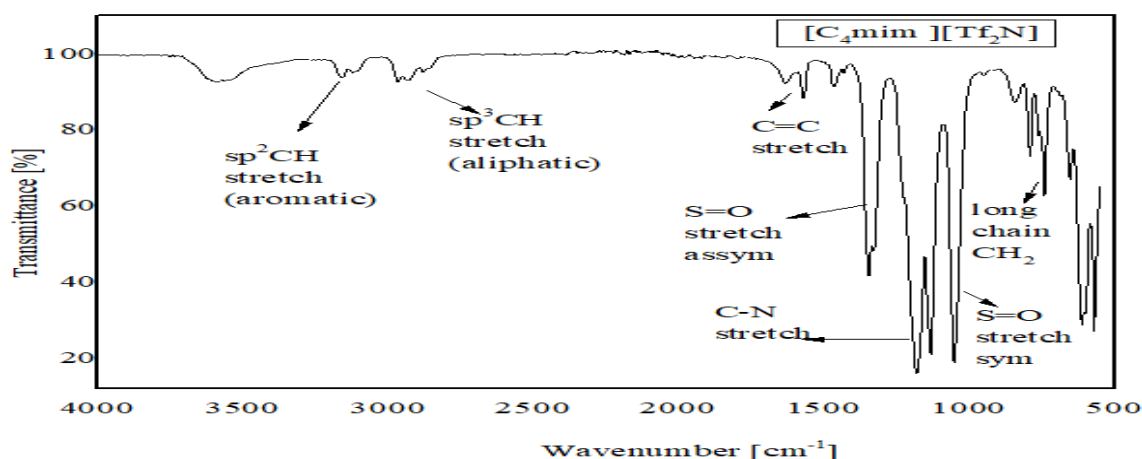


Figure 4.10 FTIR spectrum $[C_8mim][Tf_2N]$

4.2.10. FT-IR analysis for 3-Butyl-1-methylimidazolium dichloroacetate $[C_4mim][CHCl_2CO_2]$

In fig. 4.11 band at 1633 cm^{-1} indicate stretching vibration of C=O and band at 1375 cm^{-1} shows stretching vibration for C-O these band indicate formation of 3-Butyl-1-methylimidazolium dichloroacetate $[C_4mim][CHCl_2CO_2]$. Band at 1569 cm^{-1} show stretching vibration of C=C and bending vibrations for CH_2 are at 1463 cm^{-1} , peak at 1165 cm^{-1} appear due to stretching vibration of C-N of imidazolium ring, at 740 cm^{-1} peak appearance indicates presence of long chain CH_2 butyl group.

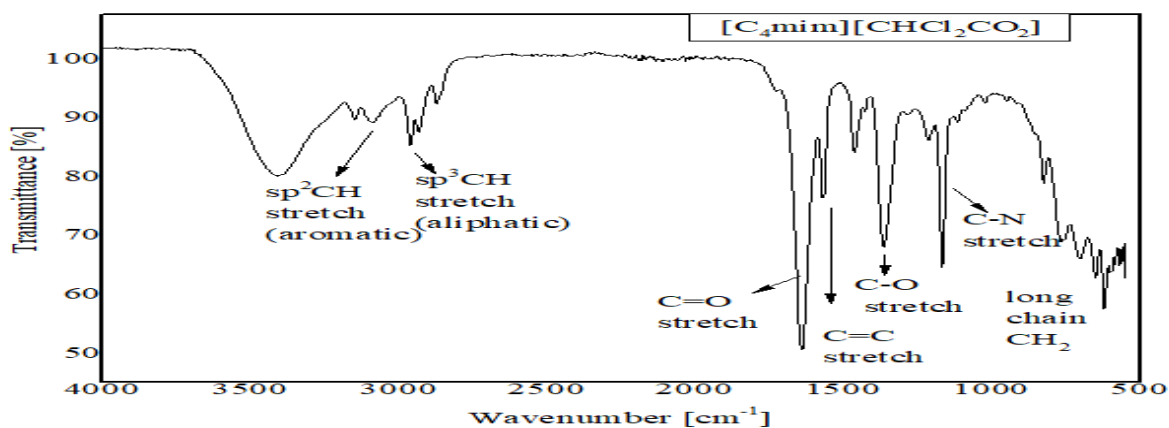


Figure 4.11 FTIR spectrum of $[C_4mim][CHCl_2CO_2]$.

4.2.11. FT-IR analysis of 1-Methyl-3-butylimidazolium tetrafluoroborate $[C_4mim][BF_4]$

fig. 4.12. indicates formation of 1-Methyl-3-butylimidazolium tetrafluoroborate $[C_4mim][BF_4]$

At 3120 cm^{-1} band appeared is due to aromatic CH stretching vibrations, 2924 cm^{-1} and 2854 cm^{-1} peaks are stretching vibrations of CH for aliphatic sp^3CH_2 and CH_3 respectively. Band at 1573 cm^{-1} show stretching vibration of C=C and bending vibrations for CH_2 are at 1463 cm^{-1} strong peak at 1169 cm^{-1} appear due to stretching vibration of C-N of imidazolium ring. At 752 cm^{-1} peak appearance indicates presence of long chain CH_2 butyl group.

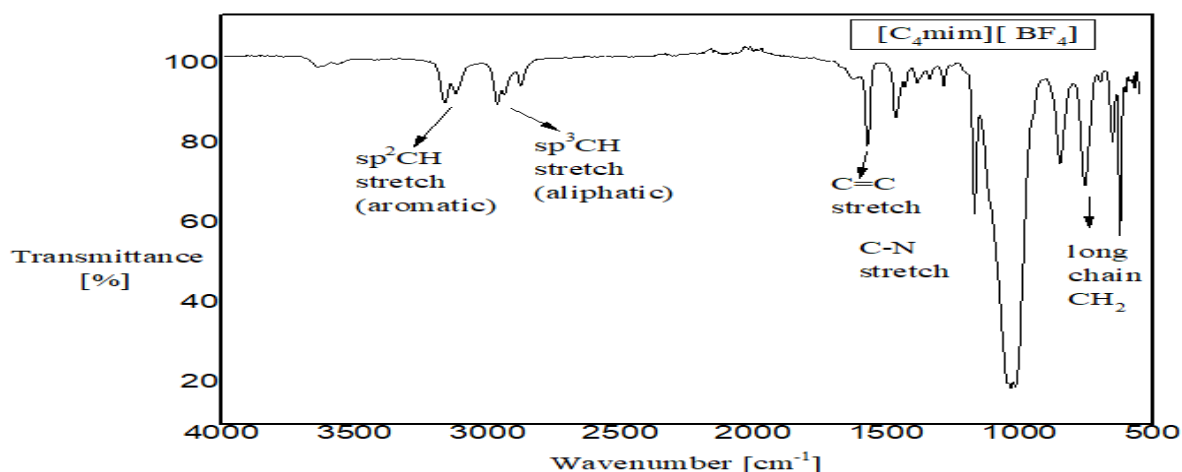


Figure 4.12 FTIR spectrum of [C₄mim][BF₄].

4.2.12. FT-IR analysis for 1-Methyl-3-butylimidazolium hydrogen sulphate [C₄mim][HSO₄]

Formation of 1-Methyl-3-butylimidazolium hydrogen sulphate was indicated by FT-IR in fig. 4.13 due to peak appearance of S=O at 1047 cm^{-1} . At 3120 cm^{-1} band appeared is due to aromatic CH stretching vibrations, 2958 cm^{-1} and 2854 cm^{-1} peaks are stretching vibrations of CH for aliphatic sp^3CH_2 and CH_3 respectively. Band at 1567 cm^{-1} show stretching vibration of C=C and bending vibrations for CH_2 are at 1463 cm^{-1} strong peak at 1165 cm^{-1} appear due to stretching vibration of C-N of imidazolium ring. At 752 cm^{-1} peak appearance indicates presence of long chain CH_2 of butyl group.

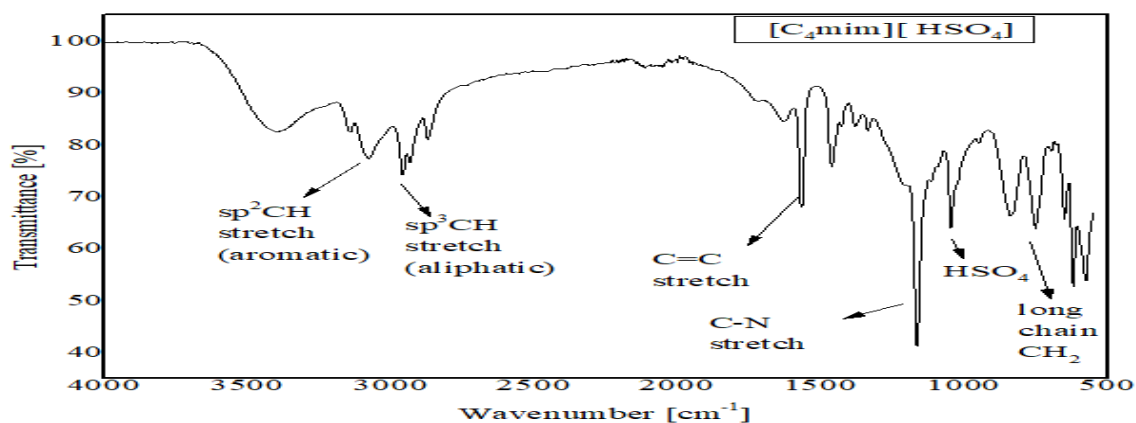


Figure 4.13 FTIR spectrum of [C4mim][HSO4]

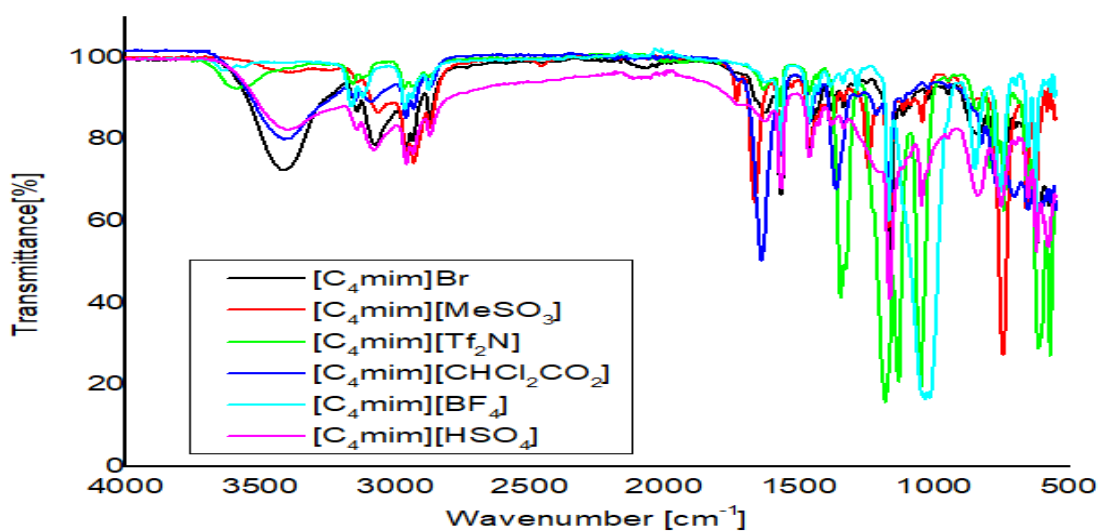


Figure 4.14 FTIR for comparison of different exchanged anions with [C4mim]

4.2.13. FT-IR analysis for Octyl pyridinium bromide [C8py]Br

FT-IR for Octyl pyridinium bromide is shown in fig.4.15 At 3120 cm^{-1} band appeared is due to aromatic CH stretching vibrations, 2924 cm^{-1} and 2855 cm^{-1} peaks are stretching vibrations of CH for aliphatic sp^3CH_2 and CH_3 respectively. A band appearing at 1633 cm^{-1} show C=N stretching vibrations of pyridinium ring, Band at 1569 cm^{-1} show stretching vibration of C=C and bending vibrations for CH_2 are at 1486 cm^{-1} strong peak at 1172 cm^{-1} appear due to stretching vibration of C-N of pyridinium ring. At 774 cm^{-1} peak appearance indicates presence of long chain CH_2 of octyl group.

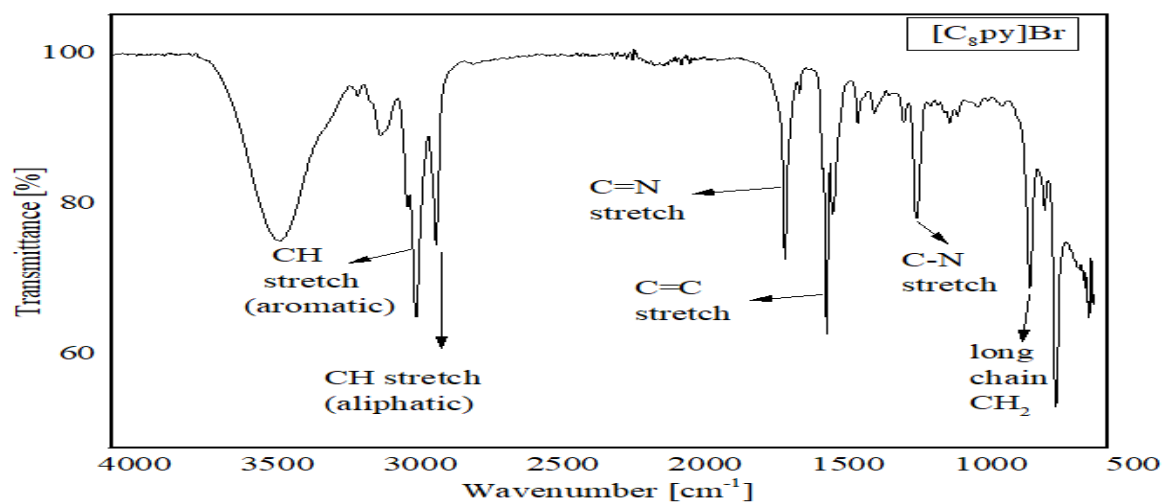


Figure 4.15 FTIR spectrum of $[C_8py][Br]$

4.2.14. FT-IR analysis for Octyl pyridinium bromide $[C_8py][MeSO_3]$

FT-IR for Octyl pyridinium methane sulphonate is shown in fig. 4.16. At 3120 cm^{-1} band appeared is due to aromatic CH stretching vibrations, 2924 cm^{-1} and 2855 cm^{-1} peaks are stretching vibrations of CH for aliphatic $sp^3\text{ CH}_2$ and CH_3 respectively. A band appearing at 1633 cm^{-1} show C=N stretching vibrations of pyridinium ring, Band at 1569 cm^{-1} show stretching vibration of C=C and bending vibrations for CH_2 are at 1487 cm^{-1} strong peak at 1174 cm^{-1} appear due to stretching vibration of C-N of pyridinium ring. S=O stretching vibration at 1042 cm^{-1} shows the exchange of methane sulphonate anion. At 774 cm^{-1} peak appearance indicates presence of long chain CH_2 of octyl group.

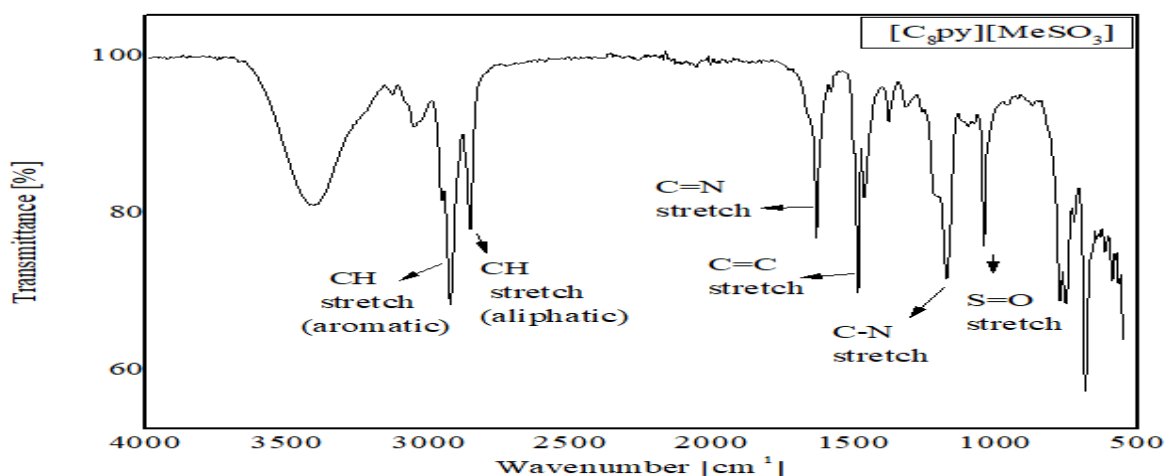


Figure 4.16 FTIR spectrum of $[C_8py][MeSO_3]$

4.2.15. FT-IR analysis for Octyl pyridinium Bis(trifluoromethane-sulfonyl)imide [C₈py]Tf₂N

FT-IR for Octyl pyridinium Bis(trifluoromethane-sulfonyl)imide [C₈mim][Tf₂N] is shown in fig.4.17 At 2924 cm⁻¹ and 2855 cm⁻¹ peaks are stretching vibrations of CH for aliphatic sp³ CH₂ and CH₃ respectively. A band appearing at 1633 cm⁻¹ show C=N stretching vibrations of pyridinium ring, Band at 1569 cm⁻¹ show stretching vibration of C=C and strong peak at 1172 cm⁻¹ appear due to stretching vibration of C-N of pyridinium ring. Bands at 1345 cm⁻¹ and at 1052 cm⁻¹ are stretching vibrations for S=O. At 774 cm⁻¹ peak appearance indicates presence of long chain CH₂ of octyl group.

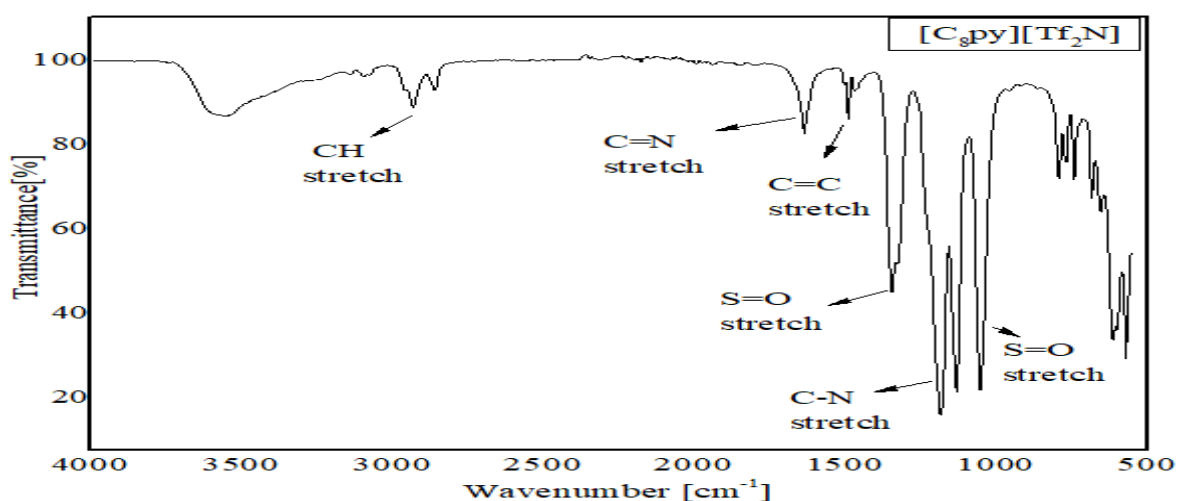


Figure 4.17 FTIR spectrum of [C₈mim][Tf₂N]

4.2.16. FT-IR analysis for Octyl pyridinium dichloroacetate [C₈py][CHCl₂CO₂]

FT-IR for Octyl pyridinium bromide is shown in fig. 4.18 At 3120 cm⁻¹ band appeared is due to aromatic CH stretching vibrations, 2925 cm⁻¹ and 2855 cm⁻¹ peaks are stretching vibrations of CH for aliphatic sp³ CH₂ and CH₃ respectively. A band appearing at 1633 cm⁻¹ show C=O stretching vibration, Band at 1569 cm⁻¹ show stretching vibration of C=C and bending vibrations for CH₂ are at 1486 cm⁻¹. At 1368 peak appearance confirm product formation as it shows stretching vibration of C-O, peak at 1172 cm⁻¹ appear due to stretching vibration of C-N of pyridinium ring. At 772 cm⁻¹ peak appearance indicates presence of long chain CH₂ of octyl group.

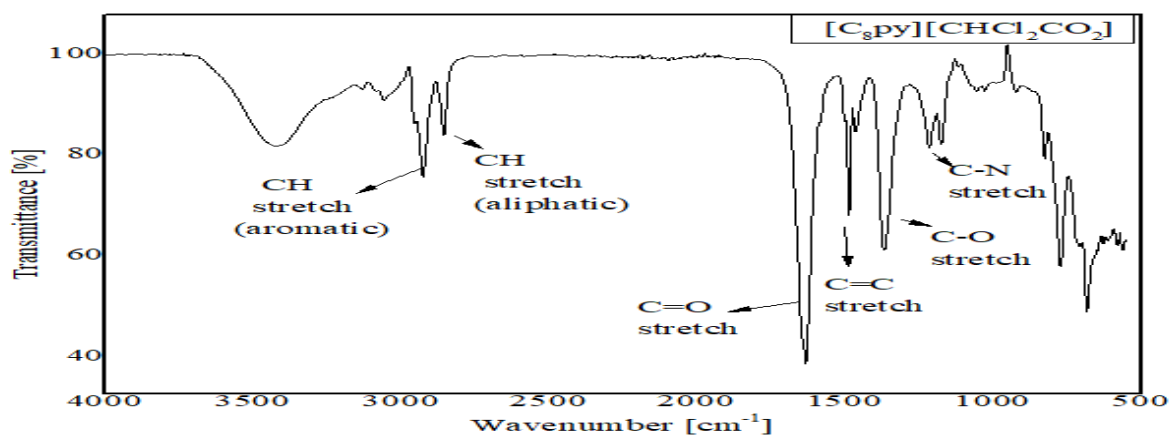


Figure 4.18 FTIR spectrum of $[C_8py][CHCl_2CO_2]$

1633 cm^{-1} indicate stretching vibration of C=O and band at 1358 cm^{-1} shows stretching vibration for C-O these band indicate formation of 3-Butyl-1-methylimidazolium dichloroacetate $[C_8py][CHCl_2CO_2]$

4.2.17. FT-IR analysis for Octyl pyridinium tetrafluoroborate $[C_8py][BF_4]$.

FT-IR for Octyl pyridinium tetrafluoroborate $[C_8py][BF_4]$ is shown in fig.4.19 At 2926 cm^{-1} and 2855 cm^{-1} peaks are stretching vibrations of CH for aliphatic sp^3 CH_2 and CH_3 respectively. A band appearing at 1633 cm^{-1} show C=N stretching vibrations of pyridinium ring, Band at 1569 cm^{-1} show stretching vibration of C=C and bending vibrations for CH_2 are at 1489 cm^{-1} peak at 1172 cm^{-1} appear due to stretching vibration of C-N of pyridinium ring. At 774 cm^{-1} peak appearance indicates presence of long chain CH_2 of octyl group.

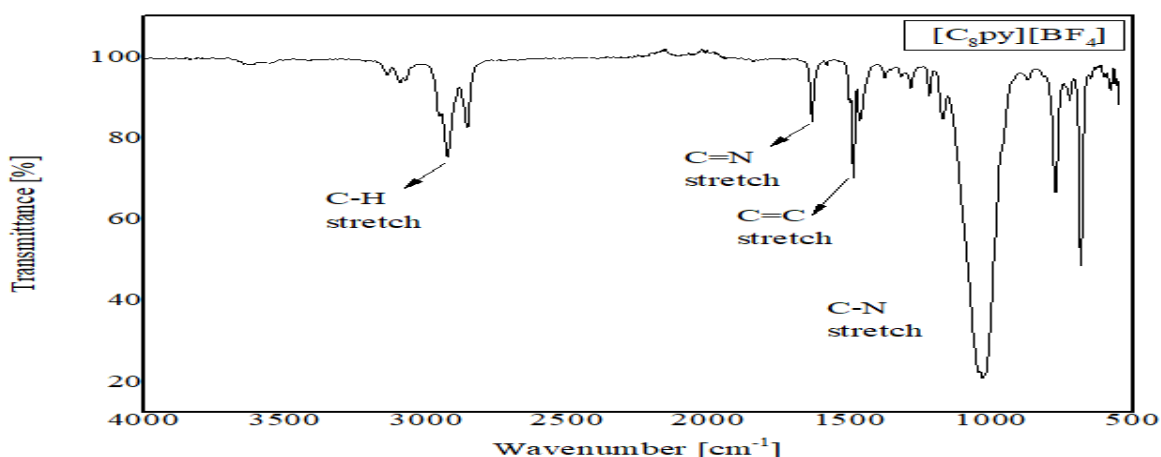


Figure 4.19 FTIR spectrum of $[C_8py][BF_4]$

Strong band appearance at 1033 cm^{-1} confirm presence of BF_4 anion so indicating formation of Octyl pyridinium tetrafluoroborate $[C_8mim][BF_4]$.

4.2.18. FT-IR analysis for Octyl pyridinium bromide [C₈py][HSO₄]

FT-IR for Octyl pyridinium hydrogen sulphate is shown in fig. 4.20 At 3120 cm⁻¹ band appeared is due to aromatic CH stretching vibrations, 2923 cm⁻¹ and 2854 cm⁻¹ peaks are stretching vibrations of CH for aliphatic sp³ CH₂ and CH₃ respectively. A band appearing at 1632 cm⁻¹ show C=N stretching vibrations of pyridinium ring, Band at 1569 cm⁻¹ show stretching vibration of C=C and bending vibrations for CH₂ are at 1486 cm⁻¹ strong peak at 1169 cm⁻¹ appear due to stretching vibration of C-N of pyridinium ring. At 1046 peak appearance show stretching vibration of S=O of HSO₄ anion and then at 774 cm⁻¹ peak appearance indicates presence of long chain CH₂ of octyl group.

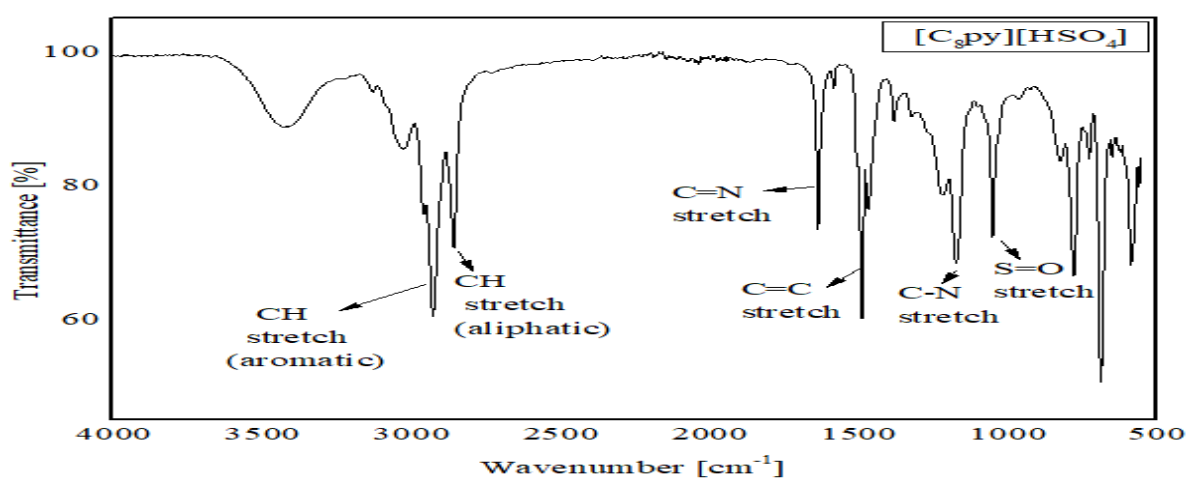


Figure 4.20 FTIR spectrum of [C₈py][HSO₄]

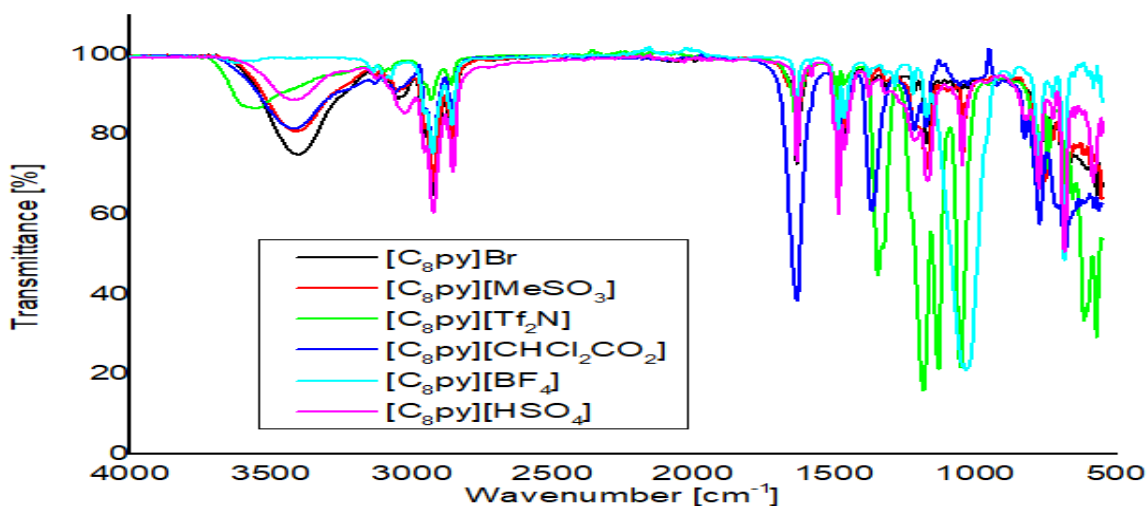


Figure 4.21 FTIR for comparison of different exchanged anions with [C₈py]

4.2.19. FT-IR analysis for Butyl pyridinium bromide [C₄py]Br

FT-IR for Butyl pyridinium bromide is shown in fig.4.22 At 3120 cm⁻¹ band appeared is due to aromatic CH stretching vibrations, 2960 cm⁻¹ and 2855 cm⁻¹ peaks are stretching vibrations of CH for aliphatic sp³ CH₂ and CH₃ respectively. A band appearing at 1632 cm⁻¹ show C=N stretching vibrations of pyridinium ring, Band at 1569 cm⁻¹ show stretching vibration of C=C and bending vibrations for CH₂ are at 1486 cm⁻¹ strong peak at 1170 cm⁻¹ appear due to stretching vibration of C-N of pyridinium ring. At 770 cm⁻¹ peak appearance indicates presence of long chain CH₂ of butyl group.

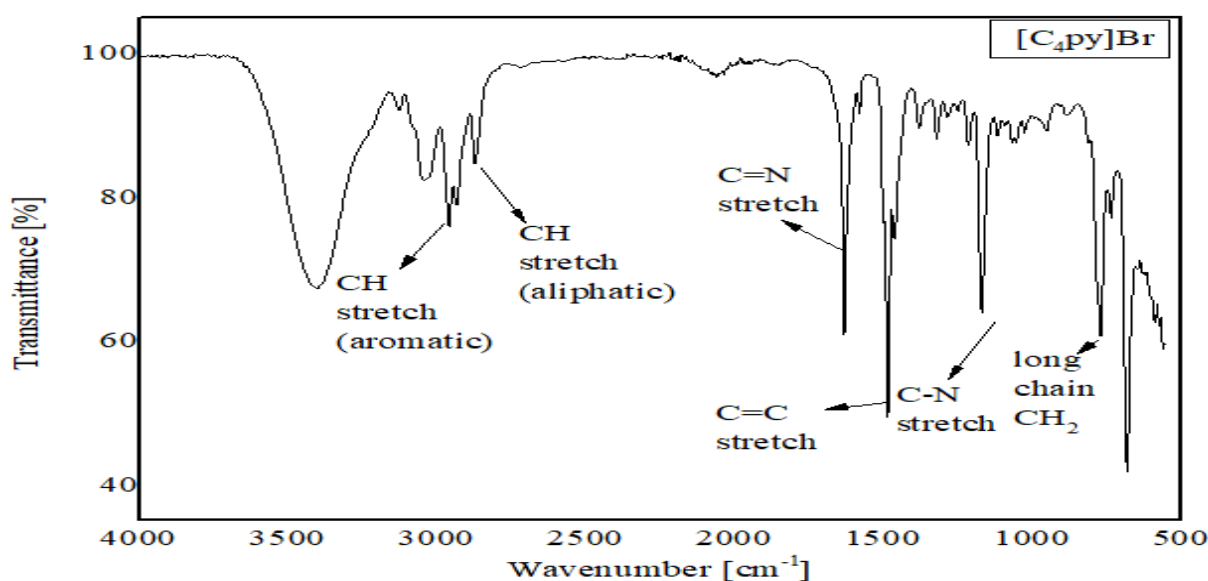


Figure 4.22 FTIR spectrum of [C₄py][Br]

4.2.20. FT-IR analysis for Butyl pyridinium bromide [C₄py][MeSO₃]

FT-IR for Butyl pyridinium methane sulphonate is shown in fig.4.23 At 2924 cm⁻¹ and 2855 cm⁻¹ peaks are stretching vibrations of CH for aliphatic sp³ CH₂ and CH₃ respectively. A band appearing at 1633 cm⁻¹ show C=N stretching vibrations of pyridinium ring, Band at 1569 cm⁻¹ show stretching vibration of C=C and bending vibrations for CH₂ are at 1487 cm⁻¹ strong peak at 1174 cm⁻¹ appear due to stretching vibration of C-N of pyridinium ring.

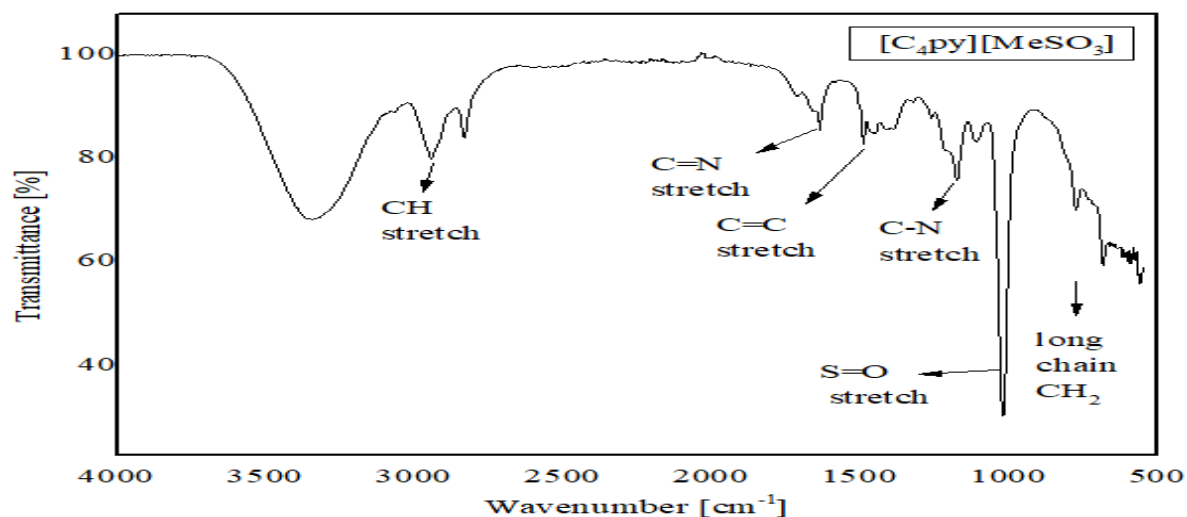


Figure 4.23 FTIR spectrum of [C₄py][MeSO₃]

S=O stretching vibration at 1042 cm⁻¹ shows the replacement of methane sulphonate anion with bromide. At 774 cm⁻¹ peak appearance indicates presence of long chain CH₂ of butyl group.

4.2.21. FT-IR analysis for Butyl pyridinium Bis(trifluoromethane-sulfonyl)imide [C₄py]Tf₂N

FT-IR for Butyl pyridinium Bis(trifluoromethane-sulfonyl)imide [C₄mim][Tf₂N] is shown in fig.4.24. A band appearing at 1636 cm⁻¹ shows C=N stretching vibrations of pyridinium ring. Band at 1569 cm⁻¹ shows stretching vibration of C=C and strong peak at 1172 cm⁻¹ appears due to stretching vibration of C-N of pyridinium ring. Bands at 1346 cm⁻¹ and at 1051 cm⁻¹ are stretching vibrations for S=O. At 740 cm⁻¹ peak appearance indicates presence of long chain CH₂ of butyl group.

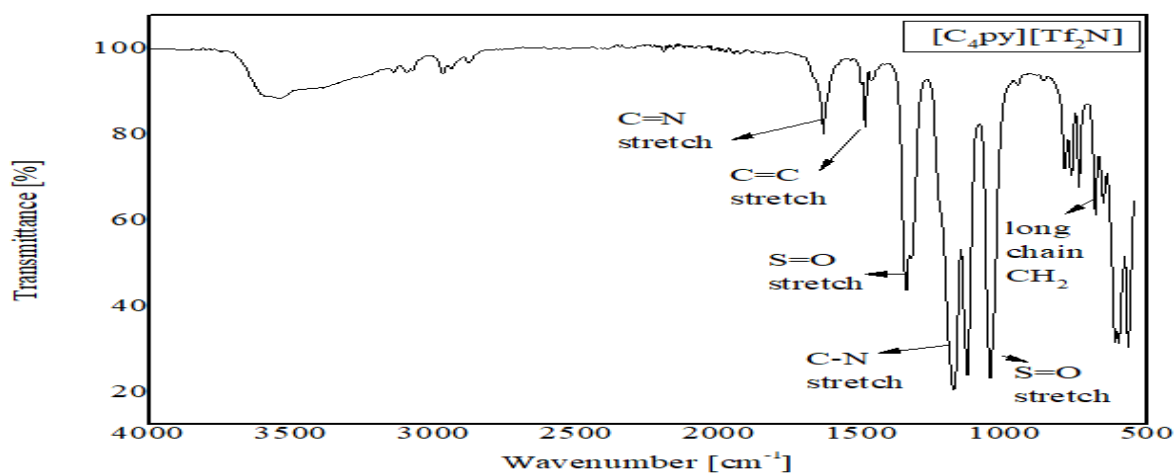


Figure 4.24 FTIR spectrum of [C₄mim][Tf₂N]

4.2.22. FT-IR analysis for Butyl pyridinium dichloroacetate [C₄py][CHCl₂CO₂]

FT-IR for Butyl pyridinium bromide is shown in fig.4.25 At 2962 cm⁻¹ and 2855 cm⁻¹ peaks are stretching vibrations of CH for aliphatic sp³ CH₂ and CH₃ respectively. A band appearing at 1633 cm⁻¹ show C=O stretching vibration, Band at 1569 cm⁻¹ show stretching vibration of C=C and bending vibrations for CH₂ are at 1486 cm⁻¹. At 1370 peak appearance confirm product formation as it shows stretching vibration of C-O, peak at 1172 cm⁻¹ appear due to stretching vibration of C-N of pyridinium ring. At 769 cm⁻¹ peak appearance indicates presence of long chain CH₂ of butyl group.

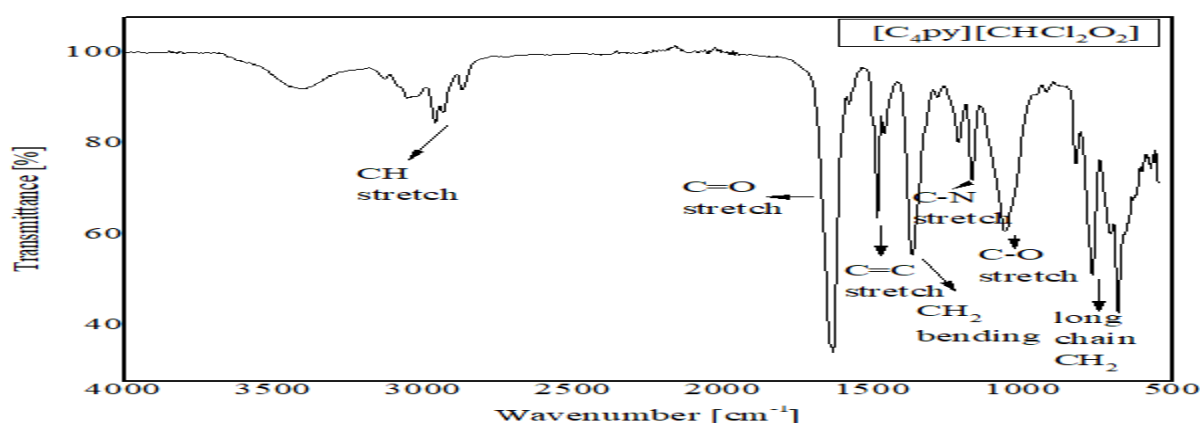


Figure 4.25 FTIR spectrum of [C₄py][CHCl₂CO₂]

4.2.23. FT-IR analysis for Butyl pyridinium tetrafluoroborate [C₄py][BF₄].

FT-IR for Butyl pyridinium tetrafluoroborate [C₄py][BF₄] is shown in fig.4.26 At 2926 cm⁻¹ and 2855 cm⁻¹ peaks are stretching vibrations of CH for aliphatic sp³ CH₂ and CH₃ respectively. A band appearing at 1635 cm⁻¹ show C=N stretching vibrations of pyridinium ring, Band at 1569 cm⁻¹ show stretching vibration of C=C and bending vibrations for CH₂ are at 1489 cm⁻¹ peak at 1172 cm⁻¹ appear due to stretching vibration of C-N of pyridinium ring. At 771 cm⁻¹ peak appearance indicates presence of long chain CH₂ of butyl group.

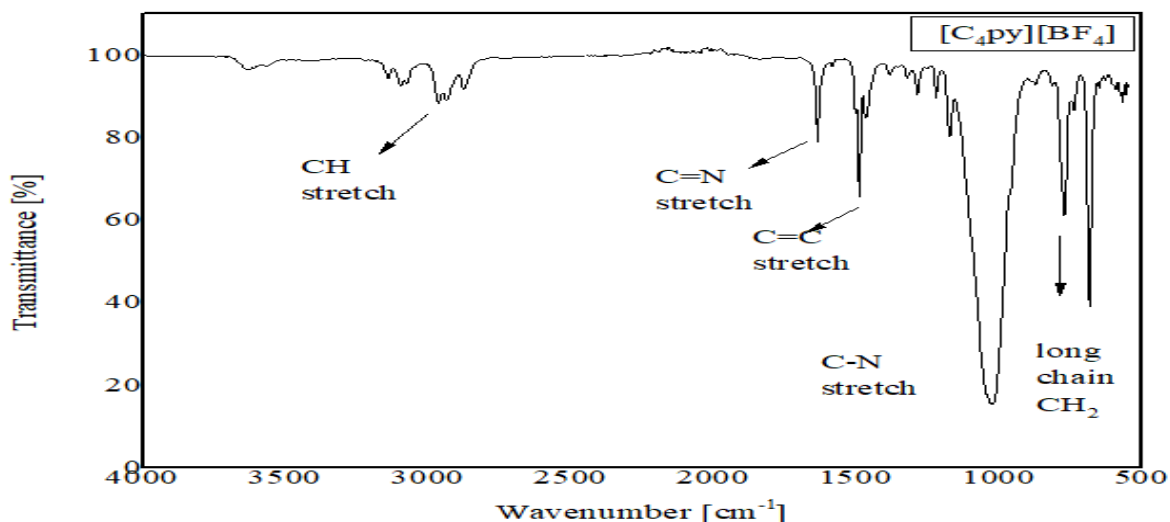


Figure 4.26 FTIR spectrum of [C₄py][BF₄]

Strong band appearance at 1049 cm⁻¹ confirm presence of BF₄ anion so indicating formation of 1-Methyl-3-octylimidazolium tetrafluoroborate [C₈mim][BF₄].

4.2.24. FT-IR analysis for Butyl pyridinium hydrogen sulphate [C₄py][HSO₄]

FT-IR for Butyl pyridinium hydrogen sulphate is shown in fig.4.27 At 3120 cm⁻¹ band appeared is due to aromatic CH stretching vibrations, 2923 cm⁻¹ and 2854 cm⁻¹ peaks are stretching vibrations of CH for aliphatic sp³ CH₂ and CH₃ respectively. A band appearing at 1632 cm⁻¹ show C=N stretching vibrations of pyridinium ring, Band at 1569 cm⁻¹ show stretching vibration of C=C and bending vibrations for CH₂ are at 1486 cm⁻¹ strong peak at 1169 cm⁻¹ appear due to stretching vibration of C-N of pyridinium ring. At 1046 peak appearance show stretching vibration of S=O of HSO₄ anion and then at 774 cm⁻¹ peak appearance indicates presence of long chain CH₂ of butyl group.

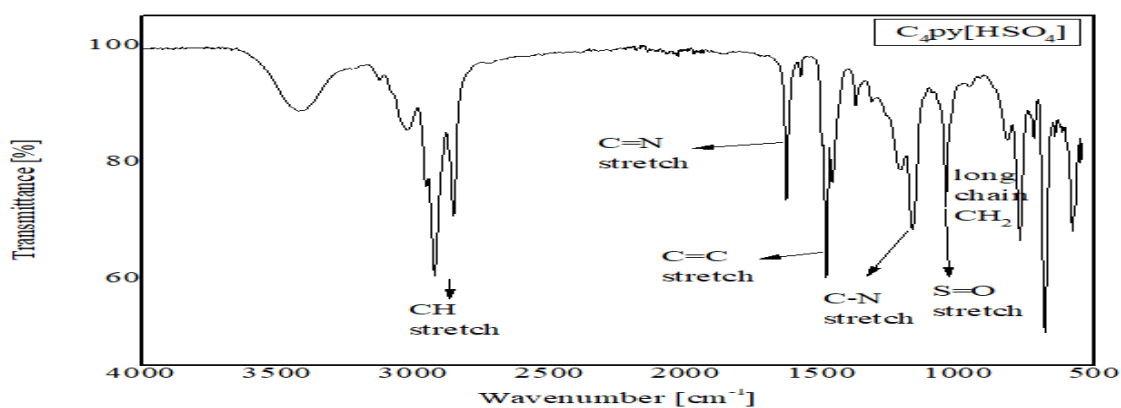


Figure 4.27 FTIR spectrum of [C₄py][HSO₄]

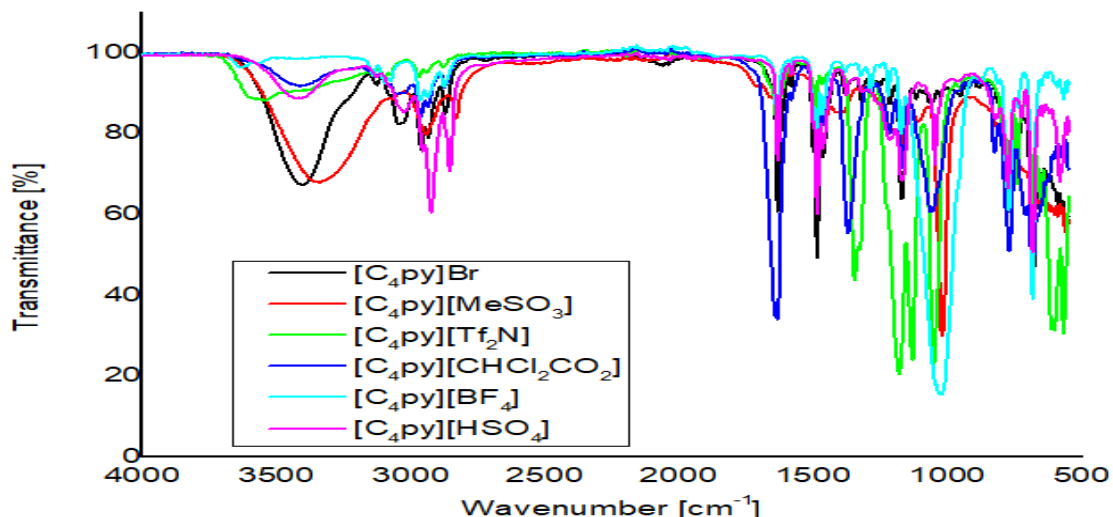


Figure 4.28 FTIR for comparison of different exchanged anions with [C₄py]

4.2.25. FT-IR analysis of Mono-butyl tri-octyl phosphonium Bromide [P₄₈₈₈][Br]

FT-IR for Mono-butyl tri-octyl phosphonium Bromide [P₄₈₈₈][Br] is shown in fig.4.29. At 2960 cm⁻¹ and 2854 cm⁻¹ peaks are stretching vibrations of CH for aliphatic sp³ CH₂ and CH₃ respectively and bending vibrations for CH₂ are at 1463 cm⁻¹. At 746 cm⁻¹ peak appearance indicates presence of long chain CH₂ in butyl and octyl groups attached to phosphorous.

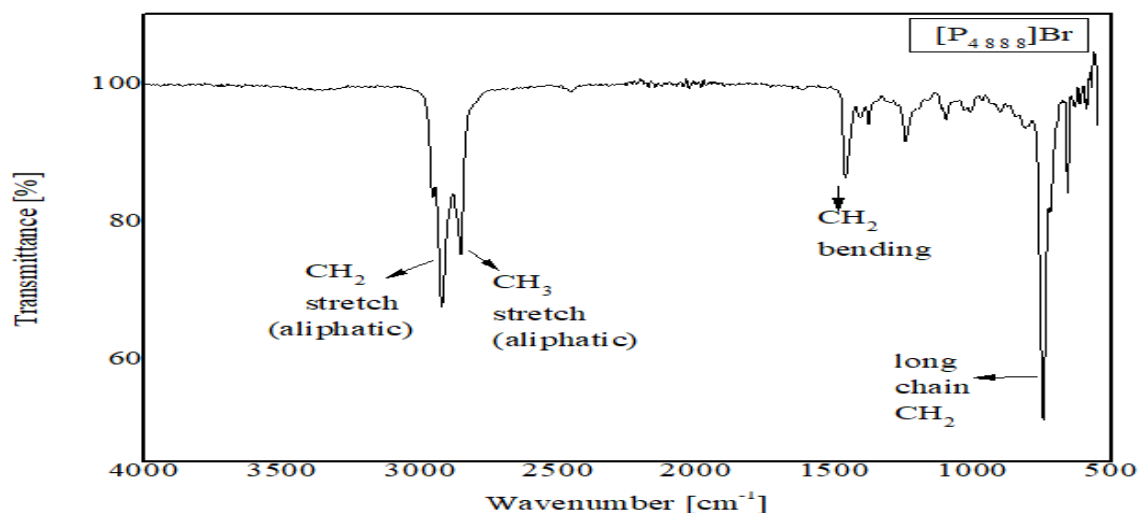


Figure 4.29 FT-IR spectrum of [P₄₈₈₈][Br]

4.2.26. FT-IR analysis of Mono-butyl tri-octyl phosphonium methane sulphonate [P₄₈₈₈][MeSO₃]

FT-IR for Mono-butyl tri-octyl phosphonium methane sulphonate [P₄₈₈₈][MeSO₃] is shown in fig. 4.30. At 2920 cm⁻¹ and 2854 cm⁻¹ peaks are stretching vibrations of CH for aliphatic

sp^3 CH_2 and CH_3 respectively and bending vibrations for CH_2 are at 1461 cm^{-1} . At 749 cm^{-1} peak appearance indicates presence of long chain CH_2 in butyl and octyl groups attached to phosphorous.

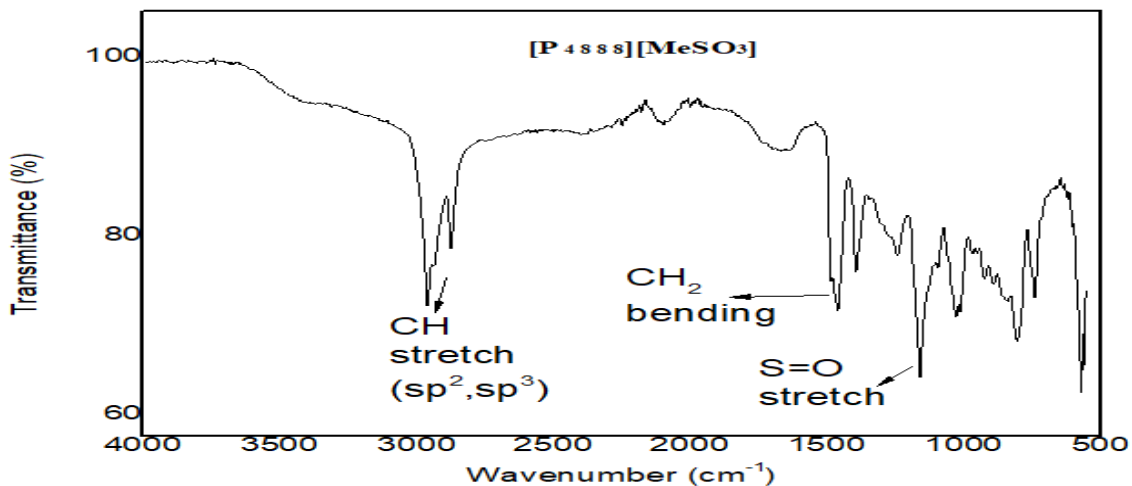


Figure 4.30 FTIR spectrum of $[P_{4888}][MeSO_3]$

4.2.27. FT-IR analysis of Mono-butyl tri-octyl phosphonium Bis(trifluoromethane-sulfonyl) imide $[N_{2244}][Tf_2N]$

FT-IR shown in fig. 4.31 is for Mono-butyl tri-octyl phosphonium Bis(trifluoromethane-sulfonyl)imide $[N_{2244}][Tf_2N]$. At 2929 cm^{-1} and 2854 cm^{-1} peaks are stretching vibrations of CH for aliphatic sp^3 CH_2 and CH_3 respectively and bending vibrations for CH_2 are at 1463 cm^{-1} . S=O stretching vibration at 1347 cm^{-1} and at 1056 cm^{-1} are present indicating replacement of Bis(trifluoromethane-sulfonyl)imide with bromide anion. At 746 cm^{-1} peak appearance indicates presence of long chain CH_2 in butyl and octyl groups attached to phosphorous.

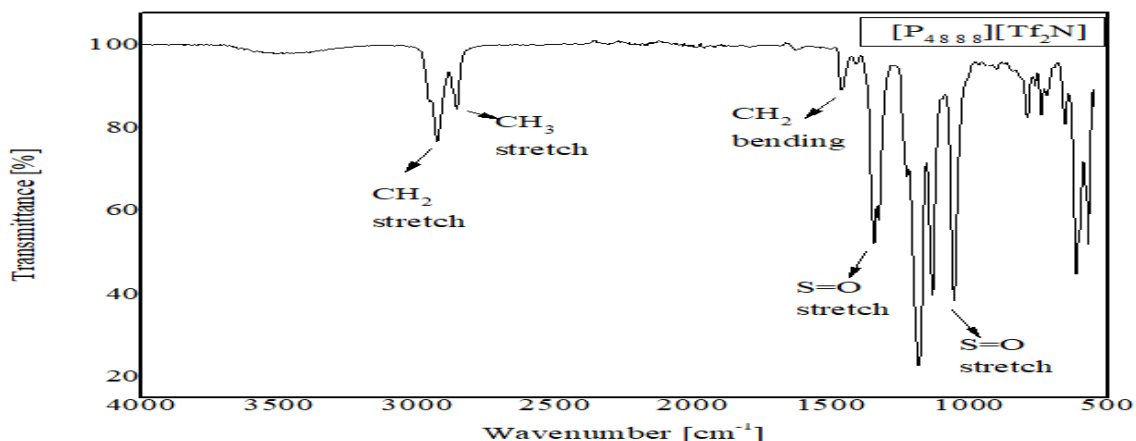


Figure 4.31 FTIR spectrum of [P₄₈₈₈][Tf₂N]

4.2.28. FT-IR analysis of Butyl-Tri-octyl phosphonium dichloroacetate

[P₄₈₈₈][CHCl₂CO₂]

FT-IR for Mono-butyl tri-octyl phosphonium dichloroacetate [P₄₈₈₈][CHCl₂CO₂] is shown in fig.4.32 At 2923 cm⁻¹ and 2854 cm⁻¹ peaks are stretching vibrations of CH for aliphatic sp³ CH₂ and CH₃ respectively and bending vibrations for CH₂ are at 1463 cm⁻¹. C=O stretching vibration at 1651 cm⁻¹ and C-O stretching vibrations at 1376cm⁻¹ indicate replacement of dichloroacetate with bromide anion. At 711 cm⁻¹ peak appearance indicates presence of long chain CH₂ in butyl and octyl groups attached to phosphorous.

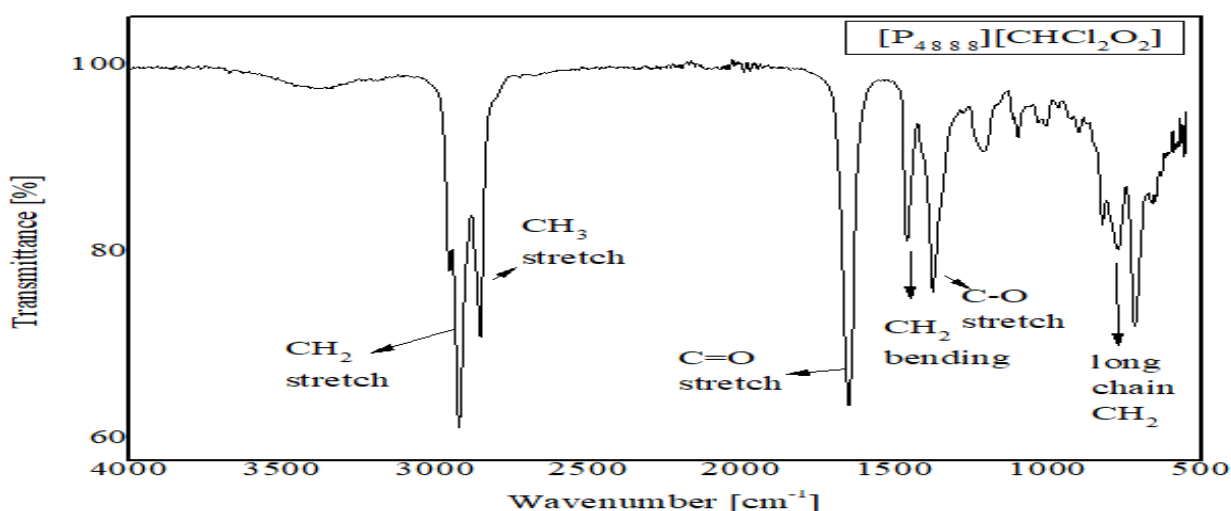


Figure 4.32 FTIR spectrum of [P₄₈₈₈][CHCl₂CO₂]

4.2.29. FT-IR analysis of Tri-octyl mono-butyl phosphonium tetrafluoroborate [P₄₈₈₈][BF₄]

FT-IR for Mono-butyl tri-octyl phosphonium tetrafluoroborate [P₄₈₈₈][BF₄] is shown in fig. 4.33 At 2924 cm⁻¹ and 2855 cm⁻¹ peaks are stretching vibrations of CH for aliphatic sp³ CH₂ and CH₃ respectively and bending vibrations for CH₂ are at 1463 cm⁻¹. At 751 cm⁻¹ peak appearance indicates presence of long chain CH₂ in butyl and octyl groups attached to phosphorous.

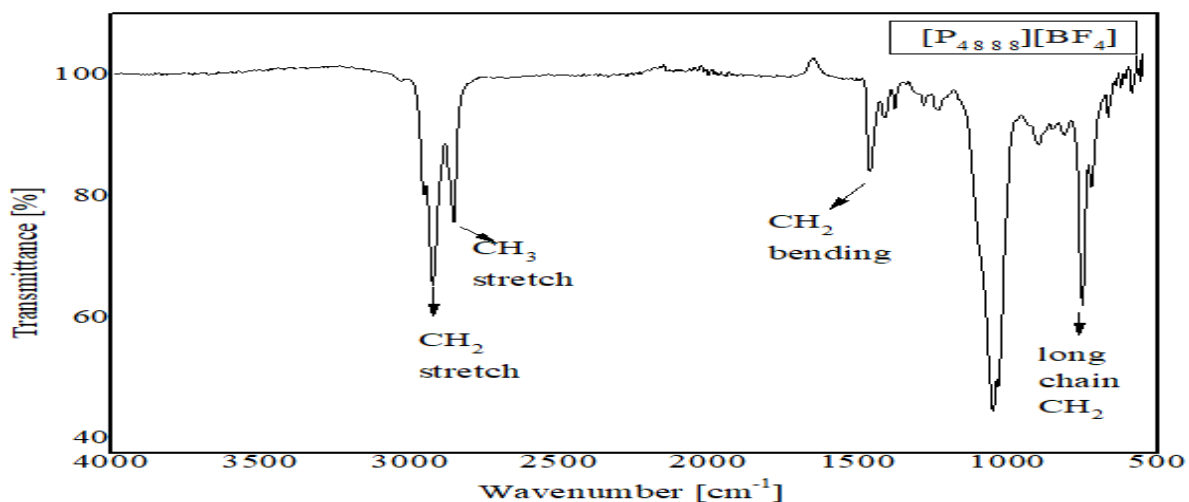


Figure 4.33 FTIR spectrum of [P₄₈₈₈][BF₄]

4.2.30. Tri-octyl mono-butyl phosphonium hydrogen sulphate [P₄₈₈₈][HSO₄]

FT-IR for Mono-butyl tri-octyl phosphonium hydrogen sulphate [P₄₈₈₈][HSO₄] is shown in fig. 4.34 At 2923 cm⁻¹ and 2854 cm⁻¹ peaks are stretching vibrations of CH for aliphatic sp³ CH₂ and CH₃ respectively and bending vibrations for CH₂ are at 1460 cm⁻¹. S=O stretching vibrations at 1236 cm⁻¹ and 1161 cm⁻¹ indicate replacement of hydrogen sulphate with bromide anion. At 719 cm⁻¹ peak appearance indicates presence of long chain CH₂ in butyl and octyl groups attached to phosphorous.

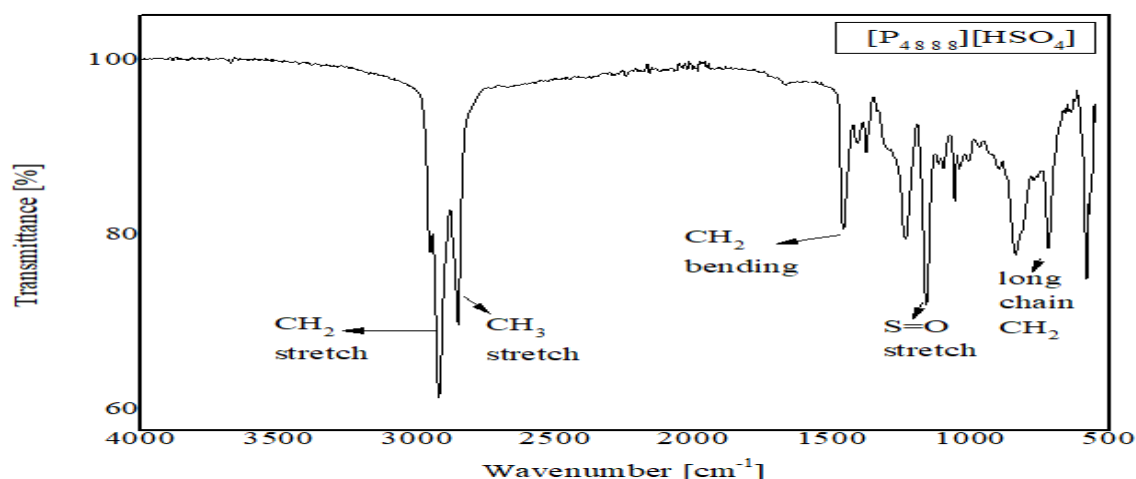


Figure 4.34 FTIR spectrum of [P₄₈₈₈][HSO₄]

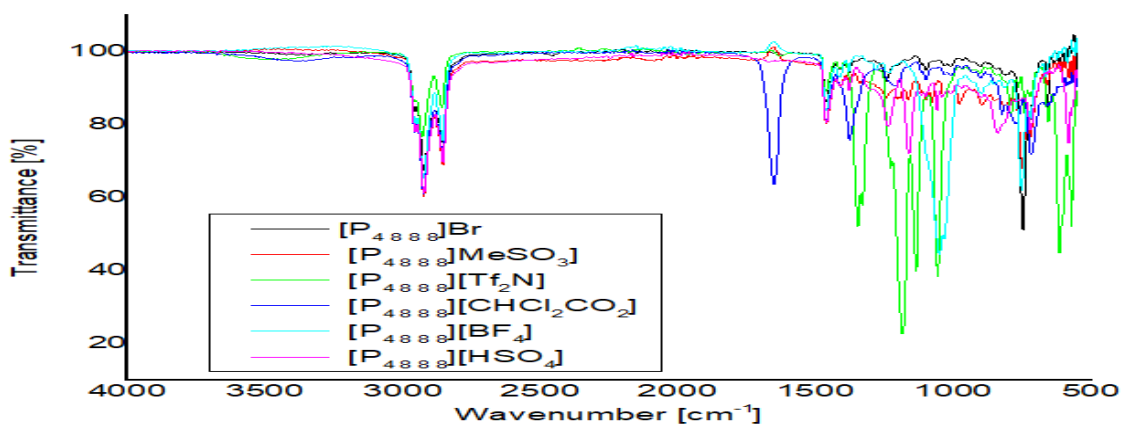


Figure 4.35 FTIR for comparison of different exchanged anions with [P₄₈₈₈]

4.2.31. FT-IR analysis of Di-butyl di-ethyl ammonium bromide [N₂₂₄₄]⁺Br⁻

FT-IR for Di-butyl di-ethyl ammonium bromide [N₂₂₄₄]⁺Br⁻ is shown in fig.4.36. At 2960 cm⁻¹ and 2854 cm⁻¹ peaks are stretching vibrations of CH for aliphatic sp³ CH₂ and CH₃ respectively and bending vibrations for CH₂ and CH₃ are at 1463 cm⁻¹ and 1395 cm⁻¹ respectively. Strong peak at 1160 cm⁻¹ appears due to stretching vibration of C-N of alkyl group bond to nitrogen. At 743 cm⁻¹ peak appearance indicates presence of long chain CH₂ in butyl and ethyl groups.

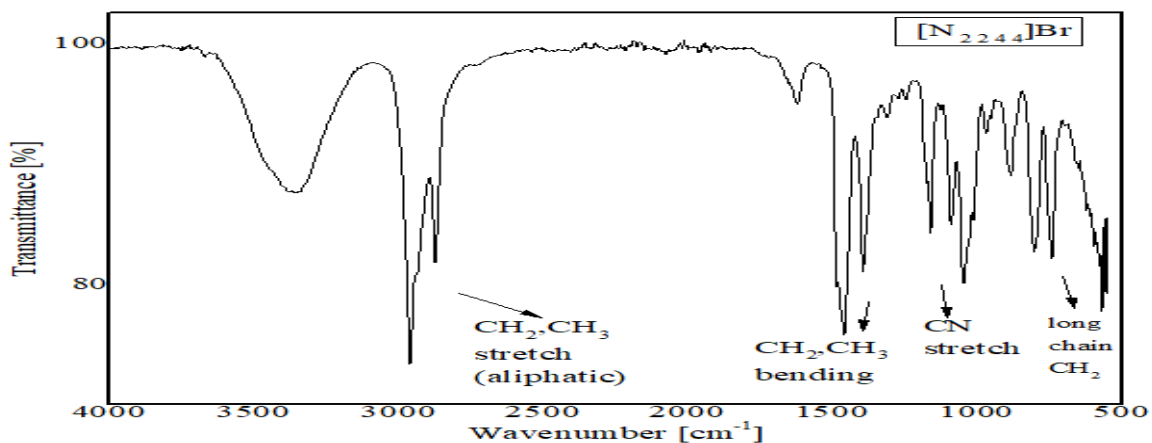


Figure 4.36 FTIR spectrum of $[N_{2,2,4,4}]\text{Br}$

4.2.32. FT-IR analysis of Di-butyl di-ethyl ammonium methanesulphonate

$[N_{2,2,4,4}][\text{MeSO}_3]$

FT-IR for Di-butyl di-ethyl ammonium methanesulphonate $[N_{2,2,4,4}][\text{MeSO}_3]$ is shown in fig.4.37. At 2960 cm^{-1} and 2854 cm^{-1} peaks are stretching vibrations of CH for aliphatic sp^3 CH_2 and CH_3 respectively and bending vibrations for CH_2 and CH_3 are at 1459 cm^{-1} and 1395 cm^{-1} respectively. Peak at 1202 cm^{-1} appear due to stretching vibration of C-N of alkyl group bond to nitrogen. At 1038 cm^{-1} band appearance show the stretching vibration of S=O of methanesulphonate and at 743 cm^{-1} peak appearance indicates presence of long chain CH_2 in butyl and ethyl groups.

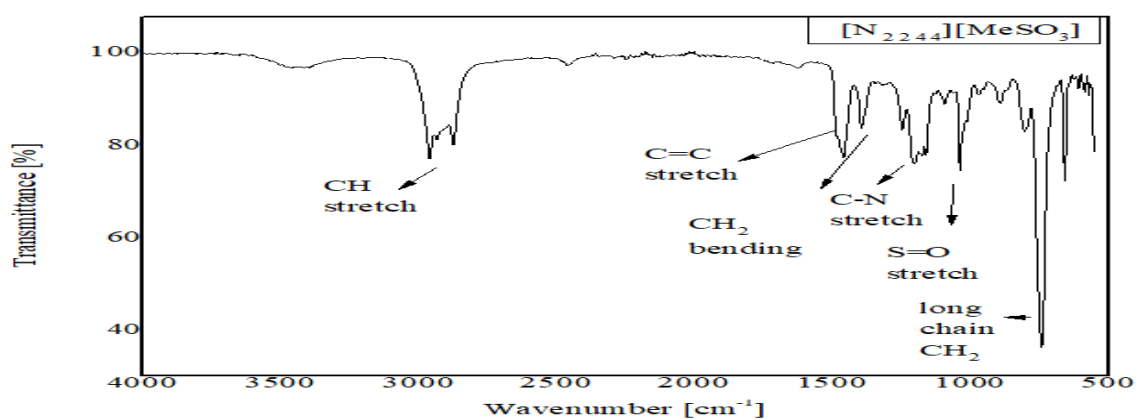


Figure 4.37 FTIR spectrum of $[N_{2,2,4,4}][\text{MeSO}_3]$

4.2.33. FT-IR analysis Di-butyl di-ethyl ammonium Bis(trifluoromethane-sulfonyl) imide $[N_{2.2.4.4}][Tf_2N]$

FT-IR for Di-butyl di-ethyl ammonium Bis(trifluoromethane-sulfonyl)imide $[N_{2.2.4.4}][Tf_2N]$ is shown in fig.4.38 At 2960 cm^{-1} and 2854 cm^{-1} peaks are stretching vibrations of CH for aliphatic $sp^3\text{ CH}_2$ and CH_3 respectively. At 1348 cm^{-1} and 1052 cm^{-1} band appearance show the stretching vibration of S=O of lithium Bis(trifluoromethane-sulfonyl)imide and at 739 cm^{-1} peak appearance indicate presence of long chain CH_2 in butyl and ethyl groups.

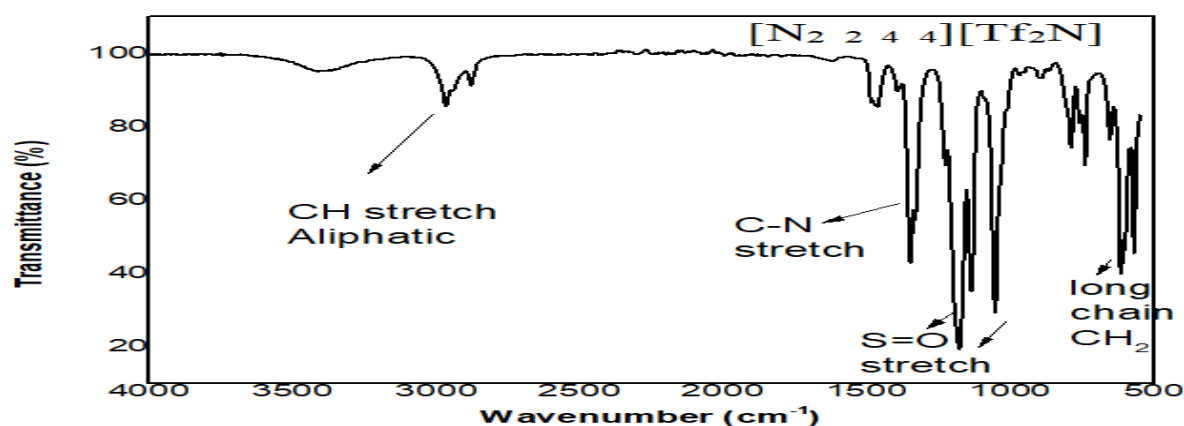


Figure 4.38 FTIR spectrum of $[N_{2.2.4.4}][Tf_2N]$

4.2.34. FT-IR analysis of Di-butyl di-ethyl ammonium dichloroacetate $[N_{2.2.4.4}][CHF_2CO_2]$

FT-IR for Di-butyl di-ethyl ammonium dichloroacetate $[N_{2.2.4.4}][CHF_2CO_2]$ is shown in fig. 4.39 At 2961 cm^{-1} and 2854 cm^{-1} peaks are stretching vibrations of CH for aliphatic $sp^3\text{ CH}_2$ and CH_3 respectively and bending vibrations for CH_2 and CH_3 are at 1459 cm^{-1} 1370 cm^{-1} respectively. Strong peak at 1646 cm^{-1} is due to C=O stretching vibrations of dichloroacetate anion then peak at 1160 cm^{-1} appear due to stretching vibration of C-N of alkyl group bond to nitrogen. At 710 cm^{-1} peak appearance indicates presence of long chain CH_2 in butyl and ethyl groups.

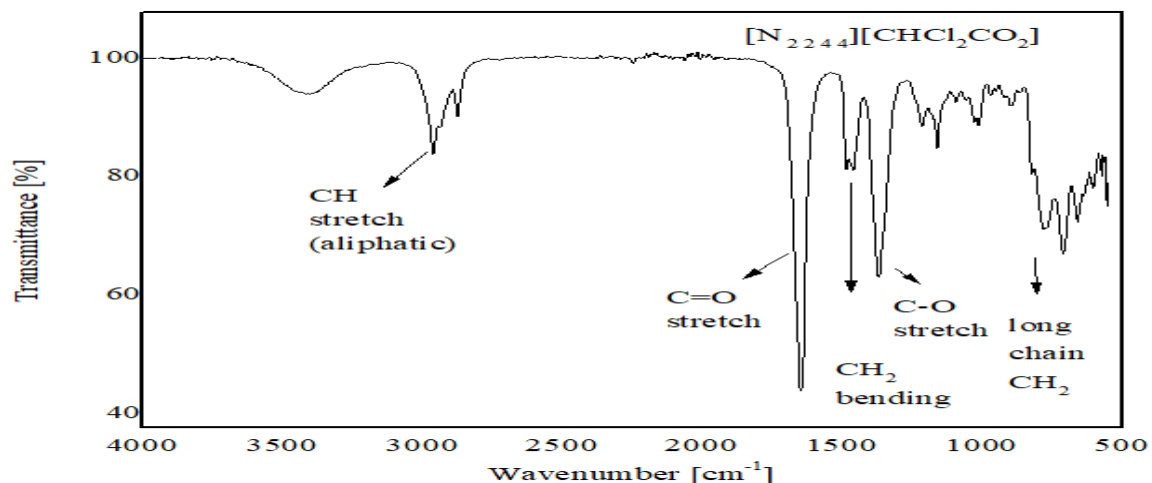


Figure 4.39 FTIR spectrum of $[N_{2,2,4,4}][CHF_2CO_2]$

4.2.35. FT-IR analysis for Di-butyl di-ethyl ammonium hydrogen tetrafluoroborate $[N_{2,2,4,4}][BF_4]$

FT-IR for Di-butyl di-ethyl ammonium hydrogen tetrafluoroborate $[N_{2,2,4,4}][BF_4]$ is shown in fig.4.40. At 2960 cm^{-1} and 2854 cm^{-1} peaks are stretching vibrations of CH for aliphatic sp^3 CH₂ and CH₃ respectively and bending vibrations for CH₂ and CH₃ are at 1459 cm^{-1} and 1393 cm^{-1} respectively. At 751 cm^{-1} peak appearance indicates presence of long chain CH₂ in butyl and ethyl groups.

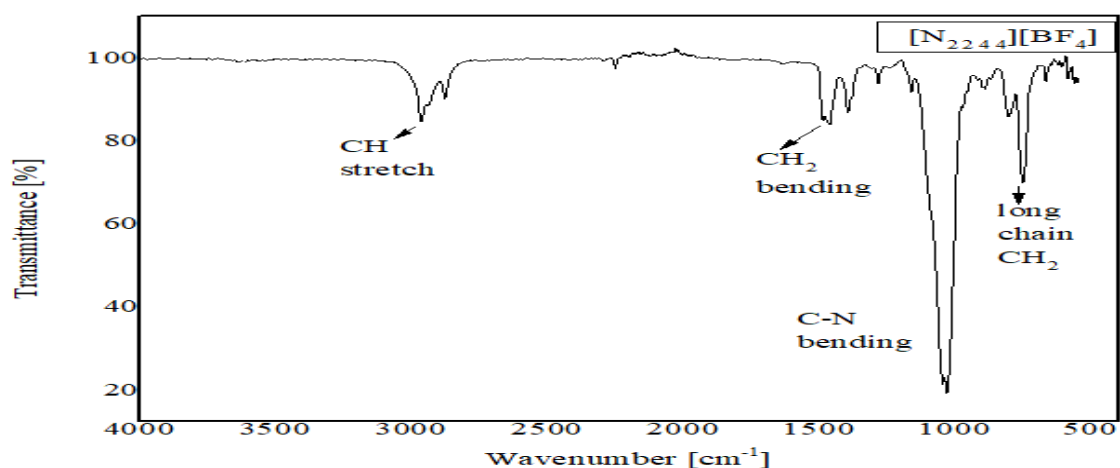


Figure 4.40 FTIR spectrum of $[N_{2,2,4,4}][BF_4]$

Strong band appearance at 1049 cm^{-1} confirms presence of BF_4 anion, so confirming formation of 1-Methyl-3-octylimidazolium tetrafluoroborate $[C_8mim][BF_4]$.

4.2.36. FT-IR analysis for Di-butyl di-ethyl ammonium hydrogen sulphate



FT-IR for Di-butyl di-ethyl ammonium hydrogen sulphate $[N_{2,2,4,4}][HSO_4]$ is shown in fig.4.41. At 2960 cm^{-1} and 2854 cm^{-1} peaks are stretching vibrations of CH for aliphatic sp^3 CH_2 and CH_3 respectively and bending vibrations for CH_2 and CH_3 are at 1459 cm^{-1} 1393 cm^{-1} respectively. Strong peak at 1160 cm^{-1} appear due to stretching vibration of C-N of alkyl group bond to nitrogen at 1027 cm^{-1} peak appearance is due to S=O stretching vibrations of hydrogen sulphate anion. At 739 cm^{-1} peak appearance indicates presence of long chain CH_2 in butyl and ethyl groups.

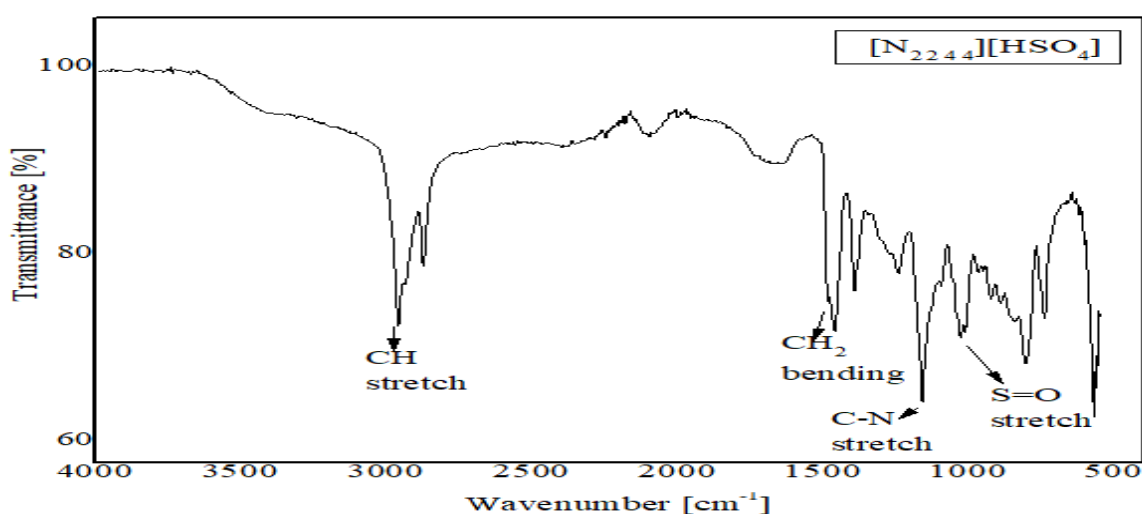


Figure 4.41 FTIR spectrum of $[N_{2,2,4,4}][HSO_4]$

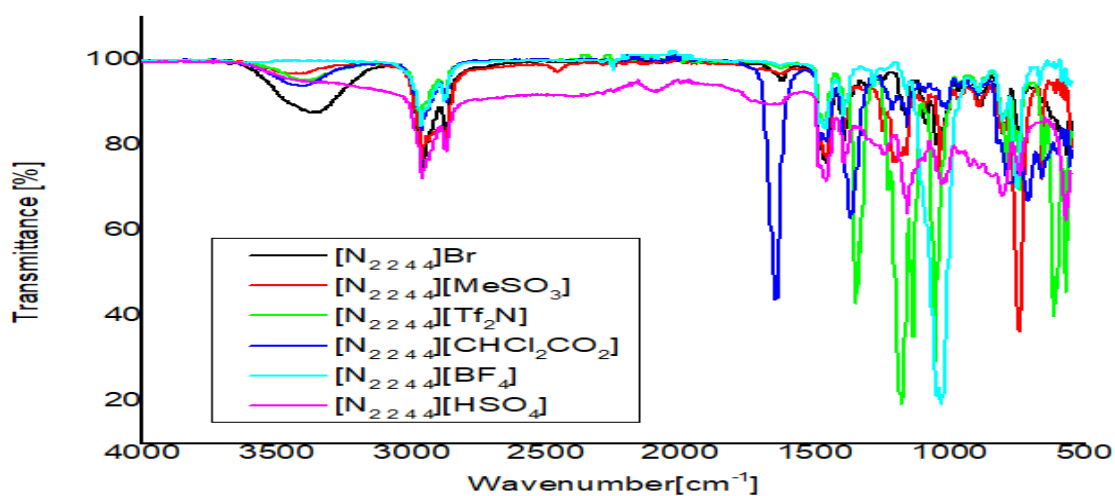


Figure 4.42 FTIR for comparison of different exchanged anions with $[N_{2,2,4,4}]$

4.3 Nuclear magnetic resonance spectroscopy(NMR)

4.3.1 [C₈mim]Br NMR

¹H NMR ppm (CDCl₃); 0.37-0.47 (m, 3H;CH₃), 0.78-0.86 (m, 2H;CH₂),1.44-1.47 (m, 10H;CH₂),3.60-3.70 (m, 3H;NCH₃), 3.87-3.90 (m, 2H;NCH₂) ,7.21-7.22 (s, 1H;CH=CH) , 7.360-7.367 (s, 1H;CH=CH), 9.529-9.531 (s, 1H;N-CH-N)

[C₄mim]Br NMR

¹H NMR ppm (CDCl₃); 0.88-0.92 (m, 3H;CH₃), 1.28-1.32 (m, 2H;CH₂), 1.70-1.90 (m, 2H;CH₂), 3.9-4.1 (m, 3H;NCH₃), 4.18-4.32 (m, 2H;NCH₂) , 7.40-7.49 (s, 1H;CH=CH) , 7.50-7.60 (s, 1H;CH=CH), 9.90-10.10 (s, 1H;N-CH-N)

[C₄py]Br NMR

¹H NMR ppm (CDCl₃); 0.85-0.91 (m,CH₃), 1.28-1.32 (m, 2H;CH₂),1.90-1.99 (m, 2H;CH₂),4.88-4.99 (m, 2H;NCH₂), 8.10-8.20(m,1H; CH-CH), 8.55-8.65(m,1H;CHCHCH), 9.45-9.55 (m, 1H;NCH)

4.4. Anti-bacterial Susceptibility of 36 different ionic liquids

4.4.1. Sample preparation:

The samples of equal density and potency were prepared using distilled water. Each sample was tested in triplicate.

4.4.2. Anti-bacterial susceptibility Test 1 using Agar Well Diffusion Assay

A total of 36 samples were used to check their antibacterial activity against pathogenic bacteria. Fresh bacterial culture of 24 hours was used to make the lawn in petri dishes in triplicate. About 100 µl of each equalized bacterial sample was spread on each petri plate. Using a sterilized borer, 3mm wells were made at equal distance. Positive and negative controls were used in equal volume by volume ratio at every plate. About 25µl of each sample solution was poured in each well and then incubated for 24 hours at 37°C. Negative Control: Distilled water
Positive Control: Levofloxacin

Majority of ionic liquids exhibited antibacterial activity against tested bacteria.

	<i>Escherichia coli</i>	<i>Enterobacter aerogenes</i>	<i>Klebsiella pneumoniae</i>	<i>Proteus vulgaris</i>	<i>Pseudomonas aeruginosa</i>	<i>Streptococcus pneumoniae</i>	<i>Streptococcus pyogenes</i>
- Control	0	0	0	0	0	0	0
+ Control	17	27	12	25	27	25	30
[Camim] Br	21	25	19	20	25	22	14
[Camim] [CH ₃ SO ₃]	21	27	20	18	24	17	13
[Camim] [TF ₂ N]	15	17	17	10	17	20	20
[Camim] [CHCl ₂ CO ₂]	19	17	16	17	20	23	15
[Camim] [BF ₄]	18	22	15	19	15	17	20
[Camim] [HSO ₄]	12	17	17	17	11	0	20

	<i>Escherichia coli</i>	<i>Enterobacter aerogenes</i>	<i>Klebsiella pneumoniae</i>	<i>Protens vulgaris</i>	<i>Pseudomonas aeruginosa</i>	<i>Streptococcus pneumoniae</i>	<i>Streptococcus pyogenes</i>
[C ₄ mim] Br	0	10	0	01	4	0	8
[Camim] [CH ₃ SO ₃]	17	0	0	0	14	0	0
[Camim] [TF ₂ N]	17	17	14	10	10	0	10
[Camim] [CHCl ₂ CO ₂]	7	15	0	0	12	0	0
[Camim] [BF ₄]	10	0	0	0	0	0	13
[Camim] [HSO ₄]	0	20	20	17	21	0	10
C ₈ py]Br	0	0	0	0	0	0	0
[C ₈ py] [CH ₃ SO ₃]	0	16	14	0	0	0	0
[C ₈ py] [TF ₂ N]	0	13	6	0	0	0	0

	<i>Escherichia coli</i>	<i>Enterobacter aerogenes</i>	<i>Klebsiella pneumoniae</i>	<i>Proteus vulgaris</i>	<i>Pseudomonas aeruginosa</i>	<i>Streptococcus pneumoniae</i>	<i>Streptococcus pyogenes</i>
[C ₈ py] [CHCl ₂ CO ₂]	0	20	15	0	0	0	0
[C ₈ py] [BF ₄]	0	20	18	0	0	0	0
[C ₈ py] [HSO ₄]	0	18	14	0	0	0	0
[C ₄ py] Br	0	6	0	0	0	0	0
[C ₄ py] [CH ₃ SO ₃]	0	9	0	0	0	0	0
[C ₄ py] [Tf ₂ N]	0	13	0	0	0	0	0
[C ₄ py] [CHCl ₂ CO ₂]	0	12	0	0	0	0	0
[C ₄ py] [BF ₄]	0	13	0	0	0	0	0
C ₄ py] [HSO ₄]	0	17	0	0	0	0	0

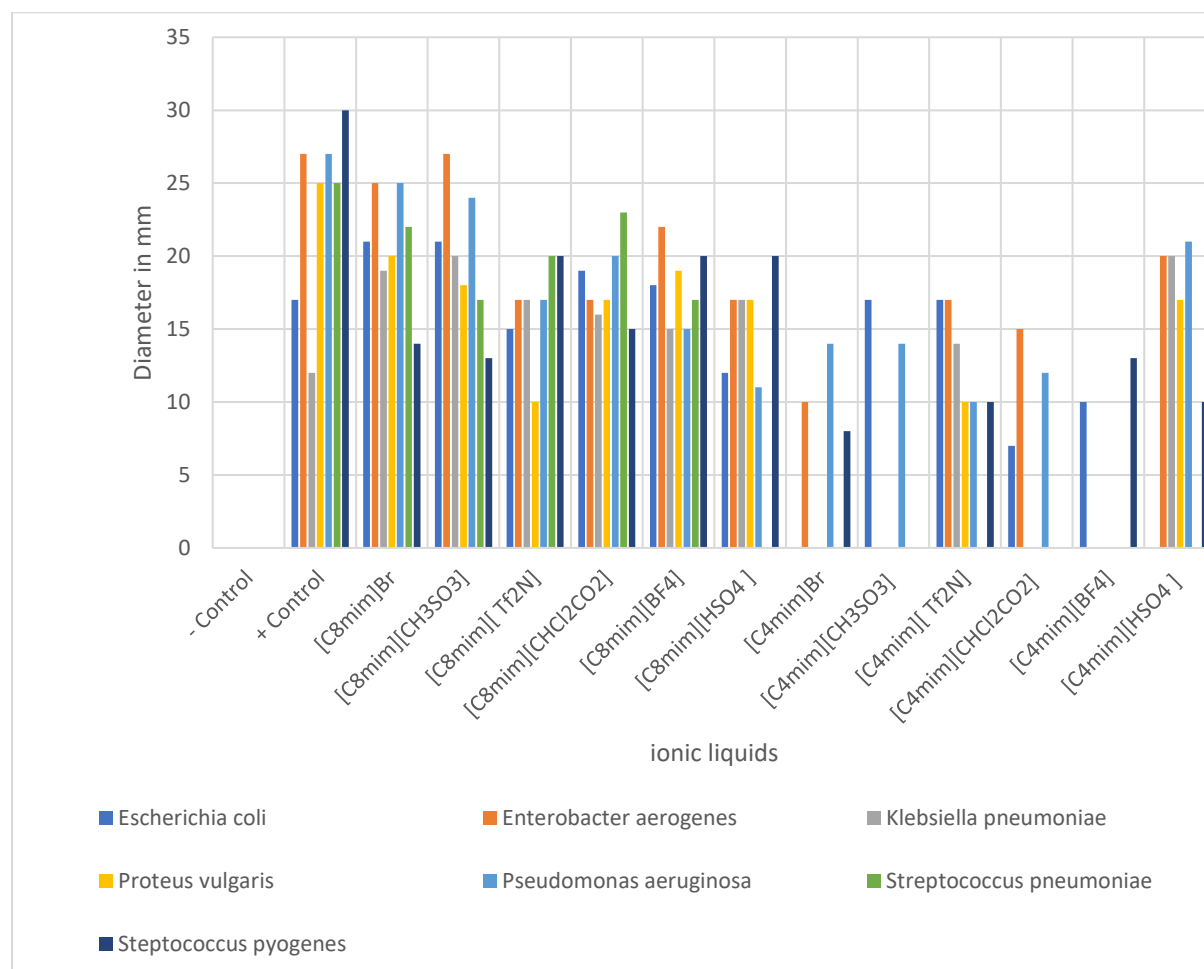
	<i>Escherichia coli</i>	<i>Enterobacter aerogenes</i>	<i>Klebsiella pneumoniae</i>	<i>Proteus vulgaris</i>	<i>Pseudomonas aeruginosa</i>	<i>Streptococcus pneumoniae</i>	<i>Streptococcus pyogenes</i>
[P ₄₈₈₈] Br	0	9	0	0	0	0	0
[P ₄₈₈₈][CH ₃ SO ₃]	12	14	0	0	0	0	0
[P ₄₈₈₈][TF ₂ N]	9	9	0	0	0	0	0
[P ₄₈₈₈] [CHCl ₂ CO ₂]	11	13	0	0	0	0	0
[P ₄₈₈₈] [BF ₄]	10	14	0	0	0	0	0
[P ₄₈₈₈][HSO ₄]	0	13	0	0	0	0	0
[N ₂₂₄₄]Br	16	12	0	0	0	0	0
[N ₂₂₄₄][CH ₃ SO ₃]	0	0	0	0	0	0	0
[N ₂₂₄₄][TF ₂ N]	0	0	0	0	0	0	0
[N ₂₂₄₄][CHCl ₂ O ₂]	0	0	0	0	0	0	0
[N ₂₂₄₄] [BF ₄]	0	0	0	7	0	0	0
[N ₂₂₄₄] [HSO ₄]	0	0	11	10	0	0	0

Table 4.1 Zone of Inhibition (Diameter in mm) of ionic liquids against most common bacteria

4.5. Antibacterial Activity Graphs

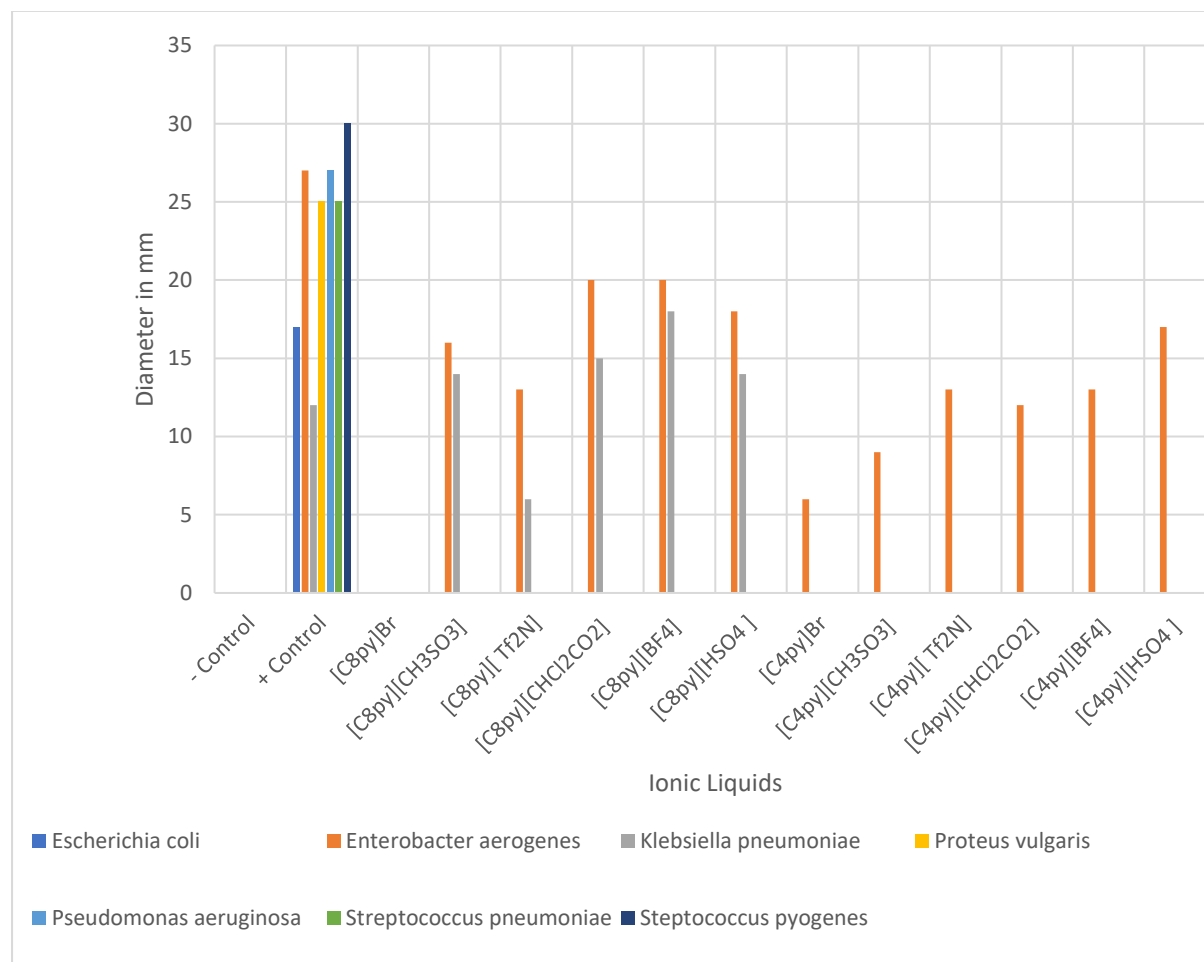
4.5.1. Imidazolium based ionic liquids antibacterial activity graph

Imidazolium based ionic liquids show highest antibacterial activity against all tested bacteria and were even more antibacterial as compare to the positive control.



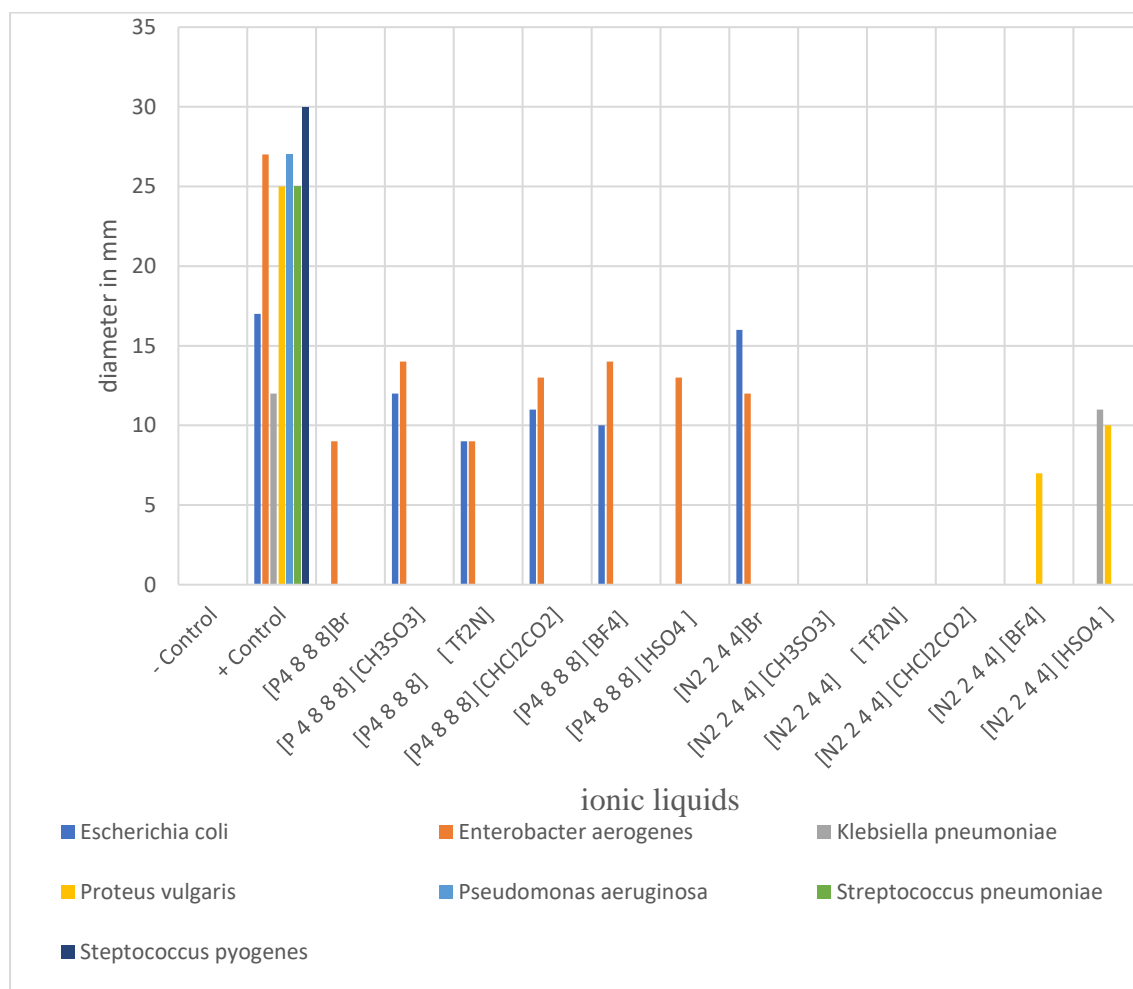
4.5.2. Pyridinium based ionic liquids antibacterial activity graph

Octyl Pyridinium based ionic liquids show antibacterial activity against *Klebsiella pneumoniae* and *Enterobacter aerogenes*. While Butyl Pyridinium based ionic liquids show antibacterial activity only against *Enterobacter aerogenes*



4.5.3. Phosphonium and Ammonium based ionic liquids antibacterial graph

Phosphonium based ionic liquids and $[N_{2,2,4,4}]Br$ were antibacterial against *Enterobacter aerogenes* and *Escherichia coli*. $[N_{2,2,4,4}] [BF_4]$ show antibacterial property against *Proteus vulgaris*, $[N_{2,2,4,4}] [HSO_4]$ was antibacterial against *Proteus vulgaris* and *Klebsiella pneumoniae*.



4.6 Antibacterial Paint

Among 36 samples 3 samples showing highest antibacterial activity were selected

- [C₈mim]Br
- C₈mim][CH₃SO₃]
- [C₈py][CHCl₂CO₂]

and their different compositions such as 2%, 5%, 10% in paint were prepared to check their antibacterial activity. These samples of paint were coated on microplates and bacterial sample was sprayed on to slides, slides antibacterial activity was tested.

Following are the results of Antibacterial activity of paint samples coated on microplates.

Out conclusion: There is no bacterial growth in any of the paint composition.

Sample description	<i>E. coli</i>	<i>P. aeruginosa</i>
Only media	0.967	0.853
2% [C ₈ mim]Br + Paint	0.041	0.053
5% [C ₈ mim]Br + Paint	0.040	0.076
10% [C ₈ mim]Br + Paint	0.040	0.050
2% [C ₈ mim][CH ₃ SO ₃] + Paint	0.042	0.050
5% [C ₈ mim][CH ₃ SO ₃] + Paint	0.040	0.048
10% [C ₈ mim][CH ₃ SO ₃] + Paint	0.043	0.048
2% [C ₈ py][CHCl ₂ CO ₂] + Paint	0.043	0.059
5% [C ₈ py][CHCl ₂ CO ₂] + Paint	0.036	0.050
10% [C ₈ py][CHCl ₂ CO ₂] + Paint	0.040	0.047
2% [C ₈ mim]Br + 2% [C ₈ mim][CH ₃ SO ₃] + 2% [C ₈ py][CHCl ₂ CO ₂] + Paint	0.042	0.048
German paint	0.045	0.056

Chapter 5

5. CONCLUSION

Thirty six Ionic Liquids were prepared cationic parts were Imidazolium, Pyridinium, Quaternary ammonium and phosphonium with varying chain lengths and anionic parts were Bromide, Sodium Methane sulphonate, Lithium Bis(trifluoro methane-sulfonyl)imide, Sodium Dichloroacetate and Sodium Tetrafluoroborate, Potassium Hydrogen sulphate. The prepared ionic liquids were characterized with different characterization techniques TLC, FTIR and NMR.

Then 25 μ L solution of these thirty six samples were taken and tested for their antibacterial activity against most commonly occurring bacteria in environment which were *Pseudomonas aeruginosa*, *Streptococcus pyogenes*, *Streptococcus pneumoniae*, *Proteus vulgaris*, *Klebsiella pneumoniae*, *Enterobacter aerogenes* and *Escherichia coli*. Imidazolium based ionic liquids show highest antibacterial activity against all tested bacteria and were even more antibacterial as compare to the positive control, Pyridinium based ionic liquids show antibacterial activity against *Klebsiella pneumoniae* and *Enterobacter aerogenes*. Phosphonium based ionic liquids and [N_{2 2 4 4}]Br were antibacterial against *Enterobacter aerogenes* and *Escherichia coli*. [N_{2 2 4 4}] [BF₄] show antibacterial property against *Proteus vulgaris*, [N_{2 2 4 4}] [HSO₄] was antibacterial against *Proteus vulgaris*, *Klebsiella pneumoniae*.

Among 36 samples 3 samples showing highest antibacterial activity were selected

- [C₈mim]Br
- C₈mim][CH₃SO₃]
- [C₈py][CHCl₂CO₂]

All samples were highly antibacterial against *E. coli* and *P. aeruginosa*

REFERENCES

- [1] E. M. Fox, Y. Jiang, and K. S. Gobius, "Key pathogenic bacteria associated with dairy foods: On-farm ecology and products associated with foodborne pathogen transmission," *International Dairy Journal*, vol. 84, pp. 28-35, 2018.
- [2] F. Hitzenbichler, M. Simon, T. Holzmann, M. Iberer, M. Zimmermann, B. Salzberger, *et al.*, "Antibiotic resistance in E. coli isolates from patients with urinary tract infections presenting to the emergency department," *Infection*, vol. 46, pp. 325-331, 2018.
- [3] J. Otter, T. Galletly, F. Davies, J. Hitchcock, M. Gilchrist, E. Dyakova, *et al.*, "Planning to halve Gram-negative bloodstream infection: getting to grips with healthcare-associated Escherichia coli bloodstream infection sources," *Journal of Hospital Infection*, vol. 101, pp. 129-133, 2019.
- [4] L. H. Gould, R. K. Mody, K. L. Ong, P. Clogher, A. B. Cronquist, K. N. Garman, *et al.*, "Increased recognition of non-O157 Shiga toxin-producing Escherichia coli infections in the United States during 2000–2010: epidemiologic features and comparison with E. coli O157 infections," *Foodborne pathogens and disease*, vol. 10, pp. 453-460, 2013.
- [5] C. L. Swaggerty, N. Corcionivoschi, S. C. Ricke, and T. R. Callaway, "The First 30 Years of Shiga Toxin-Producing Escherichia coli in Cattle Production: Incidence, Preharvest Ecology, and Management," in *Food and Feed Safety Systems and Analysis*, ed: Elsevier, 2018, pp. 117-131.
- [6] A. Davin-Regli, "Enterobacter aerogenes and Enterobacter cloacae; versatile bacterial pathogens confronting antibiotic treatment," *Frontiers in microbiology*, vol. 6, p. 392, 2015.
- [7] A. B. Cabral, M. A. V. Maciel, J. F. Barros, M. M. Antunes, C. M. M. B. de Castro, and A. C. S. Lopes, "Clonal spread and accumulation of β -lactam resistance determinants in Enterobacter aerogenes and Enterobacter cloacae complex isolates from infection and colonization in patients at a public hospital in Recife, Pernambuco, Brazil," *Journal of medical microbiology*, vol. 66, pp. 70-77, 2017.
- [8] C. L. Gorrie, M. Mirčeta, R. R. Wick, D. J. Edwards, N. R. Thomson, R. A. Strugnell, *et al.*, "Gastrointestinal carriage is a major reservoir of Klebsiella pneumoniae infection in intensive care patients," *Clinical Infectious Diseases*, vol. 65, pp. 208-215, 2017.
- [9] M. K. Paczosa and J. Meccas, "Klebsiella pneumoniae: going on the offense with a strong defense," *Microbiol. Mol. Biol. Rev.*, vol. 80, pp. 629-661, 2016.
- [10] A. L. Hamilton, M. A. Kamm, S. C. Ng, and M. Morrison, "Proteus spp. as putative gastrointestinal pathogens," *Clinical microbiology reviews*, vol. 31, pp. e00085-17, 2018.
- [11] S. Guermazi-Toumi, S. Boujljel, M. Assoudi, R. Issaoui, S. Tlili, and M. E. Hlaiem, "Susceptibility profiles of bacteria causing urinary tract infections in Southern Tunisia," *Journal of global antimicrobial resistance*, vol. 12, pp. 48-52, 2018.
- [12] S. Jain, W. H. Self, R. G. Wunderink, S. Fakhran, R. Balk, A. M. Bramley, *et al.*, "Community-acquired pneumonia requiring hospitalization among US adults," *New England Journal of Medicine*, vol. 373, pp. 415-427, 2015.
- [13] J. M. Musser, A. R. Hauser, M. H. Kim, P. M. Schlievert, K. Nelson, and R. K. Selander, "Streptococcus pyogenes causing toxic-shock-like syndrome and other invasive diseases: clonal diversity and pyrogenic exotoxin expression," *Proceedings of the National Academy of Sciences*, vol. 88, pp. 2668-2672, 1991.
- [14] T. Ikebe, T. Matsumura, H. Nihonmatsu, H. Ohya, R. Okuno, C. Mitsui, *et al.*, "Spontaneous mutations in Streptococcus pyogenes isolates from streptococcal toxic shock syndrome patients play roles in virulence," *Scientific reports*, vol. 6, p. 28761, 2016.
- [15] S. T. Micek, A. E. Lloyd, D. J. Ritchie, R. M. Reichley, V. J. Fraser, and M. H. Kollef, "Pseudomonas aeruginosa bloodstream infection: importance of appropriate initial antimicrobial treatment," *Antimicrobial agents and chemotherapy*, vol. 49, pp. 1306-1311, 2005.
- [16] V. Kochkodan and N. Hilal, "A comprehensive review on surface modified polymer membranes for biofouling mitigation," *Desalination*, vol. 356, pp. 187-207, 2015.

- [17] P. Gupta, S. Sarkar, B. Das, S. Bhattacharjee, and P. Tribedi, "Biofilm, pathogenesis and prevention—a journey to break the wall: a review," *Archives of microbiology*, vol. 198, pp. 1-15, 2016.
- [18] A. Kramer, I. Schwebke, and G. Kampf, "How long do nosocomial pathogens persist on inanimate surfaces? A systematic review," *BMC infectious diseases*, vol. 6, p. 130, 2006.
- [19] P. Rusin, S. Maxwell, and C. Gerba, "Comparative surface-to-hand and fingertip-to-mouth transfer efficiency of gram-positive bacteria, gram-negative bacteria, and phage," *Journal of Applied Microbiology*, vol. 93, pp. 585-592, 2002.
- [20] S. J. Dancer, "Control of transmission of infection in hospitals requires more than clean hands," *Infection Control & Hospital Epidemiology*, vol. 31, pp. 958-960, 2010.
- [21] J. A. Otter, S. Yezli, and G. L. French, "The role of contaminated surfaces in the transmission of nosocomial pathogens," in *Use of biocidal surfaces for reduction of healthcare acquired infections*, ed: Springer, 2014, pp. 27-58.
- [22] Z. Saleem, M. A. Hassali, B. Godman, F. K. Hashmi, and F. Saleem, "A multicenter point prevalence survey of healthcare-associated infections in Pakistan: Findings and implications," *American journal of infection control*, vol. 47, pp. 421-424, 2019.
- [23] R. Wali, A.-u. Haque, and Z. Fadool, "Healthcare-associated infections among pediatric oncology patients in Pakistan: risk factors and outcome," *The Journal of Infection in Developing Countries*, vol. 6, pp. 416-421, 2012.
- [24] Z. Saleem, M. A. Hassali, A. Versporten, B. Godman, F. K. Hashmi, H. Goossens, *et al.*, "A multicenter point prevalence survey of antibiotic use in Punjab, Pakistan: findings and implications," *Expert review of anti-infective therapy*, vol. 17, pp. 285-293, 2019.
- [25] B. Mehrad, N. M. Clark, G. G. Zhanel, and J. P. Lynch III, "Antimicrobial resistance in hospital-acquired gram-negative bacterial infections," *Chest*, vol. 147, pp. 1413-1421, 2015.
- [26] S. Gantz, A. Copeland, and C. A. Zapka, "Sanitizer composition with probiotic/prebiotic active ingredient," ed: Google Patents, 2018.
- [27] T. C. V. Penna, P. G. Mazzola, and A. M. S. Martins, "The efficacy of chemical agents in cleaning and disinfection programs," *BMC Infectious Diseases*, vol. 1, p. 16, 2001.
- [28] M. Laroussi, "Low temperature plasma-based sterilization: overview and state-of-the-art," *Plasma processes and polymers*, vol. 2, pp. 391-400, 2005.
- [29] G. McDonnell and A. D. Russell, "Antiseptics and disinfectants: activity, action, and resistance," *Clinical microbiology reviews*, vol. 12, pp. 147-179, 1999.
- [30] R. K. Chhetri, A. Baun, and H. R. Andersen, "Acute toxicity and risk evaluation of the CSO disinfectants performic acid, peracetic acid, chlorine dioxide and their by-products hydrogen peroxide and chlorite," *Science of the Total Environment*, vol. 677, pp. 1-8, 2019.
- [31] A. M. Agarkhed, M. A. Bapat, A. Majumdar, P. Mallemala, M. S. Mathapathi, and N. Tomar, "A topical antimicrobial composition," ed: Google Patents, 2019.
- [32] A. Bridier, R. Briandet, V. Thomas, and F. Dubois-Brissonnet, "Resistance of bacterial biofilms to disinfectants: a review," *Biofouling*, vol. 27, pp. 1017-1032, 2011.
- [33] M. A. Kohanski, D. J. Dwyer, B. Hayete, C. A. Lawrence, and J. J. Collins, "A common mechanism of cellular death induced by bactericidal antibiotics," *Cell*, vol. 130, pp. 797-810, 2007.
- [34] M. A. Fischbach and C. T. Walsh, "Antibiotics for emerging pathogens," *Science*, vol. 325, pp. 1089-1093, 2009.
- [35] J. L. Martínez, "Antibiotics and antibiotic resistance genes in natural environments," *Science*, vol. 321, pp. 365-367, 2008.
- [36] J. Elfersy, "Methods and compositions for antimicrobial surfaces," ed: Google Patents, 2015.
- [37] T. Kuratsuji and H. Shimizu, "Polyamide based antibacterial powder paint composition," ed: Google Patents, 2006.
- [38] K. C. Anyaogu, A. V. Fedorov, and D. C. Neckers, "Synthesis, characterization, and antifouling potential of functionalized copper nanoparticles," *Langmuir*, vol. 24, pp. 4340-4346, 2008.

- [39] M. A. Ruggiero, "Paint containing high levels of a pyrrhione salt plus a copper salt," ed: Google Patents, 1991.
- [40] L. Hochmannova and J. Vytrasova, "Photocatalytic and antimicrobial effects of interior paints," *Progress in organic coatings*, vol. 67, pp. 1-5, 2010.
- [41] T. Zuccheri, M. Colonna, I. Stefanini, C. Santini, and D. Gioia, "Bactericidal activity of aqueous acrylic paint dispersion for wooden substrates based on TiO₂ nanoparticles activated by fluorescent light," *Materials*, vol. 6, pp. 3270-3283, 2013.
- [42] J. Wang, J. Li, S. Qian, G. Guo, Q. Wang, J. Tang, *et al.*, "Antibacterial surface design of titanium-based biomaterials for enhanced bacteria-killing and cell-assisting functions against periprosthetic joint infection," *ACS applied materials & interfaces*, vol. 8, pp. 11162-11178, 2016.
- [43] N. S. Allen, M. Edge, J. Verran, J. Stratton, J. Maltby, and C. Bygott, "Photocatalytic titania based surfaces: environmental benefits," *Polymer degradation and stability*, vol. 93, pp. 1632-1646, 2008.
- [44] J. N. Pendleton and B. F. Gilmore, "The antimicrobial potential of ionic liquids: A source of chemical diversity for infection and biofilm control," *International journal of antimicrobial agents*, vol. 46, pp. 131-139, 2015.
- [45] D. Pittet, B. Allegranzi, J. Boyce, and W. H. O. W. A. f. P. S. F. G. P. S. C. C. G. o. Experts, "The World Health Organization guidelines on hand hygiene in health care and their consensus recommendations," *Infection Control & Hospital Epidemiology*, vol. 30, pp. 611-622, 2009.
- [46] W. H. Organization, "Report on the burden of endemic health care-associated infection worldwide," 2011.
- [47] O. Bondarenko, K. Juganson, A. Ivask, K. Kasemets, M. Mortimer, and A. Kahru, "Toxicity of Ag, CuO and ZnO nanoparticles to selected environmentally relevant test organisms and mammalian cells in vitro: a critical review," *Archives of toxicology*, vol. 87, pp. 1181-1200, 2013.
- [48] S. Suppi, K. Kasemets, A. Ivask, K. Künnis-Beres, M. Sihtmäe, I. Kurvet, *et al.*, "A novel method for comparison of biocidal properties of nanomaterials to bacteria, yeasts and algae," *Journal of hazardous materials*, vol. 286, pp. 75-84, 2015.
- [49] R. R. Khaydarov, R. A. Khaydarov, Y. Estrin, S. Evgrafova, T. Scheper, C. Endres, *et al.*, "Silver nanoparticles," in *Nanomaterials: Risks and Benefits*, ed: Springer, 2009, pp. 287-297.
- [50] A. Kumar, P. K. Vemula, P. M. Ajayan, and G. John, "Silver-nanoparticle-embedded antimicrobial paints based on vegetable oil," *Nature materials*, vol. 7, p. 236, 2008.
- [51] R. D. Holtz, B. A. Lima, A. G. Souza Filho, M. Brocchi, and O. L. Alves, "Nanostructured silver vanadate as a promising antibacterial additive to water-based paints," *Nanomedicine: Nanotechnology, Biology and Medicine*, vol. 8, pp. 935-940, 2012.
- [52] R. Kaegi, B. Sinnet, S. Zuleeg, H. Hagendorfer, E. Mueller, R. Vonbank, *et al.*, "Release of silver nanoparticles from outdoor facades," *Environmental pollution*, vol. 158, pp. 2900-2905, 2010.
- [53] P. AshaRani, "Low Kah Mun G, Hande MP, Valiyaveettil S," *Cytotoxicity and genotoxicity of silver nanoparticles in human cells. ACS Nano*, vol. 3, pp. 279-290, 2009.
- [54] K. Krishnamoorthy, M. Premanathan, M. Veerapandian, and S. J. Kim, "Nanostructured molybdenum oxide-based antibacterial paint: effective growth inhibition of various pathogenic bacteria," *Nanotechnology*, vol. 25, p. 315101, 2014.
- [55] S. Chen, Y. Guo, H. Zhong, S. Chen, J. Li, Z. Ge, *et al.*, "Synergistic antibacterial mechanism and coating application of copper/titanium dioxide nanoparticles," *Chemical Engineering Journal*, vol. 256, pp. 238-246, 2014.
- [56] A. S. Adeleye, E. A. Oranu, M. Tao, and A. A. Keller, "Release and detection of nanosized copper from a commercial antifouling paint," *Water research*, vol. 102, pp. 374-382, 2016.
- [57] Y. Chen, H. Ding, and S. Sun, "Preparation and characterization of ZnO nanoparticles supported on amorphous SiO₂," *Nanomaterials*, vol. 7, p. 217, 2017.

- [58] S. S. Dunne, M. Ahonen, M. Modic, F. R. Crijns, M. M. Keinänen-Toivola, R. Meinke, *et al.*, "Specialized cleaning associated with antimicrobial coatings for reduction of hospital-acquired infection: opinion of the COST Action Network AMiCI (CA15114)," *Journal of Hospital Infection*, vol. 99, pp. 250-255, 2018.
- [59] M. P. Muller, C. MacDougall, M. Lim, I. Armstrong, A. Bialachowski, S. Callery, *et al.*, "Antimicrobial surfaces to prevent healthcare-associated infections: a systematic review," *Journal of Hospital Infection*, vol. 92, pp. 7-13, 2016.
- [60] A. Abbaszadegan, A. Gholami, S. Abbaszadegan, Z. S. Aleyasin, Y. Ghahramani, S. Dorostkar, *et al.*, "The effects of different ionic liquid coatings and the length of alkyl chain on antimicrobial and cytotoxic properties of silver nanoparticles," *Iranian endodontic journal*, vol. 12, p. 481, 2017.
- [61] K. M. Docherty and C. F. Kulpa Jr, "Toxicity and antimicrobial activity of imidazolium and pyridinium ionic liquids," *Green Chemistry*, vol. 7, pp. 185-189, 2005.
- [62] O. Forero Doria, R. Castro, M. Gutierrez, D. Gonzalez Valenzuela, L. Santos, D. Ramirez, *et al.*, "Novel alkylimidazolium ionic liquids as an antibacterial alternative to pathogens of the skin and soft tissue infections," *Molecules*, vol. 23, p. 2354, 2018.
- [63] H. Hajfarajollah, B. Mokhtarani, K. A. Noghabi, A. Sharifi, and M. Mirzaei, "Antibacterial and antiadhesive properties of butyl-methylimidazolium ionic liquids toward pathogenic bacteria," *RSC Advances*, vol. 4, pp. 42751-42757, 2014.
- [64] S. Anvari, H. Hajfarajollah, B. Mokhtarani, M. Enayati, A. Sharifi, and M. Mirzaei, "Antibacterial and anti-adhesive properties of ionic liquids with various cationic and anionic heads toward pathogenic bacteria," *Journal of Molecular Liquids*, vol. 221, pp. 685-690, 2016.
- [65] Z. Zheng, Q. Xu, J. Guo, J. Qin, H. Mao, B. Wang, *et al.*, "Structure-antibacterial activity relationships of imidazolium-type ionic liquid monomers, poly (ionic liquids) and poly (ionic liquid) membranes: effect of alkyl chain length and cations," *ACS applied materials & interfaces*, vol. 8, pp. 12684-12692, 2016.
- [66] J. Pernak, K. Sobaszekiewicz, and I. Mirska, "Anti-microbial activities of ionic liquids," *Green Chemistry*, vol. 5, pp. 52-56, 2003.
- [67] D. Demberelnyamba, K.-S. Kim, S. Choi, S.-Y. Park, H. Lee, C.-J. Kim, *et al.*, "Synthesis and antimicrobial properties of imidazolium and pyrrolidinium salts," *Bioorganic & medicinal chemistry*, vol. 12, pp. 853-857, 2004.
- [68] A. Cieniecka-Rostonkiewicz, J. Pernak, J. Kubis-Feder, A. Ramani, A. J. Robertson, and K. R. Seddon, "Synthesis, anti-microbial activities and anti-electrostatic properties of phosphonium-based ionic liquids," *Green Chemistry*, vol. 7, pp. 855-862, 2005.
- [69] N. Iwai, K. Nakayama, and T. Kitazume, "Antibacterial activities of imidazolium, pyrrolidinium and piperidinium salts," *Bioorganic & medicinal chemistry letters*, vol. 21, pp. 1728-1730, 2011.
- [70] J. Cybulski, A. Wiśniewska, A. Kulig-Adamiak, L. Lewicka, A. Cieniecka-Rostonkiewicz, K. Kita, *et al.*, "Long-Alkyl-Chain Quaternary Ammonium Lactate Based Ionic Liquids," *Chemistry—A European Journal*, vol. 14, pp. 9305-9311, 2008.
- [71] W. L. Hough-Troutman, M. Smiglak, S. Griffin, W. M. Reichert, I. Mirska, J. Jodynis-Liebert, *et al.*, "Ionic liquids with dual biological function: sweet and anti-microbial, hydrophobic quaternary ammonium-based salts," *New Journal of Chemistry*, vol. 33, pp. 26-33, 2009.
- [72] J. Cybulski, A. Wiśniewska, A. Kulig-Adamiak, Z. Dąbrowski, T. Praczyk, A. Michalczyk, *et al.*, "Mandelate and prolinatate ionic liquids: synthesis, characterization, catalytic and biological activity," *Tetrahedron letters*, vol. 52, pp. 1325-1328, 2011.
- [73] F. Walkiewicz, K. Materna, A. Kropacz, A. Michalczyk, R. Gwiazdowski, T. Praczyk, *et al.*, "Multifunctional long-alkyl-chain quaternary ammonium azolate based ionic liquids," *New Journal of Chemistry*, vol. 34, pp. 2281-2289, 2010.

- [74] K. N. Ibsen, H. Ma, A. Banerjee, E. E. Tanner, S. Nangia, and S. Mitragotri, "Mechanism of antibacterial activity of choline-based ionic liquids (CAGE)," *ACS Biomaterials Science & Engineering*, vol. 4, pp. 2370-2379, 2018.
- [75] R. J. V. Ferraz, "Development of novel active pharmaceutical ionic liquids and salts based on antibiotics and anti-fungal drugs," 2013.
- [76] A. Perichaud, F. Bataille, C. Baudrion, and L. Panaiva, "Antimicrobial polymers comprising quaternary ammonium groups, their use for making a material with antimicrobial properties and methods for preparing them," ed: Google Patents, 2001.
- [77] K. R. Gisser, M. S. Sibbald, W. J. Smith, J. K. Dreshar, and D. A. Prochazka, "High quality antimicrobial paint composition," ed: Google Patents, 2015.